

Full Scale Investigation of Bilge Keel Effectiveness at Forward Speed

David James Grant

Thesis submitted to the Faculty of Virginia Polytechnic
Institute and State University in partial fulfillment of
the requirements for the degree of

MASTER OF SCIENCE in Ocean Engineering

Dr. Leigh S. McCue, Chairman
Dr. Owen F. Hughes
Dr. Ali Etebari

April 28, 2008
Blacksburg, VA

Keywords: Bilge Keel, Roll Damping, Full Scale

Full Scale Investigation of Bilge Keel Effectiveness at Forward Speed

David J Grant

ABSTRACT

Ship motions in a seaway have long been of great importance, and today with advanced hull forms and higher speeds they are as important as ever. While one can now often adequately predict heave, pitch, sway, yaw and even surge, roll motions are much more difficult. Roll is the one motion that is very dependent upon viscous effects of the fluid. Recently, at David Taylor Model Basin, there have been model experiments where the bilge keels were instrumented in order to directly measure their damping force upon the vessel. To build upon this work and to validate it when applied to full scale vessels, a trial using the Italian naval vessel *Nave Bettica* was performed.

The objective of this thesis is to describe the experiment, present and analyze the results, and offer some conclusions based upon these results. The process of instrumenting the port bilge keel using strain gages and correlating their output to pressures and total forces is described. Selected results for different forward speeds are presented, with full results in the appendices. Particle image velocimetry (PIV) was also performed during the test and was used to measure the flow field in a three foot by three foot area under the aft end of the same bilge keel. Selected image series are presented, as is a methodology for using these images to calculate the center of pressure and the corresponding results.

ACKNOWLEDGEMENTS

I would like to express my sincere appreciation and gratitude to the following:

Dr. Leigh McCue, my chairman, for accepting me as one of her graduate students, for helping me through the process of putting together a thesis, and for her continued support and feedback.

Dr. Ali Etebari, my committee member, for his participation in this project and his help and guidance along the way.

Dr. Owen Hughes, my committee member, for his support and feedback as well as his instruction during my time in graduate school.

Allen Engle and **Dr. Paisan Atsavapranee** of NSWCCD for their participation in this project, as well as for getting me involved and supporting my efforts presented herein.

Jason Carneal of NSWCCD for his work above, below, and within the ship during the test as well as his incredible attitude throughout.

Scott Percival, Todd Beirne, James Herring, Jaime Corzo, and David Bochinski of NSWCCD for their participation in this project.

Claudio Lugni of INSEAN and the **Crew of the Bettica** for all of their cooperation across the Atlantic and assistance during the setup and testing.

Cailin, Marlee, and Emma Grant, my children, for constantly reminding me that, “Daddy has homework to do.”

And finally my wife, **Erin**, for her continuous love, support, and friendly taunting throughout this process.

TABLE OF CONTENTS

Chapter 1	Introduction	1
1.1	Background	1
1.2	Objectives	1
1.3	Nave Bettica	2
Chapter 2	Test Setup	4
2.1	Strain Gages	4
2.1.1	Design	4
2.1.2	Locations	6
2.1.3	Installation, Hookup, and Waterproofing	7
2.1.4	Data Collection	10
2.1.5	Calibration	10
2.2	Particle Image Velocimetry	13
2.2.1	PIV Camera	14
2.2.2	Laser Probes	14
2.2.3	Seeding	15
2.2.4	Calibration	16
Chapter 3	Test Procedure	17
3.1	Test Conditions	17
3.2	Zeroes	18
3.3	PIV Seeding	18
3.4	Forced Oscillation	18
3.5	Data Collection	19
Chapter 4	Analysis Procedure	20
4.1	Gage Calibration Values	20
4.2	FEA Model Verification	22
4.3	Bilge Keel Force	23
4.4	Data Processing	25
4.5	PIV Center of Pressure	28
Chapter 5	Results	31
5.1	Steady State Lifting Force	31
5.2	Roll Damping Results	33
5.3	Center of Pressure	42
5.4	PIV Images	43

Chapter 6	Conclusions & Discussion	48
6.1	Bilge Keel Forces	48
6.2	Center of Pressure	50
6.3	Flow Field Measurement	51
6.4	Limitations of Current Work	51
6.5	Recommendations for Future Work	52
References		54
Appendix A	Ship Characteristics	55
Appendix B	Run Logs & Channel Zeros	60
Appendix C	Complete Roll Damping Force Plots	65
Appendix D	Additional PIV Image Series	98

LIST OF FIGURES

Figure 1	<i>Nave Bettica</i> Outboard Profile	2
Figure 2	Outboard View of the FEA Model	4
Figure 3	Inboard View of the FEA Model	5
Figure 4	Bilge Keel Gage Longitudinal Locations	6
Figure 5	Bilge Keel Cross Section	7
Figure 6	Strain Gage Wiring Diagram	8
Figure 7	Installed Wireway	9
Figure 8	Installed Gages at Location 4 (BK4)	9
Figure 9	Calibration Setup	12
Figure 10	Calibration Output for Location 6 (BK6)	12
Figure 11	PIV Measurement Plane Location	13
Figure 12	Installed PIV Camera	14
Figure 13	Installed Laser Probes	15
Figure 14	Camera, Laser, and PIV Calibration Target	16
Figure 15	Shunt Calibration Diagram	20
Figure 16	FEA Analysis of 100 lbf Point Load at Location 3 (BK3)	23
Figure 17	FEA Analysis of 0.83 psi Distributed Pressure Load	24
Figure 18	Steady State Lift Forces	31
Figure 19	Steady State Individual Gage Pressures	32
Figure 20	Total Force at 0.0kts	33
Figure 21	Individual Gage Pressures at 0.0kts	33
Figure 22	Total Force at 5.0kts	34
Figure 23	Individual Gage Pressures at 5.0kts	34
Figure 24	Frequency Separated Forces at 5.0kts	35
Figure 25	Total Force at 7.5kts	35
Figure 26	Individual Gage Pressures at 7.5kts	36
Figure 27	Frequency Separated Forces at 7.5kts	36
Figure 28	Total Force at 10.0kts	37
Figure 29	Individual Gage Pressures at 10.0kts	37
Figure 30	Frequency Separated Forces at 10.0kts	38

Figure 31	Total Force at 12.5kts	38
Figure 32	Individual Gage Pressures at 12.5kts	39
Figure 33	Frequency Separated Forces at 12.5kts	39
Figure 34	Total Force at 15.0kts	40
Figure 35	Individual Gage Pressures at 15.0kts	40
Figure 36	Frequency Separated Forces at 15.0kts	41
Figure 37	Pressure Contours in Negative Roll at 5.0kts	42
Figure 38	Pressure Distribution Across Bilge Keel Span	43
Figure 39	PIV Images at 5.0kts (t = 0,1,2,3,4,5s)	44
Figure 40	PIV Images at 5.0kts (t = 6,7,8,9,10,11s)	45
Figure 41	PIV Images at 10.0kts (t = 0,1,2,3,4,5s)	46
Figure 42	PIV Images at 10.0kts (t = 6,7,8,9,10,11s)	47

LIST OF TABLES

Table 1	Strain Gage Voltage Gain Values	21
Table 2	Pressure Gain Values	24
Table 3	Moment Gain Values	25

CHAPTER 1 INTRODUCTION

1.1 Background

A collaborative effort between the United States Department of Defense and the Italian Ministry of Defense has been underway for several years to develop a 6-degree of freedom (DOF) Reynolds Averaged Navier-Stokes (RANS) model for ship maneuvering. The goal of this effort is to improve the prediction of all 6-DOF motions of surface ships operating in a seaway with particular emphasis on roll motions.

To date there has been significant effort at David Taylor Model Basin (DTMB) addressing roll damping using computation and model testing methods. In particular, two recent papers present methods for estimating bilge keel damping force using data from a typical surface combatant model with instrumented bilge keels. Atsavapranee et al. (OMAE 2007) present a method for a vessel undergoing roll-decay and Grant et al. (OMAE 2007) expand upon this bilge keel force model and extend the method to include coupled roll and heave motions in beam wave fields.

1.2 Objectives

This experiment was performed at varying forward speeds in calm water to obtain a full scale data set for bilge keel forces and flow field measurement of a modern light combatant hull form. The port bilge keel had strain gages installed at multiple locations and the data analyzed to yield bending moments at each location. The strain gage output was correlated to pressure values by assuming a uniform pressure distribution across the bilge keel span. Since there are eight gage locations on the bilge keel, this yields pressure distribution along its length. This is then integrated to give the total bilge keel force acting on the vessel.

Particle image velocimetry (PIV) was used to record the flow field under the bilge keel near its aft end within a three foot by three foot cross section. Processing these images yield in-plane velocities. The full PIV data set can be used to validate computational models and give flow visualization, clearly showing vortex formation and shedding.

1.3 Nave Bettica

The Italian Naval Vessel *Bettica* (P-492) is a modern light combatant and the third vessel in the Commandante class. The vessel's overall length is 88.6m (291ft), length at the design waterline is 80.0m (262ft) it has a maximum beam of 12.2m (40ft), a full load displacement of 1520 metric tons (1496 long tons) and full load draft of 3.2m (10.5ft). The outboard profile is shown in Figure 1. The body plan and curves of form can be found in Appendix A.

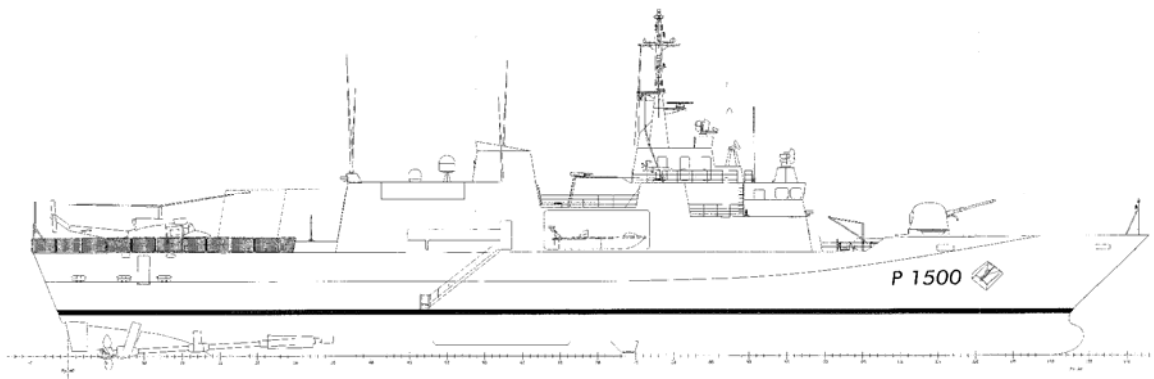


Figure 1 – Nave Bettica Outboard Profile

The vessel is equipped with both active and passive roll damping measures. The bilge keels begin approximately at midships and go aft 11m (36.1ft) with a span of 450mm (17.7in). The vessel also has active fins located 4.7m (15.4ft) forward of midships (measuring to the pivot point). These active fins are 2.0m (6.6ft) long with an average chord length of 1.9m (6.3ft). More information on the bilge keels can be found

in Chapter 2 and Appendix A, and more information on active fins can be found in Appendix A.

The ship has two small boats that are stowed on the port and starboard sides behind roll-up doors. During this experiment one of the boats was removed and the port side boat room was used as a control room. The data collection systems, lasers, and seed manifold were located here.

The *Nave Bettica* is based out of the naval arsenal in the city of Augusta, on the island of Sicily. Installation of the equipment was performed in Augusta during a dry dock period in August and September of 2007. The experiment commenced as soon as the ship had left dry dock and refueled. The testing was performed on the east side of Sicily at night.

CHAPTER 2 TEST SETUP

2.1 Strain Gages

The ship's port bilge keel was instrumented along its length with the goal of measuring the total force exerted on the hull.

2.1.1 Design

A finite element analysis using the expected pressure on the bilge keel was performed to look at bending strain. The model included all main structural elements from frame 42 to frame 75, and from the keel to the main deck. Figures 2 and 3 show the FEA model, with the main deck removed for clarity. Note that initially the plan called for the starboard side bilge keel to have the gages installed. Therefore the model was constructed for this side. Due to ship symmetry port to starboard, the model was left as the starboard side.

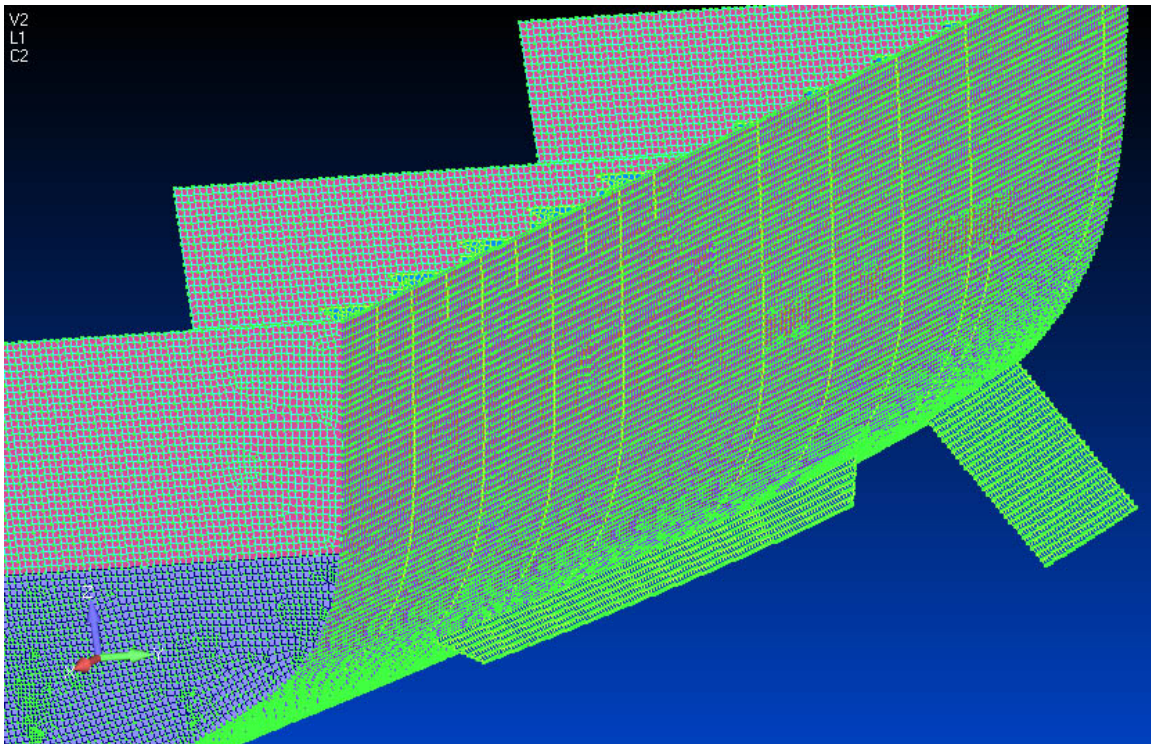


Figure 2 – Outboard View of the FEA Model

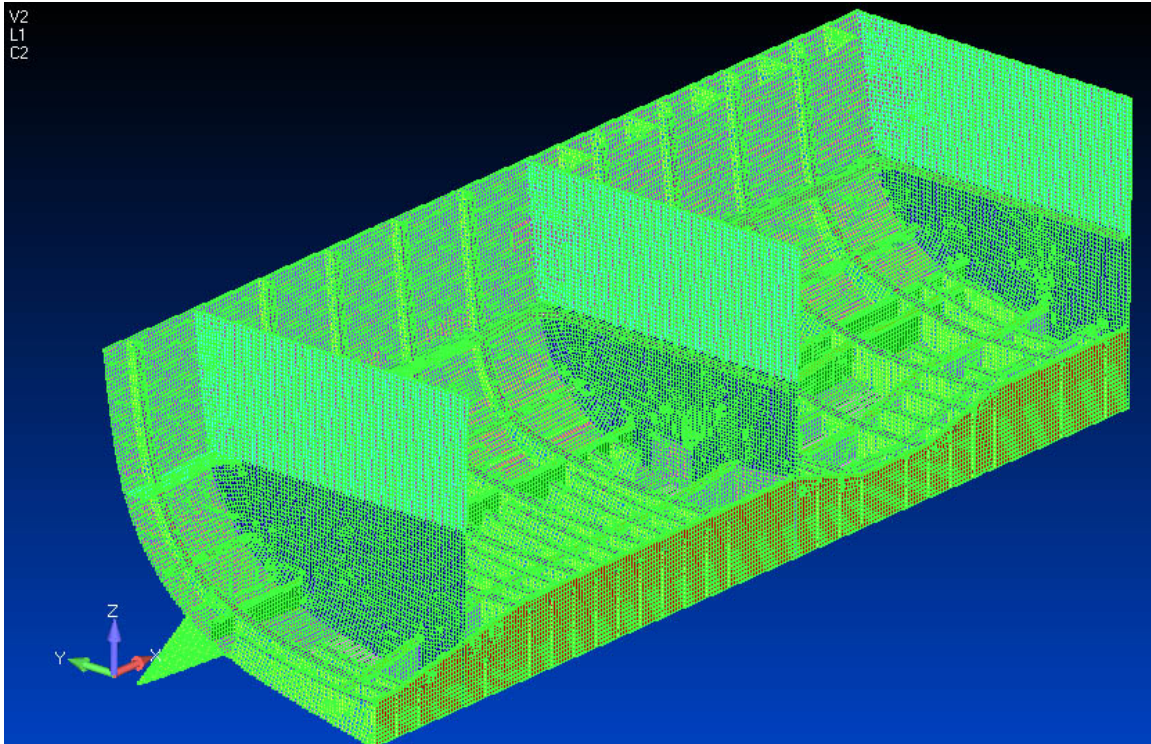


Figure 3 – Inboard View of the FEA Model

Strain was found to be maximum at locations where there was structure (frames, bulkheads, etc) behind the line of bilge keel attachment inside the vessel. From the FEA model it was anticipated that the strain seen at the gage locations would be very low, approximately 50 microstrain. The cables to the gage locations would be up to 75 feet long before reaching the amplifiers. The noise that might be seen from the vessel's machinery and electronics was a concern during the planning phase. Steps were taken to maximize the signal to noise ratio, including 50 Hz filtering, shielded cable, etc.

It is possible to measure force directly using two gages separated along the direction of measured strain by a known distance. The output of this method is the difference in bending strain between the two gages. This value gets smaller as the gages get closer. While not practical on this test, this method would typically be employed by using a full Wheatstone bridge with two gages on each side of the member. This

effectively doubles the output since one side is in compression while the other is in tension.

However, any force exerted on the member between the two gages will decrease the accuracy, meaning that the gages should be placed very close to each other relative to the overall span for pressure applications. In this case our signal would have been much too small to measure and most likely lost in the anticipated noise. For this reason it was decided to use a half bridge and only measure the bending moment at each location.

2.1.2 Locations

There were eight locations where framing intersected the bilge keel. These locations became the locations for the eight gages and are shown below in Figure 4. Note that the frame numbering starts at the aft end of the vessel. The gages were placed at one inch from the plate attaching the bilge keel to the hull. See Figure 5 for bilge keel cross section dimensions.

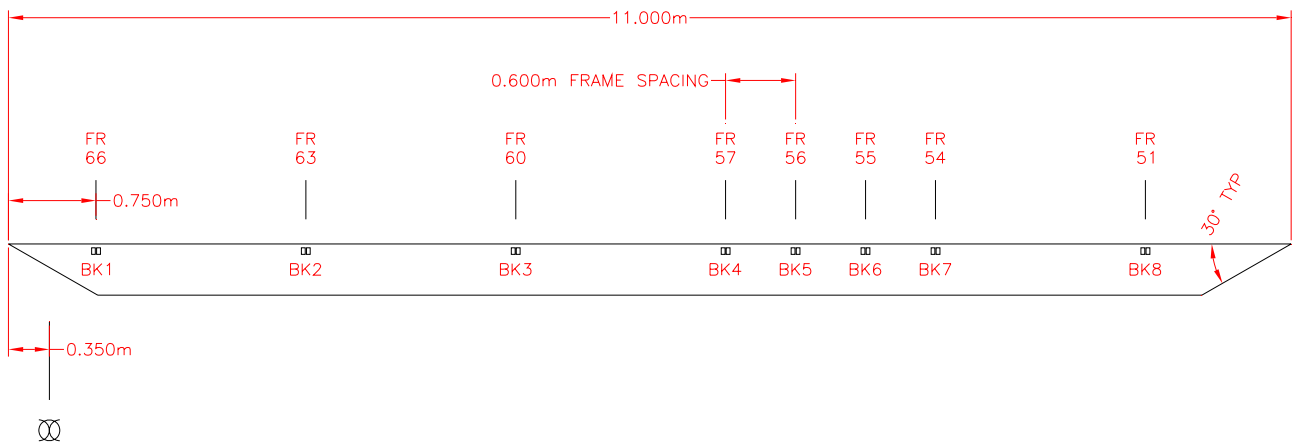


Figure 4 – Bilge Keel Gage Longitudinal Locations

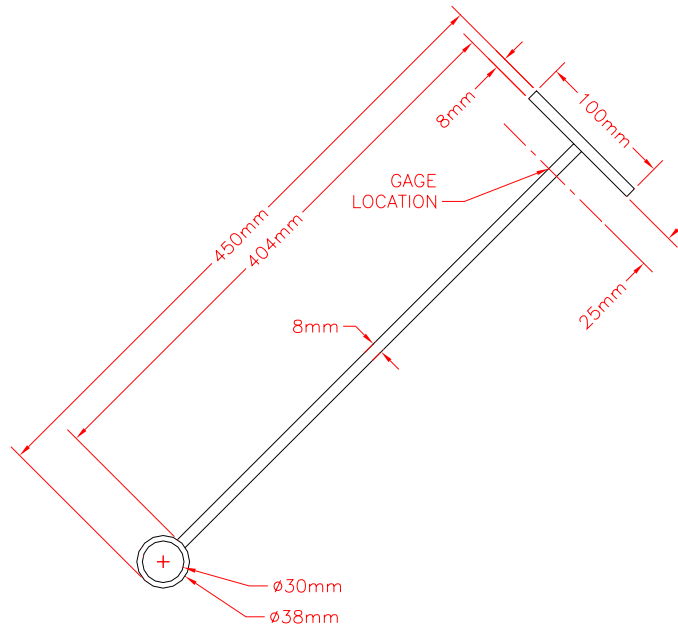


Figure 5 – Bilge Keel Cross Section

In addition to the eight locations on the bilge keel, a 9th gage set was installed on an unattached piece of 8mm steel. This was left in the cable tray above the bilge keel and was designed as a reference gage to correct for temperature changes during testing and any other strain offsets that might occur when the ship was re-floated after the drydocking period.

2.1.3 Installation, Hookup, and Waterproofing

The installed design used two linear 350 ohm gages (Vishay CEA-06-W-250A-350) to form a half bridge. Three wires were run to each gage, and precision dummy resistors were used prior to the amplifiers to complete the Wheatstone bridge (Figure 6). Vishay model 2310 amplifiers were used. Excitation voltage to each gage was measured and recorded coming from the amplifier, but was nominally 10 volts. The amplifier gain was set to 1000, and the amplifiers were adjusted to balance the bridge prior to testing.

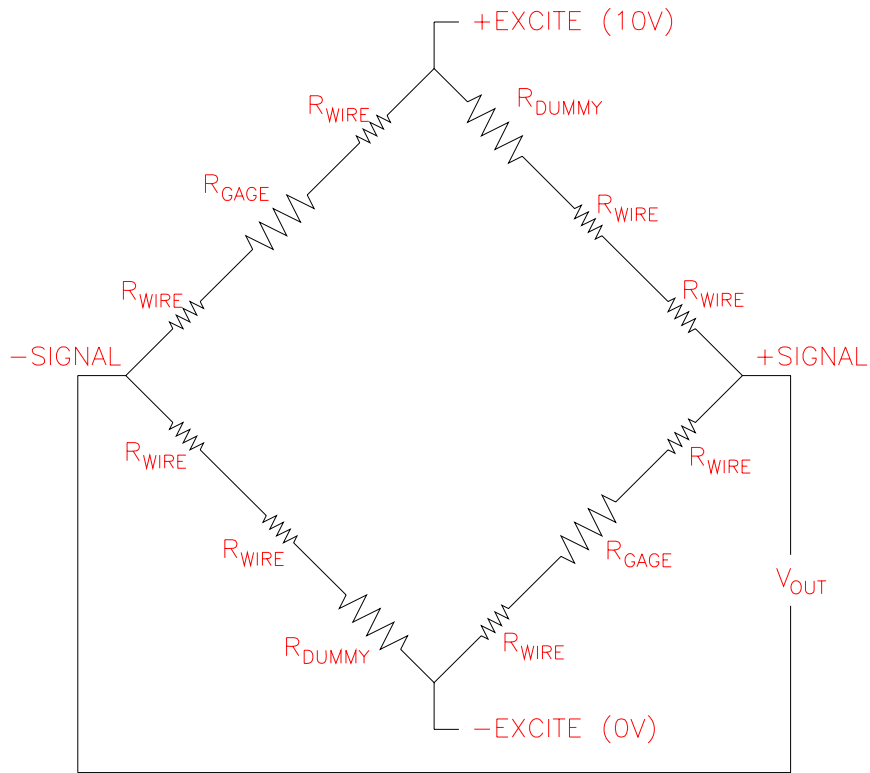


Figure 6 – Strain Gage Wiring Diagram

The cable used was water-blocked 22 AWG, with three shielded pair (Monroe Cable LS2SWAU-3). The cables were run from the amplifiers in the port boat room, down the hull, and aft along the top of the bilge keel in a removable stainless steel wireway installed for this test. Figure 7 shows the installed wireway as it turns aft along the top of the port bilge keel and Figure 8 shows the installed gages at location four (BK4).



Figure 7 – Installed Wireway

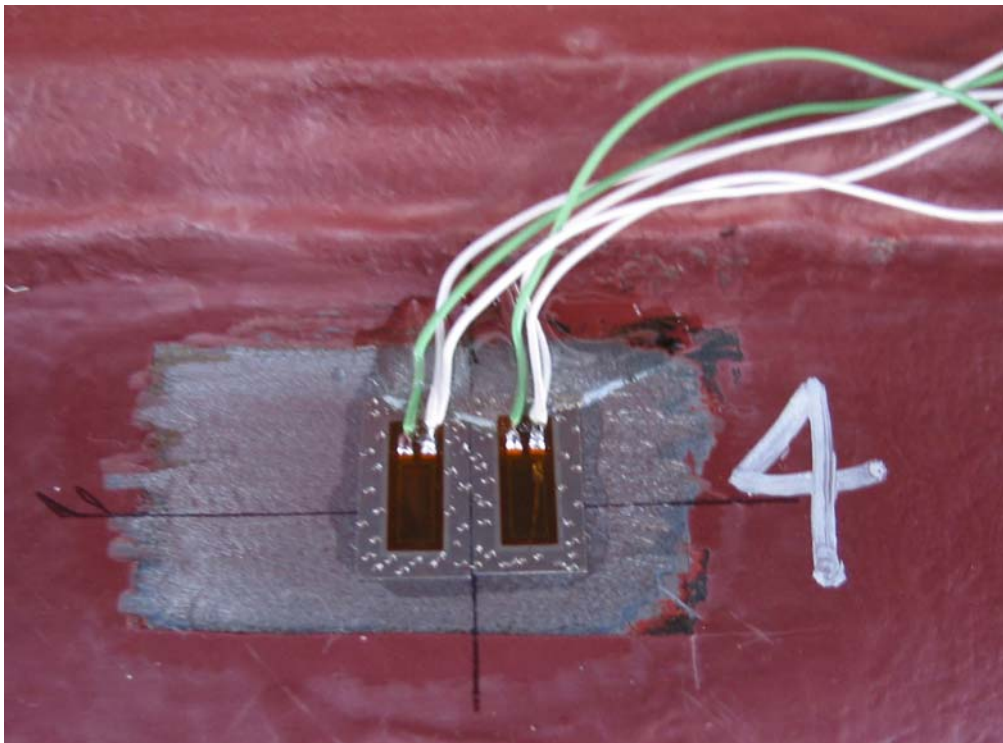


Figure 8 – Installed Gages at Location 4 (BK4)

2.1.4 Data Collection

With the exception of PIV images, all data channels were collected at 20 hertz using a PC in the control room running LabView. This computer recorded the bilge keel strain, ship motions, GPS speed and direction, and PIV synchronization signals. Nine channels from the bilge keel amplifiers and the synchronization signal were acquired using a National Instruments analogue to digital converter. A Garmin GPS unit was used for speed over ground and heading. Latitude and longitude were also recorded throughout the test. The PIV system was manually triggered for each run and a 5V synchronization pulse was recorded on an analogue channel.

All six components of ship motion were measured using a LN200 fiberoptic gyro. This gyro was aligned so that the positive X axis pointed forward, the positive Y axis pointed to starboard, and positive Z was pointed down. This means that positive roll was starboard down. The gyro was physically mounted on top of the bridge overhead at frame 68. The GPS antenna was also mounted at this location.

Ship speed through water, heading, water temperature, wind speed and direction were to be measured using the ship's instrumentation. They were noted for each run and manually recorded in the run log. Initial planning included the use of a new wave radar being installed on the ship at the same time. However, this radar was not operational by the beginning of testing and so significant wave height was estimated by the ship's crew from the bridge and recorded manually.

2.1.5 Calibration

There were two calibrations performed on the installed gages and acquisition system. The first was a shunt calibration. A shunt resistor of 846,000 ohms was applied

across each gage and the output voltage recorded. The resistance was sized to mimic 100 microstrain and therefore an output of approximately one volt at a gain of 1000. This calibration was recorded as Run 21.

The second calibration involved directly loading the bilge keel and recording the output. At each gage location, the bilge keel was loaded in both the up and down direction. Due to the geometry within the drydock, it was not possible to apply the load perfectly perpendicular to the bilge keel. Instead, the loads in the up direction were applied at 30 degrees from the ship's center plane and the loads in the down direction at 240 degrees from the center plane. The average angle of the bilge keel is 148 degrees, although it changes slightly along its length.

The load was applied using free weights hung from a line and re-directed through one pulley in the up direction and two pulleys when in the down direction. Due to friction and hysteresis in this system, a load cell was used to measure the actual applied force on the bilge keel at the point of application. Six empty compressed air tanks were used as weights. They were added and removed incrementally and a run recorded each time. Including the zero runs, this yielded 13 calibration points in each direction at each gage location. These were recorded as runs 40 to 251. Figure 9 shows the calibration setup and Figure 10 shows a sample of the calibration output.



Figure 9 – Calibration Setup
Load cell output shown on the left, weights on the right.

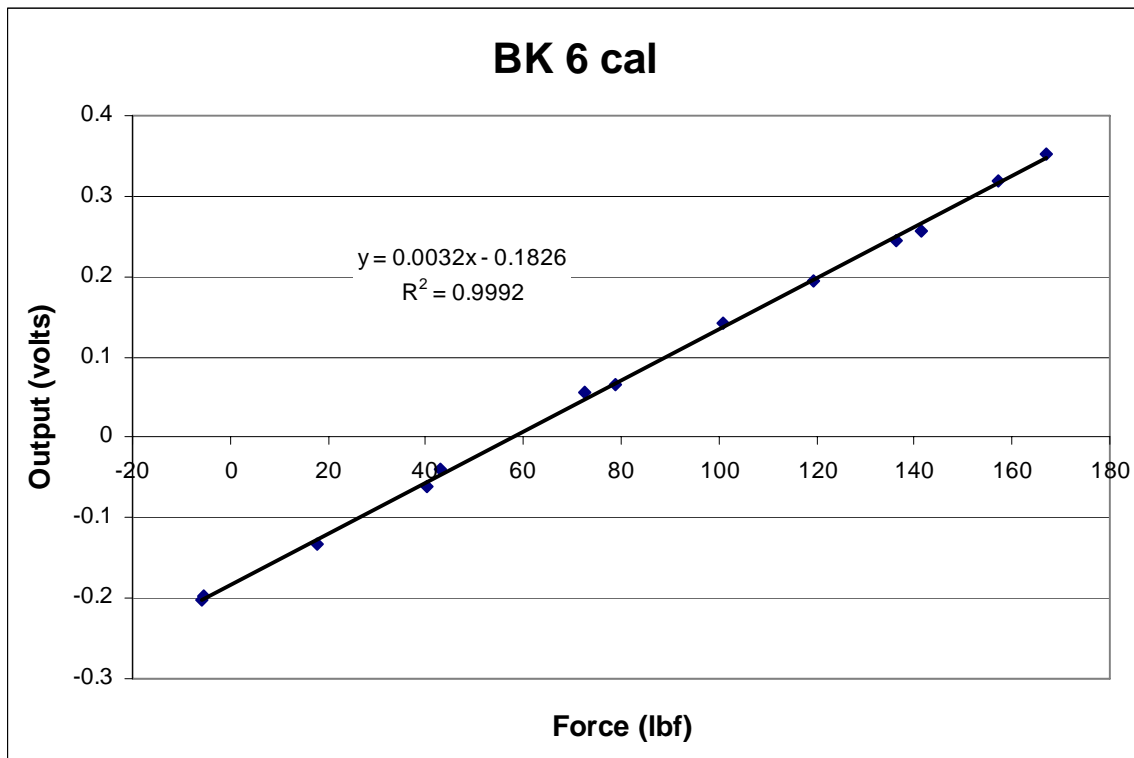


Figure 10 – Calibration Output for Location 6 (BK6)

2.2 Particle Image Velocimetry

PIV is a standard in global flow-field measurements. With one camera it is possible to get in-plane velocity measurements of a planar cross-section of flow. Using two cameras in a stereo configuration will yield all three velocity components and is referred to as stereo particle image velocimetry (SPIV). While initial plans called for using SPIV on this test, it was decided to simplify to one camera to help mitigate risk and reduce costs. The location of the PIV measurement plane is shown in Figure 11.

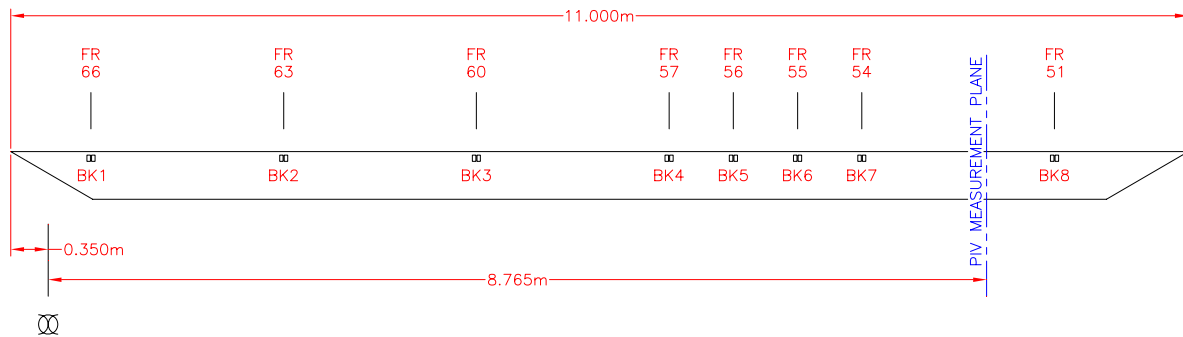


Figure 11 – PIV Measurement Plane Location

The PIV technique uses seed particles in the fluid as tracers. These particles are ideally very small (micron-sized) and neutrally buoyant. A laser sheet from a high-powered laser is used to illuminate these particles within a thin section of the flow field with two consecutive pulses separated by a very small Δt . The Δt was varied according to ship speed and recorded in the run log. A high speed camera is used to record this image pair. Then a statistical cross-correlation is performed between square subsets of the two images, essentially tracking the movement of the tracer particles and yielding the velocity vectors.

2.2.1 PIV Camera

The camera (Redlake ES 4.0, 2048 x 2048 pixels) was used in dual exposure mode at a frame rate of 6 fps. The camera was mounted in a custom waterproof enclosure with a 30m (100ft) umbilical that used the same cable tray as the strain gauges. The camera was mounted approximately two feet off the hull directly aft of the target area on a stainless steel v-strut. The camera had full adjustment in roll and slight adjustment in yaw and pitch. The camera was focused remotely during the calibration procedure. Figure 12 shows the installed camera.



Figure 12 – Installed PIV Camera

2.2.2 Laser Probes

Two flash lamp, pumped dye lasers (modified Cynosure V-Star, 585 nm, 1 J/pulse maximum) were used to form the light sheet in 10 microsecond pulses at 6 hertz. The laser was coupled into optical fibers and formed into sheets using beam-forming optics in submersible housings. Both lasers were used in tandem to illuminate the maximum

possible target area. The laser optic housings were mounted to a stainless steel v-strut similar to the camera and inboard of the target area. Figure 13 shows the installed laser probes.



Figure 13 – Installed Laser Probes

2.2.3 Seeding

In order to ensure that there would be enough reflective particulate in the water for good PIV images, a particle seeding system was installed. The chosen seeding material was diatomaceous earth. While not completely neutrally buoyant, it was found to be effective in preliminary tests for this kind of application. This was mixed into slurry and pumped to a three inch venturi-type mixing nozzle, where it was further diluted with seawater.

The main source of water came from two hydrants on the ship's fire main. The final seed mixture was then sent through a manifold to be dispersed from four seed pipes running down the side of the hull. The seed pipes were staggered so that they would form four zones running from the water line to the keel. The manifold used pneumatically controlled three-way valves to direct the seed mixture to the correct zones to get optimal seed placement downstream at the target area.

It was found that the seeding system was only required for the lower speed runs during testing. Higher speed runs achieved larger roll angles and the extra turbulence seemed to bring more of the natural surface particulate into the target area.

2.2.4 Calibration

A 36 inch by 36 inch precision calibration target was mounted to the hull and then aligned to the laser sheet. The dry dock was partially submerged in order to immerse the bilge keel and target area. A diver was used to make final adjustments to the camera angles and laser optics. The target was then illuminated and a series of calibration pictures were recorded. Once a satisfactory calibration was obtained, the dry dock was brought back to its normal position and the target was removed. A picture of the target and calibration setup can be seen in Figure 14.



Figure 14 – Camera, Laser, and PIV Calibration Target

CHAPTER 3 TEST PROCEDURE

3.1 Test Conditions

The testing was performed on the nights of October 4th, 5th, 8th, 9th, and 10th, 2007 (referred to as days one through five) in the Mediterranean, off the east coast of Sicily.

While the test was designed as a calm water test, completely calm water is very rare for a full scale trial. The first night of testing was used mainly to troubleshoot the system, and the conditions were very favorable with very light winds and ambient waves. The second night of testing also proved to be very favorable, again with very light winds and ambient waves. There was storm during the weekend before testing recommenced on day three. Days three through five had moderate wind and more significant ambient waves than days one and two as the remnants of the storm lingered.

Ship speed through water was set by the crew to the specified value and measured by the vessel's equipment. Ship speed over ground and ship direction were recorded directly from the GPS antenna by the data collection system. Water temperature, wind speed and direction were manually entered in the run log from the vessel's equipment. The significant wave height was estimated by the ships' crew on days three, four, and five and manually recorded in the run log. The run log can be found in Appendix B.

The ship generally held to a course that provided either 0 or 180 degree angle of encounter with the ambient wave field as it traversed back and forth through during each night's testing. Wind speeds varied from 0 to maximum of 18 knots. Estimated significant wave heights varied from 0 to 25 centimeters (0-10in).

3.2 Zeroes

Throughout each night of testing zeroes were taken at least every six damping runs. The ship would come to a zero speed through water, and zeros would be collected by the acquisition system. Then a run would be recorded with the ship still at zero speed. The ship would then accelerate to the designated test speed. A steady-state run with the active fins in automatic mode would be taken before damping runs commenced.

3.3 PIV Seeding

When collecting PIV runs it was evaluated whether seed would be needed. The higher speed runs did not seem to need the seed, while the 5 and 7.5 knot runs did. Higher speed runs achieved larger roll angles and the extra turbulence seemed to bring more of the natural surface particulate into the target area. The seed slurry was kept mixed in the starboard boat room. Prior to the beginning the run, water to the three inch mixing nozzle was turned on by the ship's crew. Slurry was then pumped to the mixing nozzle for the duration of the run. The three way valves were initially adjusted for optimum seed placement and did not need to be actively adjusted during the roll cycle as originally planned.

3.4 Forced Oscillation

To excite the vessel in roll the ship's crew would manually actuate the active fins at the natural roll frequency of approximately 9-10 seconds. When it appeared the maximum roll angle had been achieved the fins would be released back to the zero position. The point of release in seconds was recorded for each run.

3.5 Data Collection

Data collection for each run was started when the forced oscillations started. When used, the PIV system was started after the data collection system and a synchronization trigger was recorded by the data collection computer. 2000 frames (167 seconds) of PIV data was taken for roll decay runs and 1000 frames (83 seconds) for steady state runs. 200 seconds of data was taken by the data collection system when the PIV system was being used, and 100 seconds when there was no PIV.

CHAPTER 4 ANALYSIS PROCEDURE

4.1 Gage Calibration Values

The shunt resistor calibration was performed for each gage as described in Chapter 2. Data was collected for four to five seconds for each of the 18 individual gages. The values for each gage were averaged and the standard deviation calculated. The absolute average values of the two gages at each location were averaged to give a single value for each of the 9 gage locations. These values give a voltage output for a known change in gage resistance.

Referring back to Figure 6, it can be seen that this 846,000 ohms of added resistance is placed across the gage and the resistance in the wires down and back. Therefore the resistance of the wire needs to be included and is calculated based on wire gauge and length. The 22 awg wire used has a resistance of 0.01614 ohms/ft. The change in gage resistance can be found by evaluating the simple resistor circuit shown below in Figure 15.

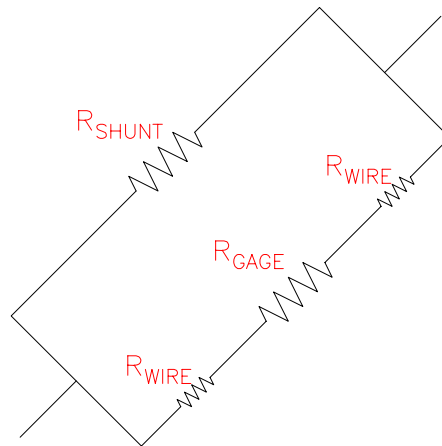


Figure 15 – Shunt Calibration Diagram

$$R_{TOTAL} = \left(\frac{1}{R_{GAGE} + 2R_{WIRE}} + \frac{1}{R_{SHUNT}} \right)^{-1}$$

$$\Delta R_{GAGE} = R_{GAGE} + 2R_{WIRE} - R_{TOTAL}$$

For this experiment the gage resistance was 350.0 ohms and the wire resistance was calculated for each gage location. With the change in resistance of the gage we can calculate the strain using the basic equation for gain factor:

$$\varepsilon = \frac{\Delta R / R}{G_f}$$

where ε is strain and G_f is the gage factor of the installed strain gage. The manufacturer listed the gage factor for this lot of gages at 2.06. While the shunt resistor was applied across a single gage, this installation used a half bridge with two gages measuring the same strain. Therefore the output signal for actual strain is doubled and our equation becomes:

$$\varepsilon = \frac{1}{2} \frac{\Delta R / R}{G_f}$$

Calibration values for obtaining strain per volt recorded are then calculated and can be seen tabulated below in Table 1.

Gage Location	Excitation volts	R_{WIRE} ohms	ΔR_{GAGE} ohms	Apparent Strain	Output volts	Gain strain/volt
BK1	9.94	0.7263	0.1459	1.012E-04	1.034	9.791E-05
BK2	9.96	0.82314	0.1461	1.013E-04	1.033	9.810E-05
BK3	9.97	0.91998	0.1463	1.014E-04	1.045	9.705E-05
BK4	9.98	1.01682	0.1464	1.015E-04	1.042	9.749E-05
BK5	9.96	1.0491	0.1465	1.016E-04	1.037	9.797E-05
BK6	9.97	1.08138	0.1465	1.016E-04	1.036	9.811E-05
BK7	9.97	1.11366	0.1466	1.017E-04	1.030	9.871E-05
BK8	9.97	1.2105	0.1467	1.018E-04	1.038	9.809E-05
BK9	9.96	0.91998	0.1463	1.014E-04	1.037	9.778E-05

Table 1 – Strain Gage Voltage Gain Values

4.2 FEA Model Verification

The FEA model examined during the experiment planning showed that strain would be maximum where the bilge keel was rigidly constrained, i.e. at the frame and bulkhead locations. For a given pressure, the strain between the supporting structure was much lower. Therefore it was decided to use the FEA model to correlate the measured strain values to a pressure load.

Rarely are large FEA models perfect, especially when looking at very localized strains such as seen at the gage locations. Ideally a calibration would have been performed on the bilge keel using a known distributed load that was representative of the loads that would be seen during vessel rolling. Since this was not feasible while in dry dock, point load calibrations were performed as described in Chapter 2.

The first thing was to check the model against the measured strain values from the point load calibrations. The point load calibrations yielded volt per load values and the shunt calibrations yielded the strain at each gage. The corresponding strain at 100 lbf was then calculated at each location for the up and down directions.

The 100 lbf point loads were applied to the FEA model and the strain at each gage location tabulated. Figure 16 shows the FEA results from one of these load cases. The point calibrations in the down direction were closer to perpendicular to the bilge keel and therefore these were the values used for comparison to the calibration. The FEA model over-predicted the strain, as is typical of coarse-mesh models. This is most likely explained by the lack of detail where the gages are and differences between the ideal model and the actual gage installation aboard the vessel. However, it is still reasonable to

assume that the relative strain distribution along the bilge keel would be would be accurate.

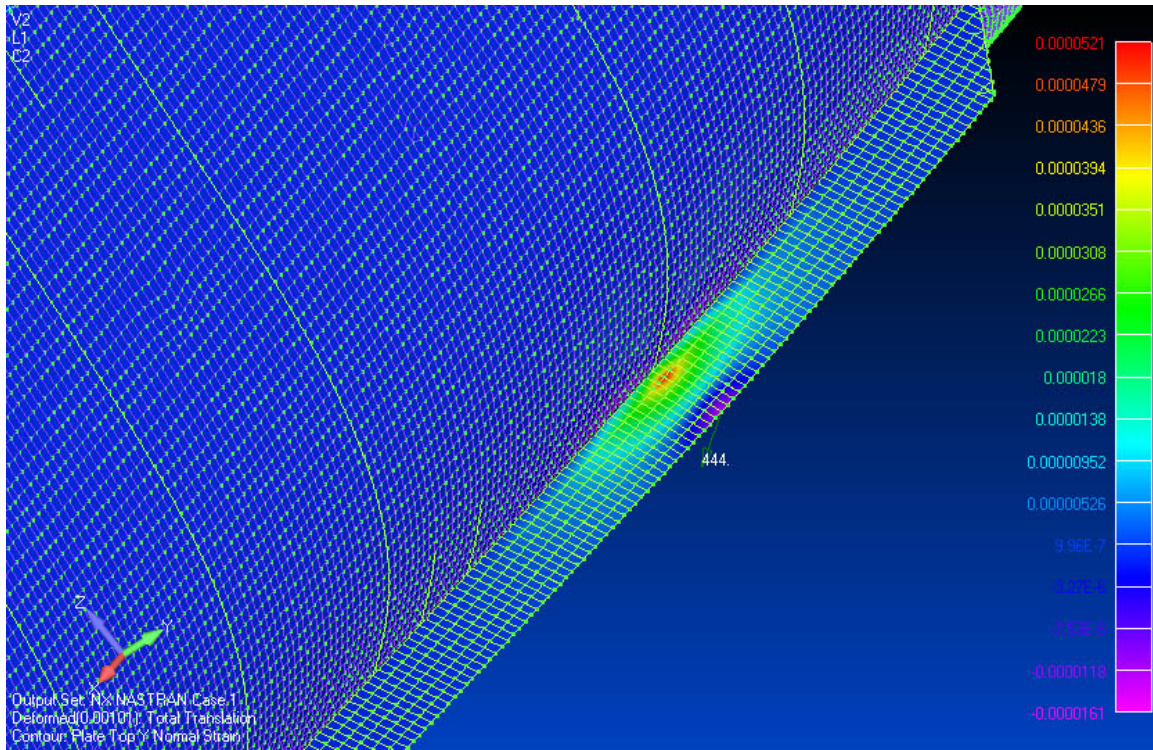


Figure 16 – FEA Analysis of 100 lbf Point Load at Location 3 (BK3)

4.3 Bilge Keel Force

Using this assumption the FEA model was loaded with a uniform pressure until the strain values were approximately 100 microstrain (0.83 psi). The FEA results are shown in Figure 17. Reducing these strain values by the differences in the point calibration for each gage location allows us to calculate a pressure gain, or applied pressure per strain at a gage. The results can be seen below in Table 2.

Gage Location	Calibration 100lbf Strain	FEA 100lbf Strain	Difference	FEA 0.83psi Strain	Actual 0.83psi Strain	Pressure Gain psi/Strain
BK1	4.422E-05	8.054E-05	82%	6.517E-05	3.578E-05	2.320E+04
BK2	3.155E-05	5.160E-05	64%	1.056E-04	6.457E-05	1.285E+04
BK3	3.463E-05	5.214E-05	51%	1.092E-04	7.252E-05	1.145E+04
BK4	3.437E-05	5.056E-05	47%	1.006E-04	6.838E-05	1.214E+04
BK5	2.810E-05	4.838E-05	72%	9.237E-05	5.366E-05	1.547E+04
BK6	3.114E-05	4.837E-05	55%	9.183E-05	5.912E-05	1.404E+04
BK7	3.275E-05	5.054E-05	54%	9.882E-05	6.404E-05	1.296E+04
BK8	4.058E-05	5.999E-05	48%	9.544E-05	6.456E-05	1.286E+04

Table 2 – Pressure Gain Values

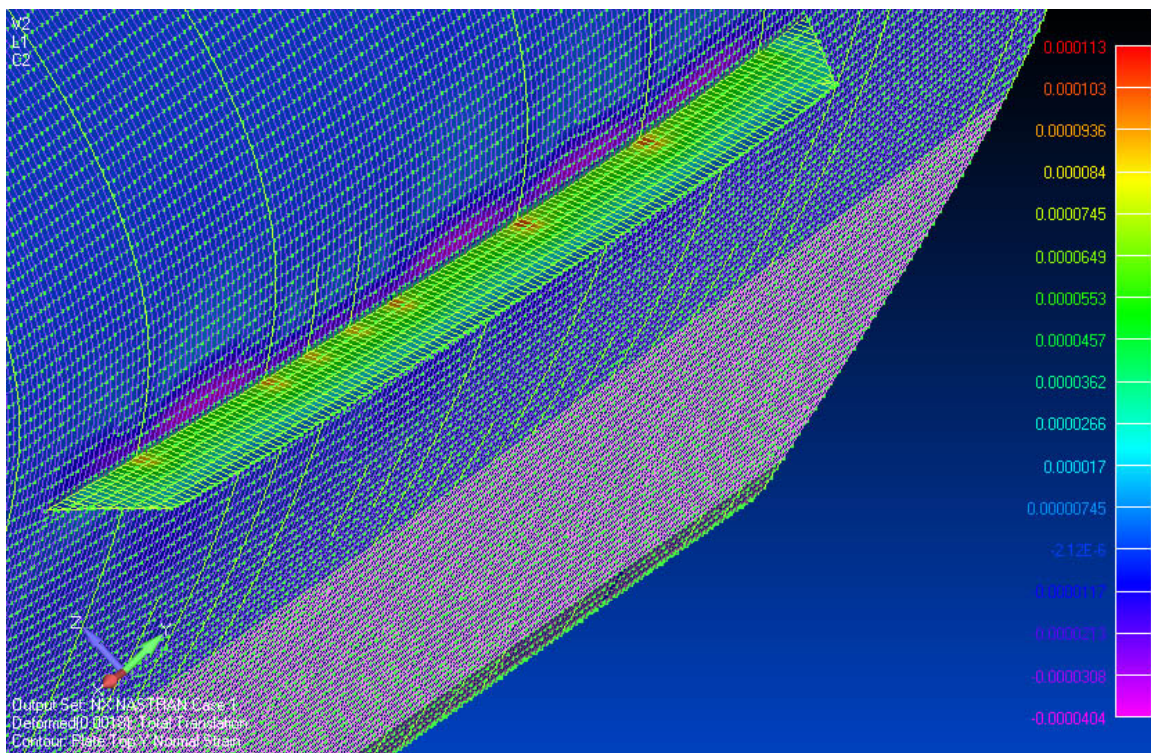


Figure 17 – FEA Analysis of 0.83psi Distributed Pressure Load

The total force on the bilge keel can be calculated by integrating the pressure distribution along its length. Trapezoidal integration was used. Since the first and last gages are not at the extreme ends of the bilge keel, the pressures at those gages will be assumed to extend to their respective extreme ends. Because there is unequal gage spacing the equation can be written as:

$$F_{TOTAL} = A_1 P_1 + \frac{A_2}{2} \left(P_1 + 2P_2 + 2P_3 + \frac{4}{3}P_4 + \frac{2}{3}P_5 + \frac{2}{3}P_6 + \frac{4}{3}P_7 + P_8 \right) + A_3 P_8$$

where P_1, P_2, \dots, P_8 are the pressures at each location and A_1 is the area forward of the first gage (251in^2), A_2 is the area between every three frames (1233in^2), and A_3 is the area aft of the last gage (594in^2).

Since the gages are actually measuring bending moment at their location, the center of pressure is required to calculate the actual force on the bilge keel if the pressure is not uniform. So far it has been assumed that the pressure was evenly distributed, therefore the center of pressure is located midway between the gage and the bilge keel tip. It is desirable to be able to have a set of gains that give the bending moment as function of recorded voltage. This allows refined center of pressure numbers to be used to calculate overall bilge keel force. These gains are shown below in Table 3.

Gage Location	Moment Gain <i>in-lb/volt</i>
BK1	3.055E+02
BK2	1.696E+02
BK3	1.494E+02
BK4	1.592E+02
BK5	2.038E+02
BK6	1.853E+02
BK7	1.721E+02
BK8	1.696E+02

Table 3 – Moment Gain Values

4.4 Data Processing

Strain gage and gyro data were recorded in comma delimited (.csv) files during the experiment. Processing of this data and most of the plotting was completed using MATLAB. Some of the MATLAB output was compiled in Excel for plotting. PIV

image pairs were processed using the software DaVis, and the resulting vector fields plotted using TecPlot 360.

To start, the run log and the zeros for each channel were examined to determine which runs would be useful. Unfortunately, the strain gage amplifiers were not powered on the first day of testing, leaving no strain gage data for those runs. Additionally, runs 271, 294, and 330-334 were excluded due to bad zeros. This left 63 roll damping runs and 34 steady state runs, including 6 zero-speed runs.

All the gages were zeroed frequently during each night's testing, including the reference gage, BK9. As a result, the values recorded from BK9 were relatively low. However the data from BK9 for each run was averaged and subtracted from the other eight channels as a steady state offset.

Steady state runs were compiled into a mean value for each run and combined into plots showing lift as a function of forward speed. In addition to the total force, the individual pressures at each gage location were plotted in order to show distribution along the length of the bilge keel.

Within the body of this thesis, one representative roll damping run at each forward speed is presented and examined in depth. Additionally, one zero run is looked at for roll damping comparison. Total force, roll angle, and tangential velocity at the bilge keel tip are presented for all roll damping runs in Appendix C.

Data was initially analyzed starting when the active fin was released back to zero by the helmsman. However, transients from the fin took one to three seconds to pass over the bilge keel. Therefore the starting point for each run became the release point plus three seconds. Thirty seconds, or approximately the time required for three roll

cycles, was analyzed. After this the rolling had decayed into a steady state condition. Total force and individual gage pressures were plotted for this sample period.

It became apparent that some of the components of the force on the bilge keel were not varying at the same frequency as the ship's roll. Therefore a Fourier analysis was performed and the first, second, and third harmonics were reconstructed and plotted.

The spectral content of the force signal can be computed by performing a Fourier analysis on the force signal. The Fourier Series representation of a signal $f(t)$ is given by the following equations, where $f(t)$ is the signal to be represented, t is time, a_i are the cosine term coefficients, b_i are the sin term coefficients, and T is the period over which the representation is performed. For this experiment, T was selected as the time between the n^{th} and $2 + n^{\text{th}}$ roll zero crossings for cycle number n . Since the ship had a steady list to port, the mean roll amplitude over the entire run was subtracted from the signal to ensure the zero crossings detected were referenced to a change from the steady state condition.

$$f_n(t) = \frac{a_0}{2} + \sum_{i=1}^n a_i \cos(n\omega t) + b_i \sin(n\omega t)$$

$$a_i = \frac{2}{T} \int_0^T f(t) \cos(k\omega t) dt$$

$$b_i = \frac{2}{T} \int_0^T f(t) \sin(k\omega t) dt$$

In order to calculate the Fourier coefficients a_i and b_i for the force signal, the Fast Fourier Transform (FFT) was used in MATLAB. The coefficients a_i are the real portion of the FFT coefficients, and the b_i coefficients are the imaginary portion. To determine the frequency content of the signals, the Power Spectral Density (PSD) of the signals was

calculated by multiplying the FFT coefficients with their complex conjugate. The equations for the FFT $X(f_i)$ of a signal $x(k)$ and a filtered signal $y(k)$ are given below. $Y(f_i)$ is the FFT of the filtered signal $y(k)$, f_i is frequency, and T is the uniform interval of the signal, and F is the inverse of T .

$$X(f_i) = \sum_{k=-\infty}^{\infty} x(k)e^{-j(2\pi f_i k T)}$$

$$Y(f_i) = H(f_i)X(f_i)$$

$$y(k) = \frac{1}{F} \int_{-F/2}^{F/2} Y(f_i)e^{-j(2\pi f_i k T)} df$$

4.5 PIV Center of Pressure

Up to this point, a uniform pressure distribution has been assumed for bilge keel across its span. The center of pressure for a uniform load is the middle of that span. The distance from this point to the gage center is the moment arm used to calculate force on the bilge keel from the actual measured moment as discussed in above. Improving upon this estimation of center of pressure would enable a similar improvement in the total force calculation for the bilge keel.

The processed PIV images yield the in-plane velocities within the target area. Knowing these u and v velocity components allows an approximate calculation of relative pressures due to the ship's rolling motions. To do this the Navier-Stokes equations are written with the pressure gradient term on the left side and the acceleration and viscous terms are left on the right hand side:

$$\nabla P = -\rho \left(\frac{\partial \vec{u}}{\partial t} + \vec{u} \cdot \nabla \vec{u} \right) + \mu (\nabla^2 \vec{u})$$

where P is pressure, ρ is the fluid density, the vector \mathbf{u} is velocity, and μ is the fluid viscosity. The pressure difference between any two points can be calculated as the line integral between them. The individual components of the equation are given below:

$$\bar{\mathbf{u}} = \langle u, v, w \rangle$$

$$\frac{\partial \bar{\mathbf{u}}}{\partial t} = \left\langle \frac{\partial u}{\partial t}, \frac{\partial v}{\partial t}, \frac{\partial w}{\partial t} \right\rangle$$

$$\nabla \bar{\mathbf{u}} = \left\langle \frac{\partial u}{\partial x}, \frac{\partial v}{\partial y}, \frac{\partial w}{\partial z} \right\rangle$$

$$\bar{\mathbf{u}} \cdot \nabla \bar{\mathbf{u}} = \left\langle u \frac{\partial u}{\partial x}, v \frac{\partial v}{\partial y}, w \frac{\partial w}{\partial z} \right\rangle$$

$$\nabla^2 \bar{\mathbf{u}} = \left\langle \frac{\partial^2 u}{\partial x^2}, \frac{\partial^2 v}{\partial y^2}, \frac{\partial^2 w}{\partial z^2} \right\rangle$$

$$\nabla P = -\rho \left\langle \frac{\partial u}{\partial t}, \frac{\partial v}{\partial t}, \frac{\partial w}{\partial t} \right\rangle - \rho \left\langle u \frac{\partial u}{\partial x}, v \frac{\partial v}{\partial y}, w \frac{\partial w}{\partial z} \right\rangle + \mu \left\langle \frac{\partial^2 u}{\partial x^2}, \frac{\partial^2 v}{\partial y^2}, \frac{\partial^2 w}{\partial z^2} \right\rangle$$

For the present case, the out-of-plane component of the velocity, w , is assumed to be constant in the z direction, and the unsteady acceleration terms are ignored. This gives us the pressure gradient described by the following equation:

$$\nabla P = -\rho \left\langle u \frac{\partial u}{\partial x}, v \frac{\partial v}{\partial y} \right\rangle + \mu \left\langle \frac{\partial^2 u}{\partial x^2}, \frac{\partial^2 v}{\partial y^2} \right\rangle$$

A complete calculation of the pressures would also need to include the ambient pressure, P_0 . While this is impossible to determine from what we have, some improved center of pressure estimate can still be performed. The desired value is a center of pressure, which will depend upon the relative and not absolute magnitudes of the pressures across the span, making P_0 unnecessary.

For each of the five forward speed roll damping cases examined, the velocity fields from the PIV images were processed in MATLAB. Line integrals were performed in both the x and y directions and averaged, with the pressures normalized to the pressure at the intersection of the hull and bilge keel to yield the pressures in the test plane. Pressure values along the line of the bilge keel were then extracted from the processed image and exported to Excel. Only images of the lower side of the bilge keel are available. Pressures along the bilge keel were taken from images with velocities in both directions of roll and compared. The resulting pressure profile for each side of the bilge keel was plotted across the span, with the pressures at the tip set to zero to give a common value at that point.

CHAPTER 5 RESULTS

5.1 Steady State Lifting Force

The average total lift force on the port bilge keel for each steady state run can be seen plotted in Figure 18. Note that ship motions were measured with positive Z in the down direction and positive roll was starboard down. Keeping consistent with this, the lift is plotted with positive being aligned with the Z axis and therefore negative lift is actually in the up direction.

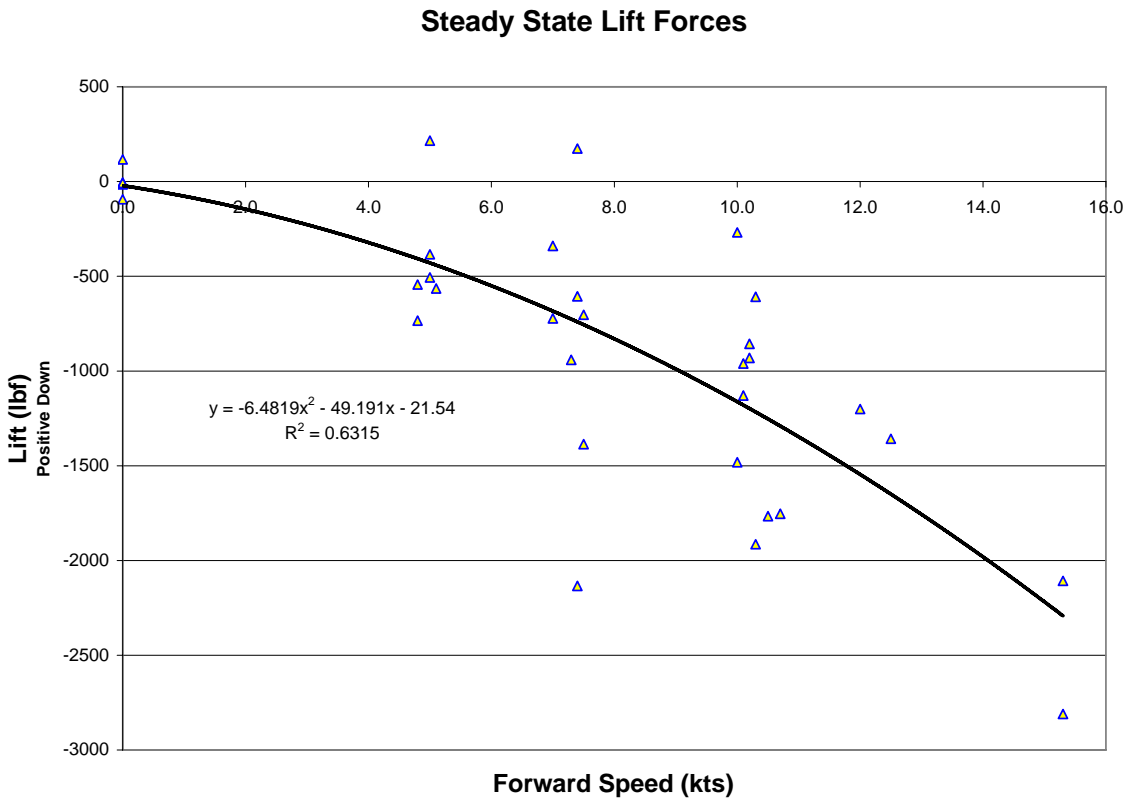


Figure 18 – Steady State Lift Forces

The scatter in the data seems to derive from the scatter in the zero values collected for each channel. However, when outlying zeros and corresponding runs were excluded, the quadratic fitted through the data changed very little, with only the r-squared value improving. With no better reason to exclude these runs, they have been left in the data set plotted.

To obtain an idea of the pressure or lift distribution along the length of the bilge keel, the individual pressures at each gage location were plotted and quadratics fit through each set of points. This can be found below in Figure 19. Note that most of the increase in lift due to forward speed happens at the leading edge. This is seen later in the roll damping data as well.

Individual Gage Pressures

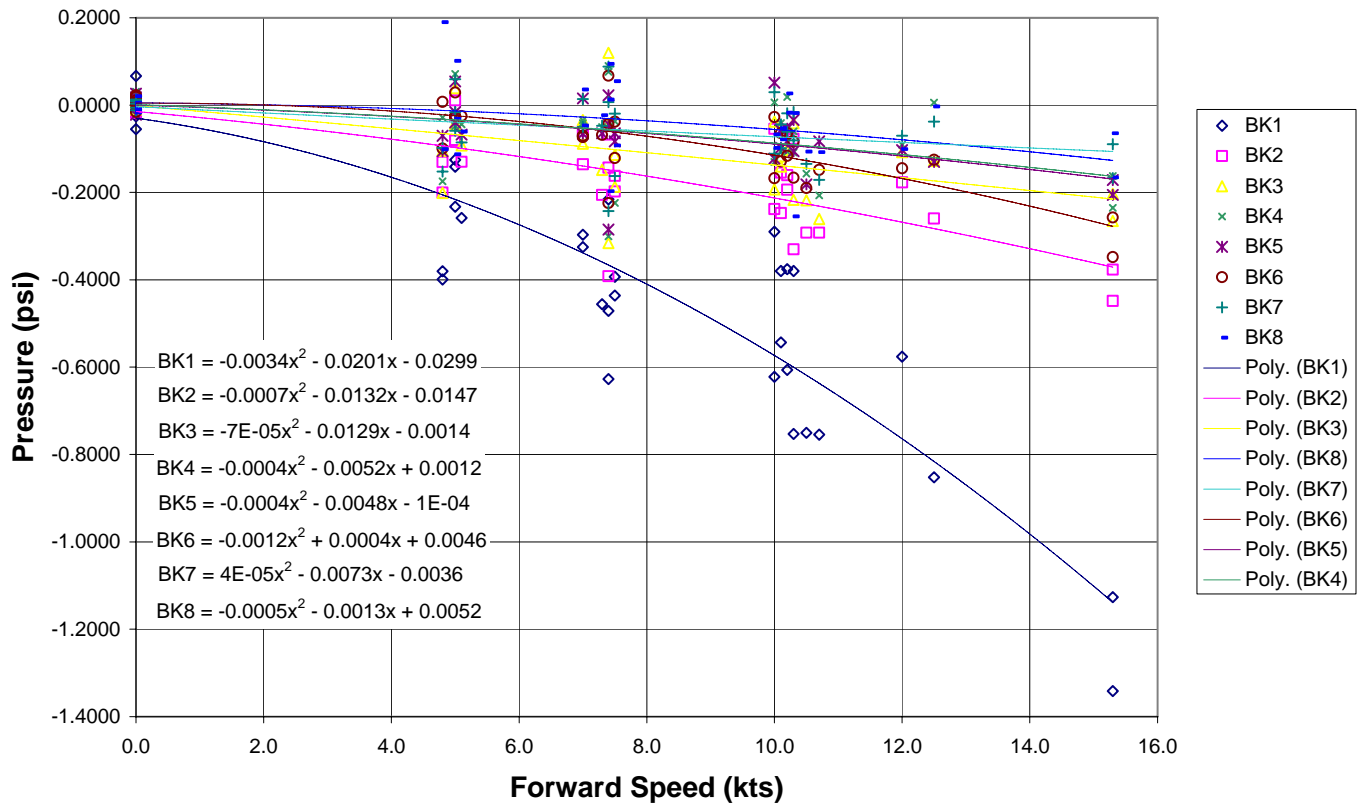


Figure 19 – Steady State Individual Gage Pressures

5.2 Roll Damping Results

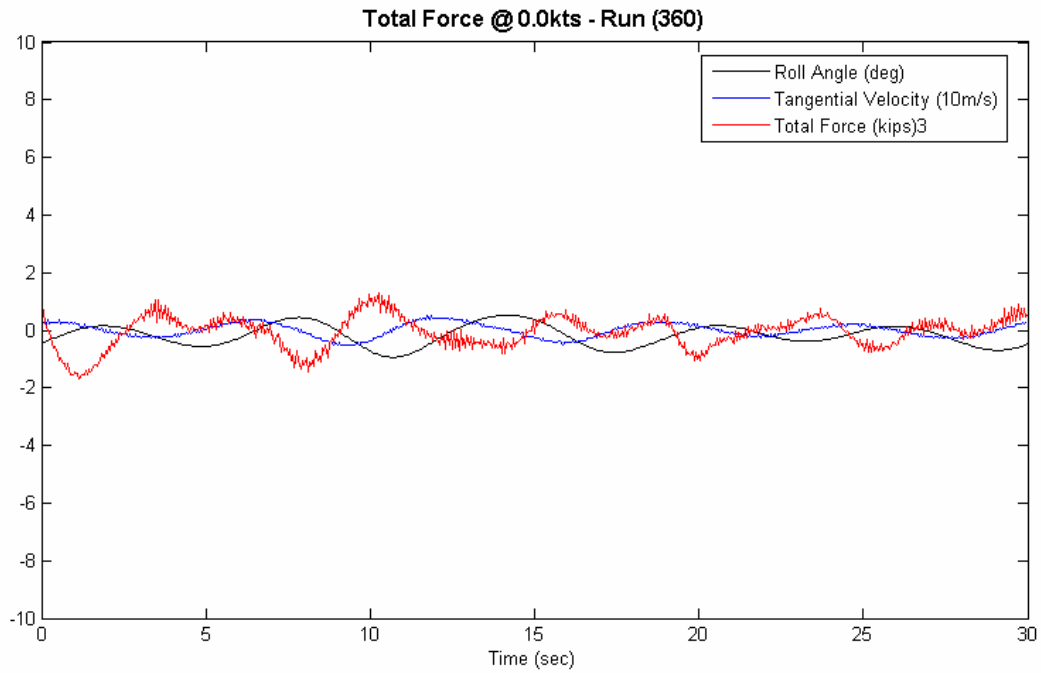


Figure 20 – Total Force at 0.0kts

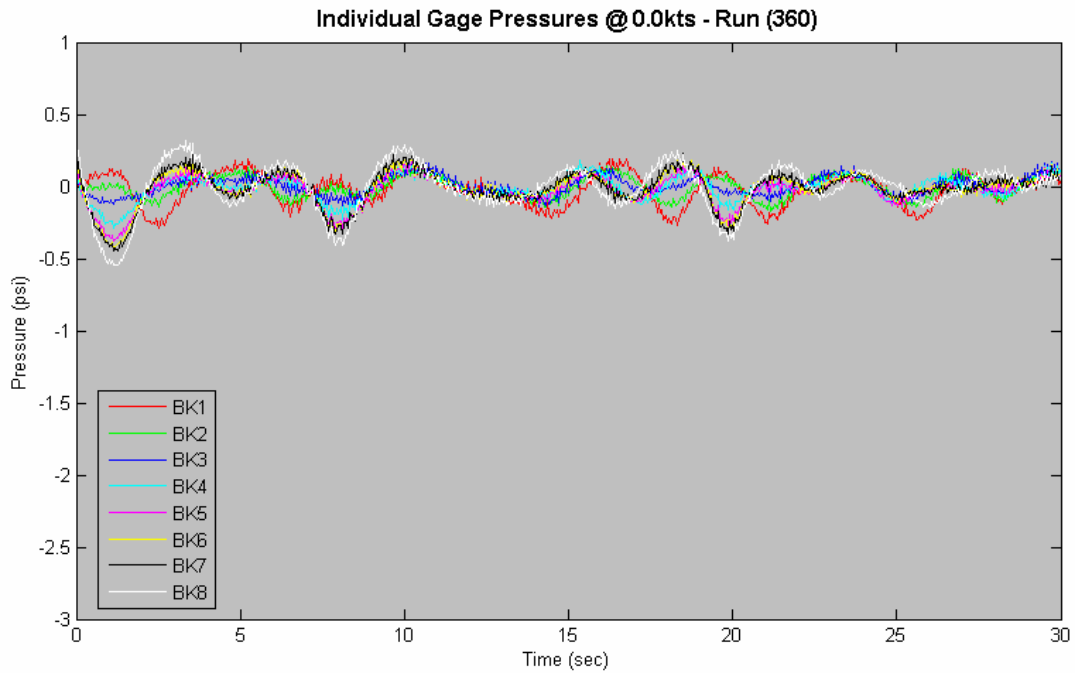


Figure 21 – Individual Gage Pressures at 0.0kts

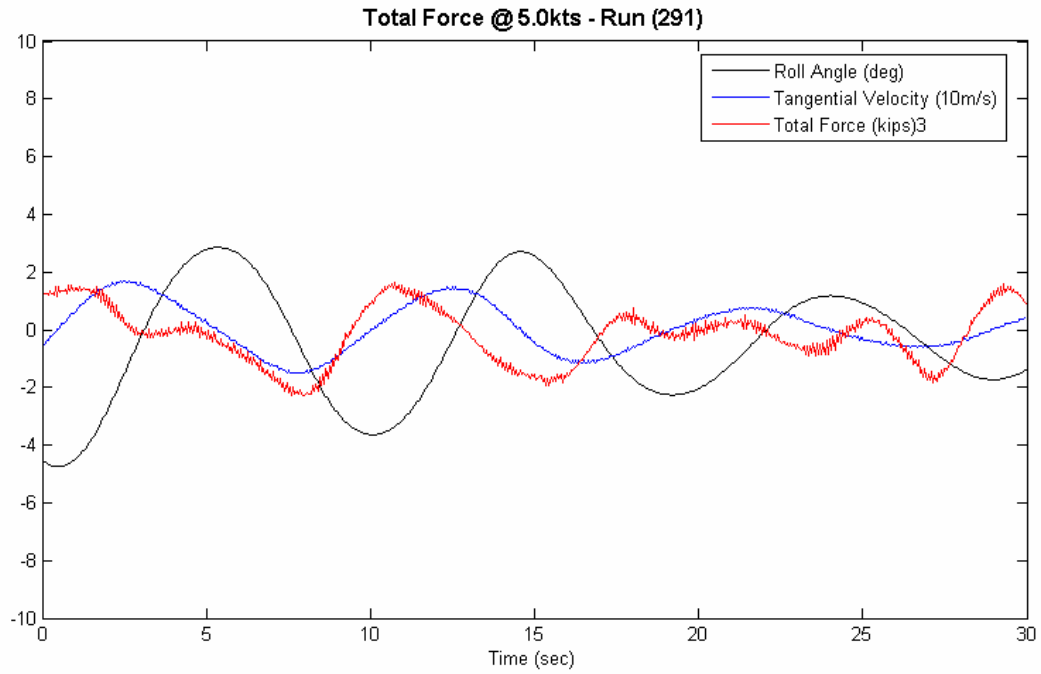


Figure 22 – Total Force at 5.0kts

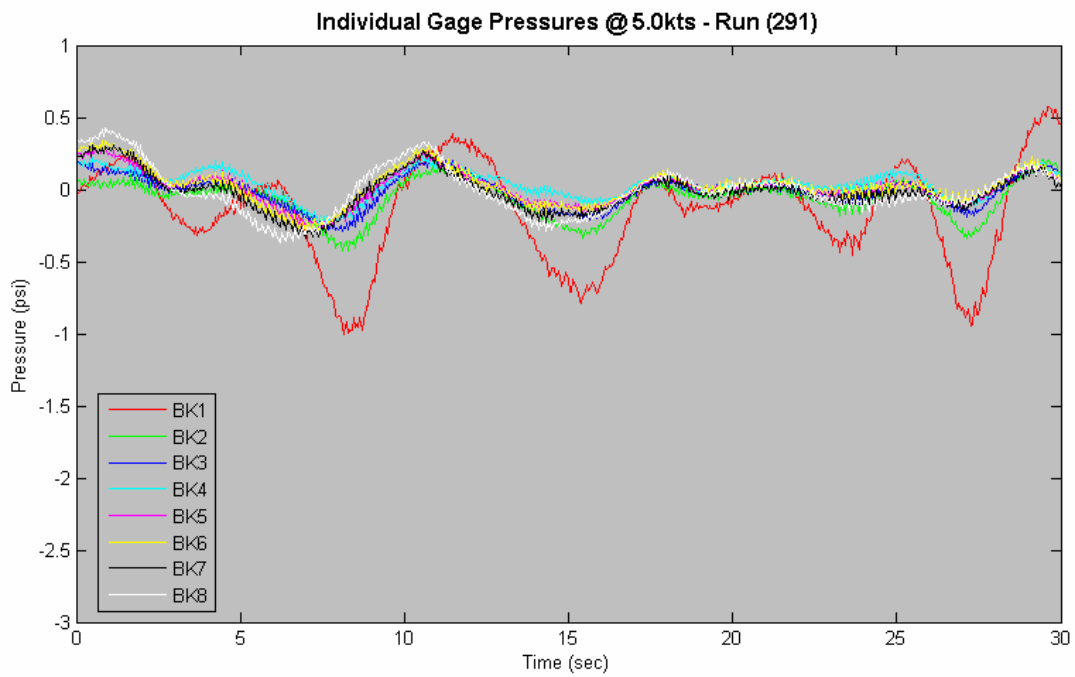


Figure 23 – Individual Gage Pressures at 5.0kts

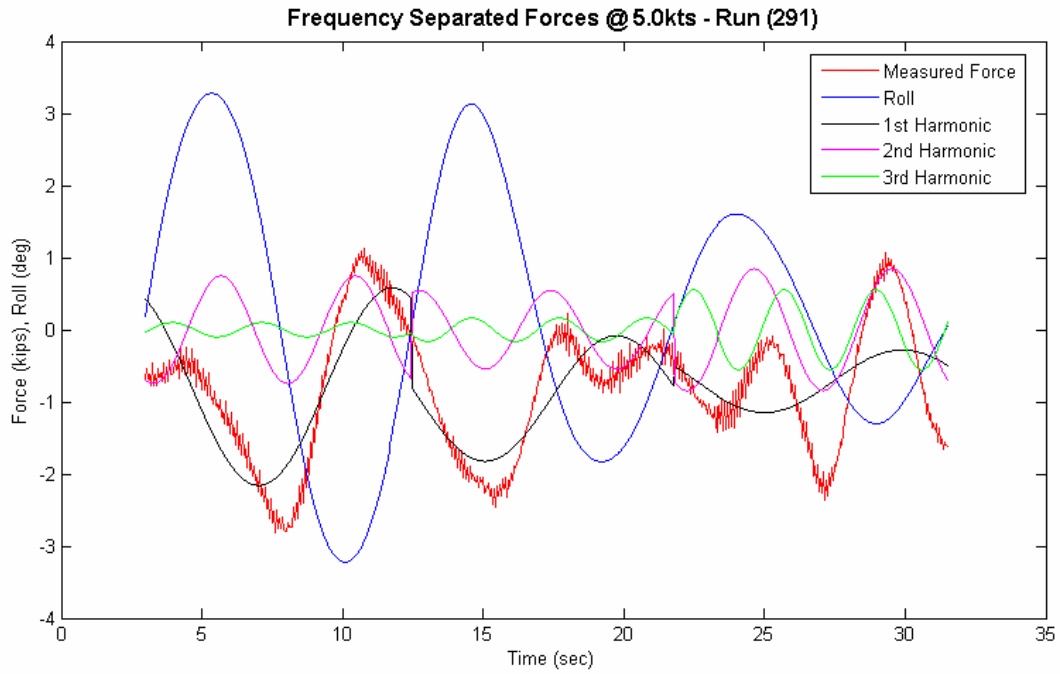


Figure 24 – Frequency Separated Forces at 5.0kts

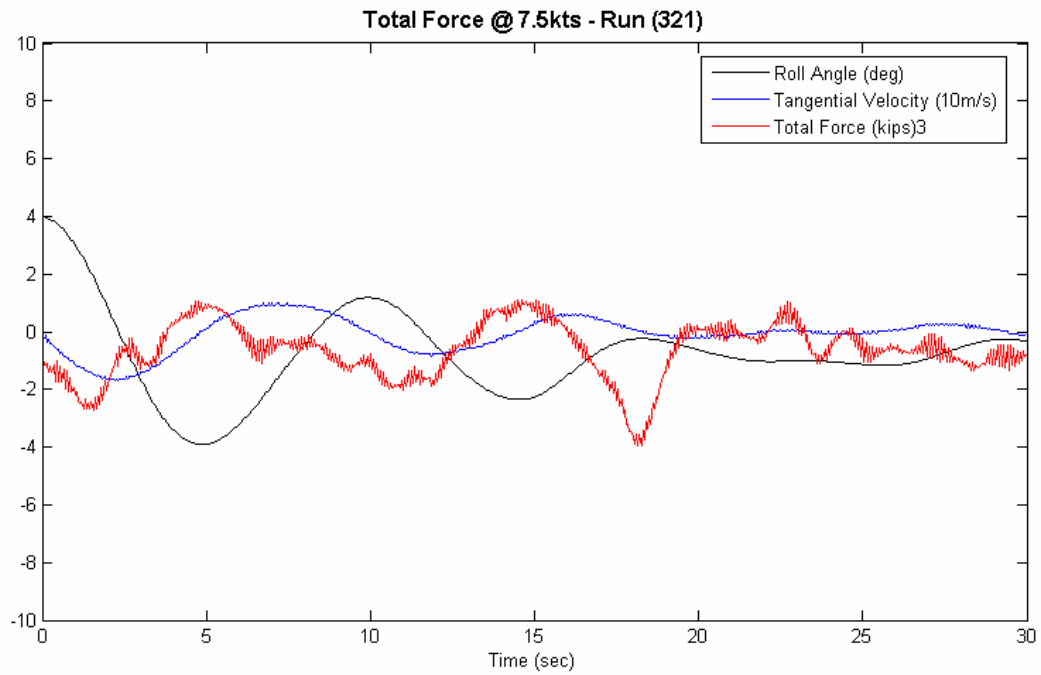


Figure 25 – Total Force at 7.5kts

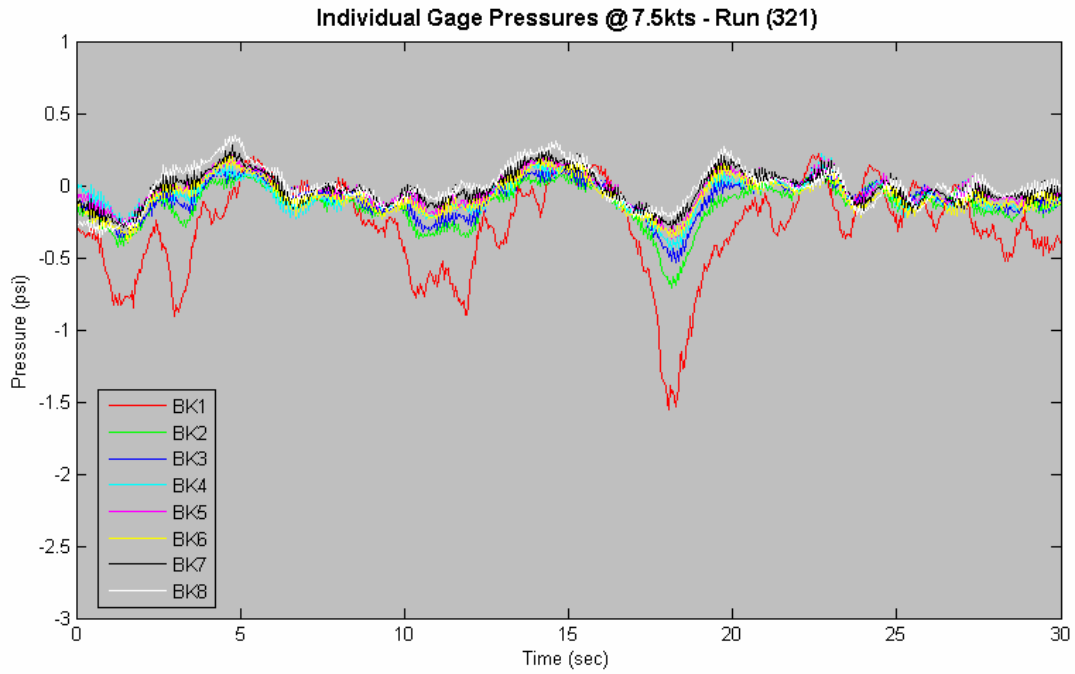


Figure 26 – Individual Gage Pressures at 7.5kts

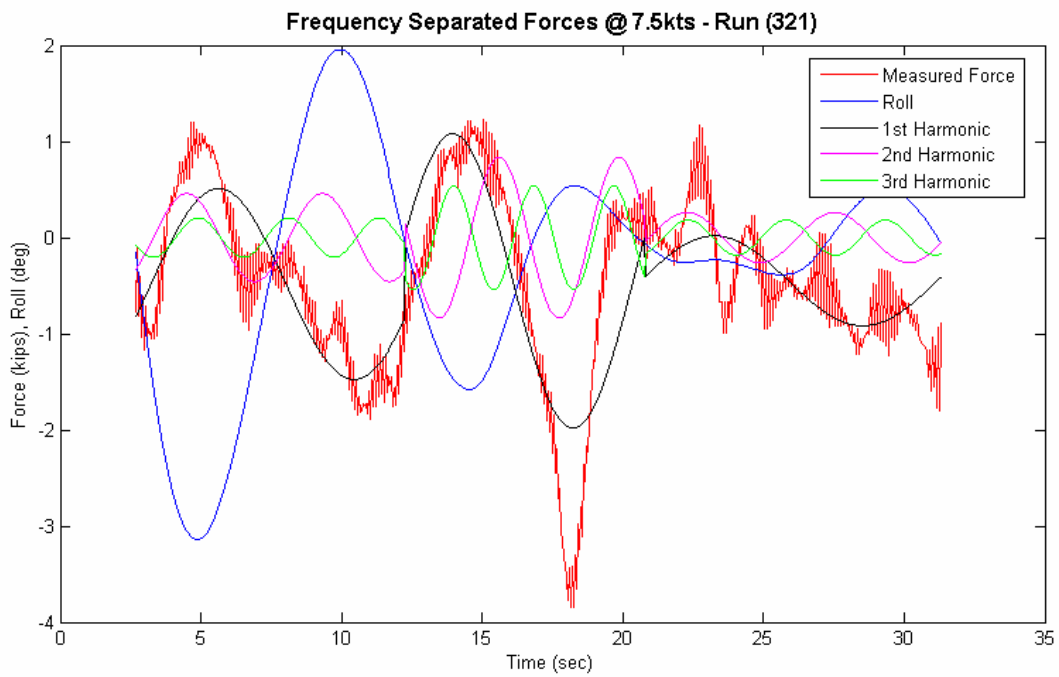


Figure 27 – Frequency Separated Forces at 7.5kts

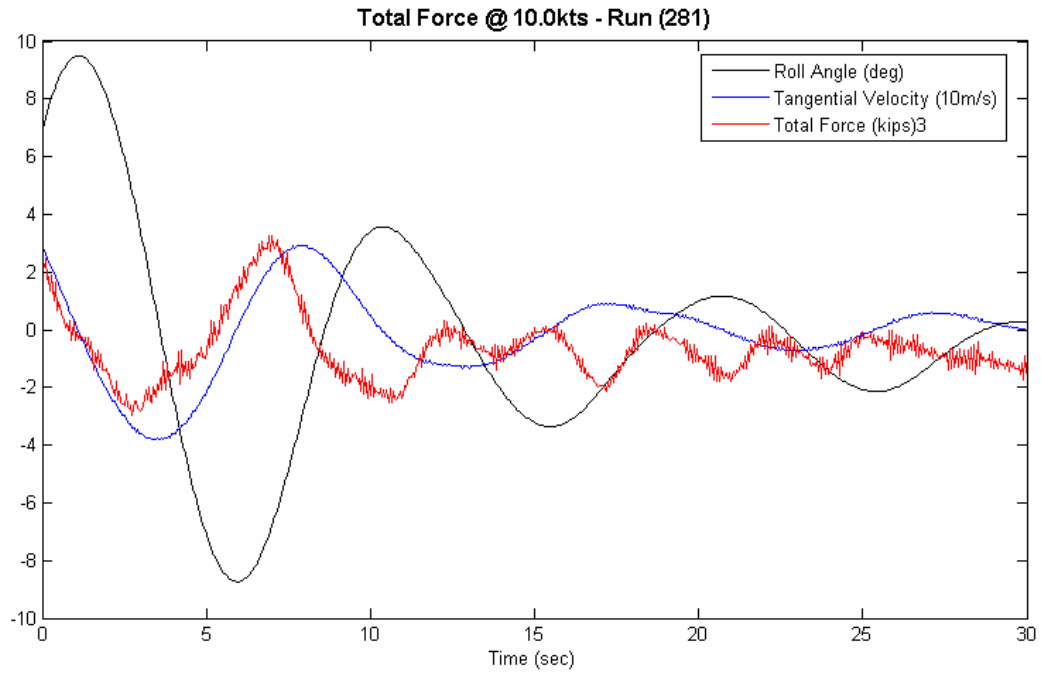


Figure 28 – Total Force at 10.0kts

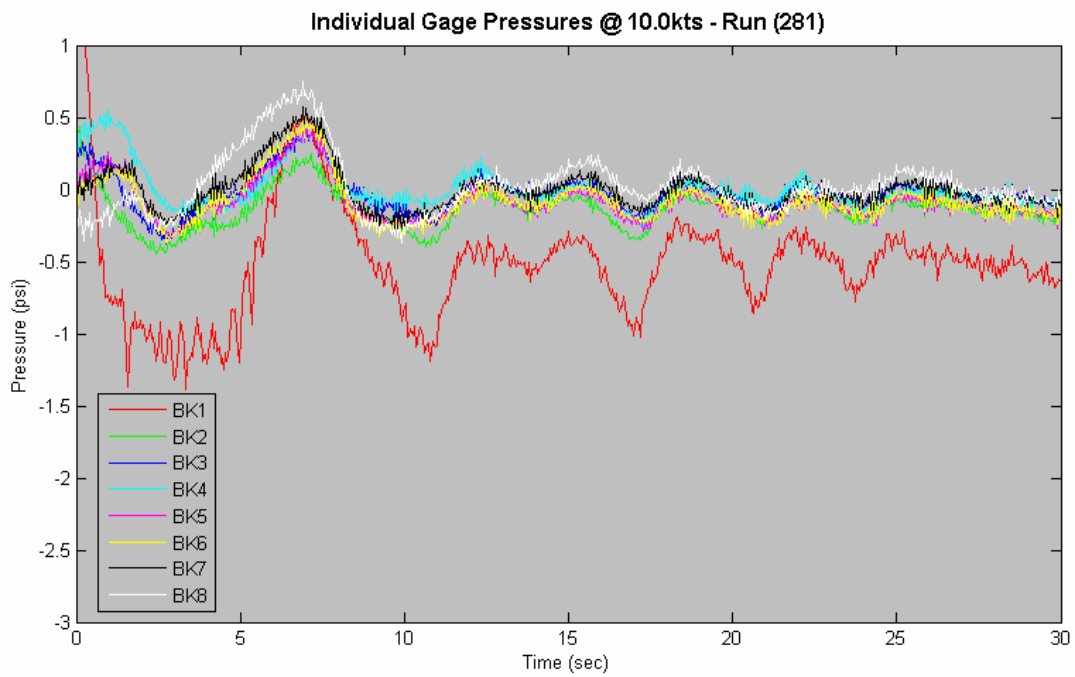


Figure 29 – Individual Gage Pressures at 10.0kts

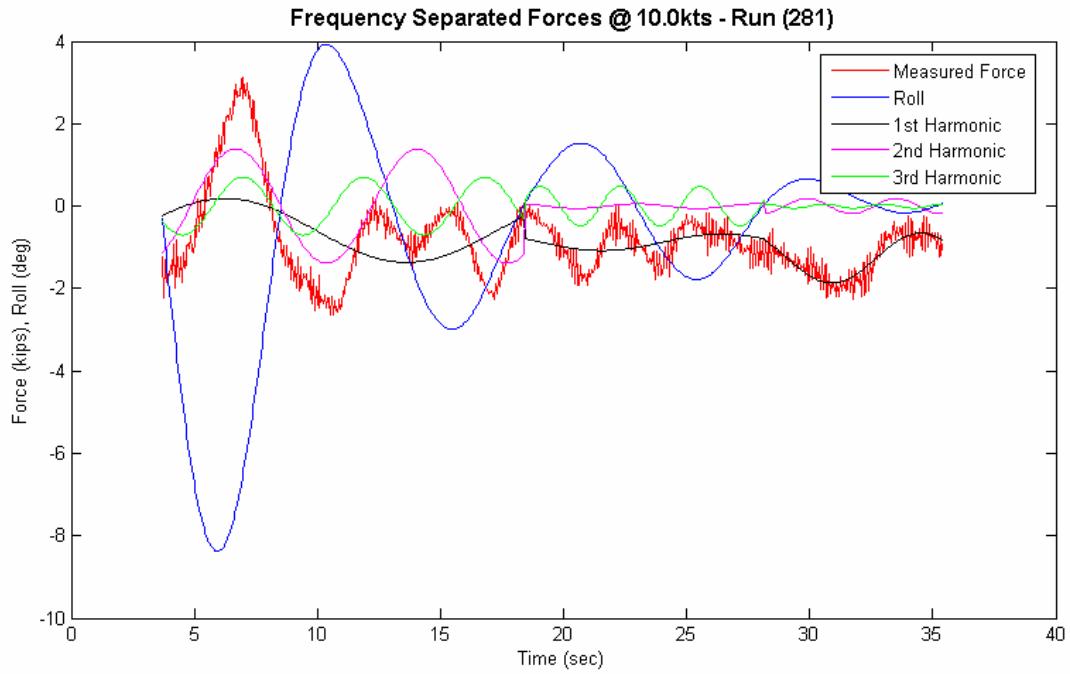


Figure 30 – Frequency Separated Forces at 10.0kts

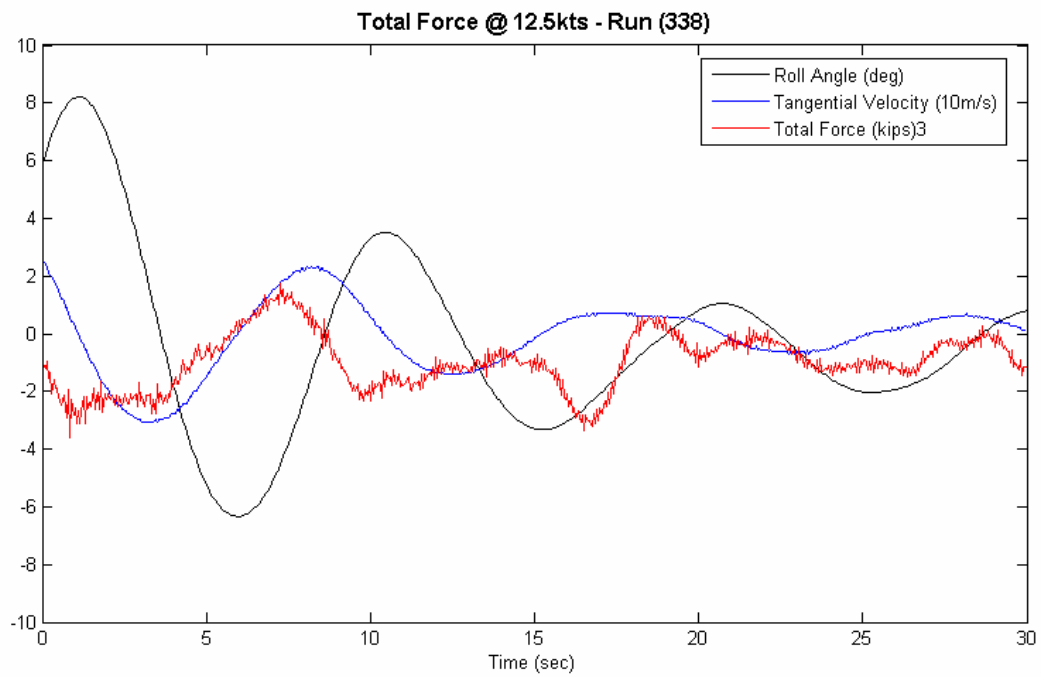


Figure 31 – Total Force at 12.5kts

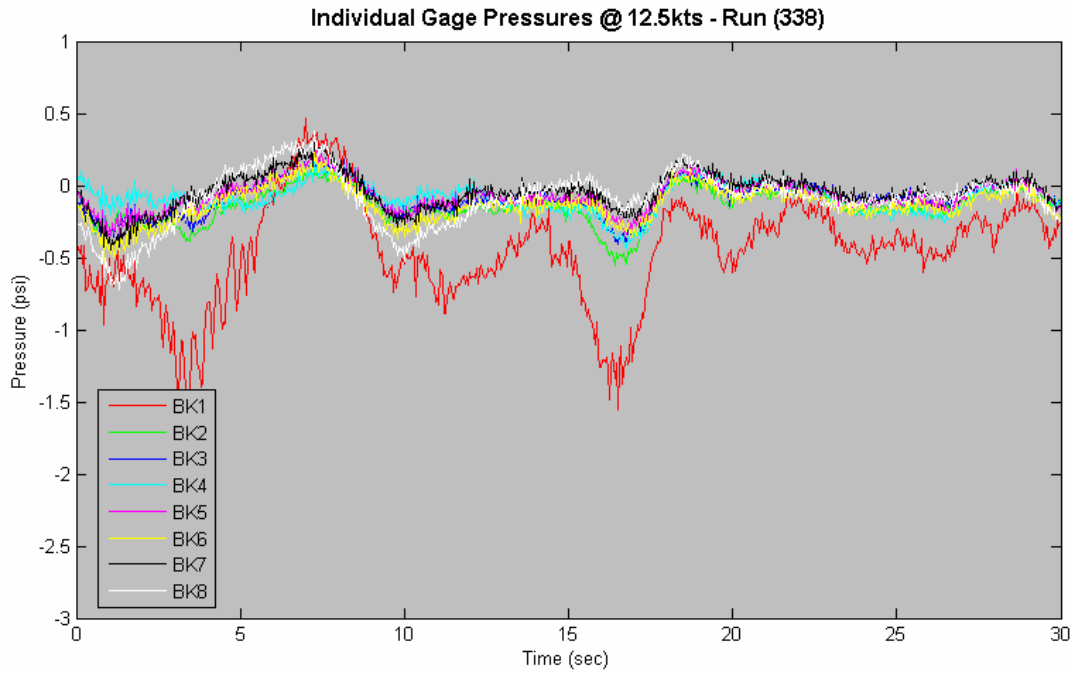


Figure 32 – Individual Gage Pressures at 12.5kts

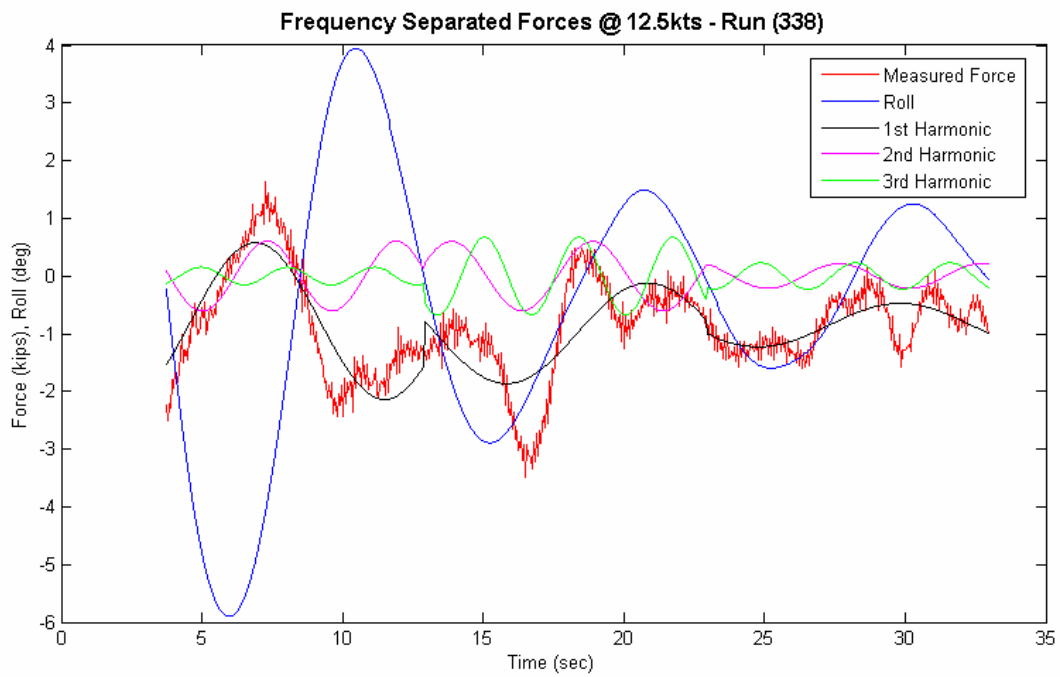


Figure 33 – Frequency Separated Forces at 12.5kts

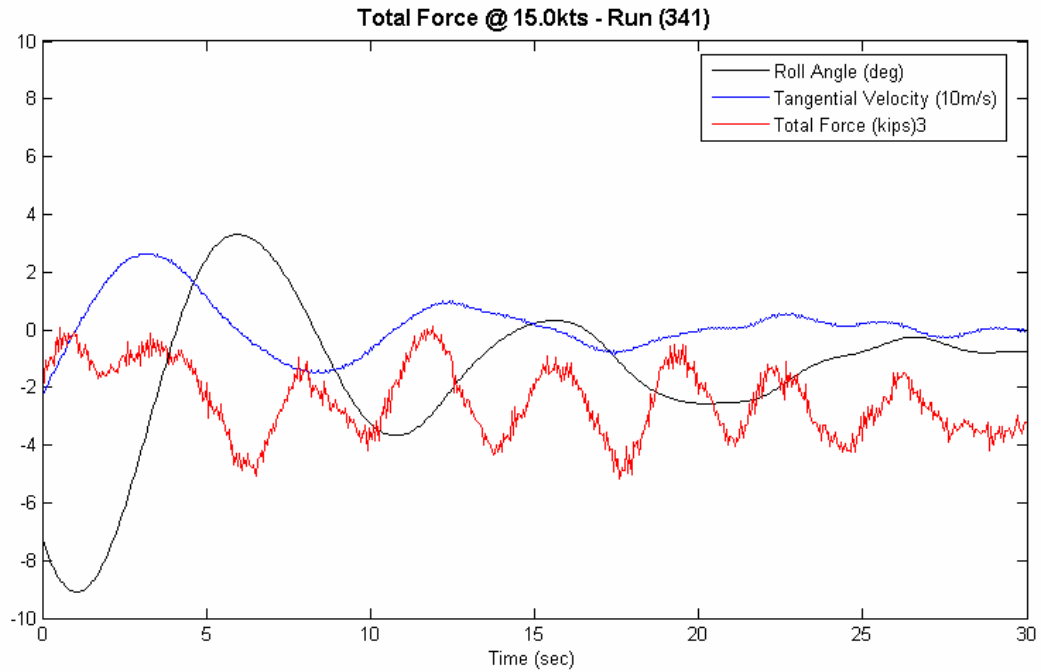


Figure 34 – Total Force at 15kts

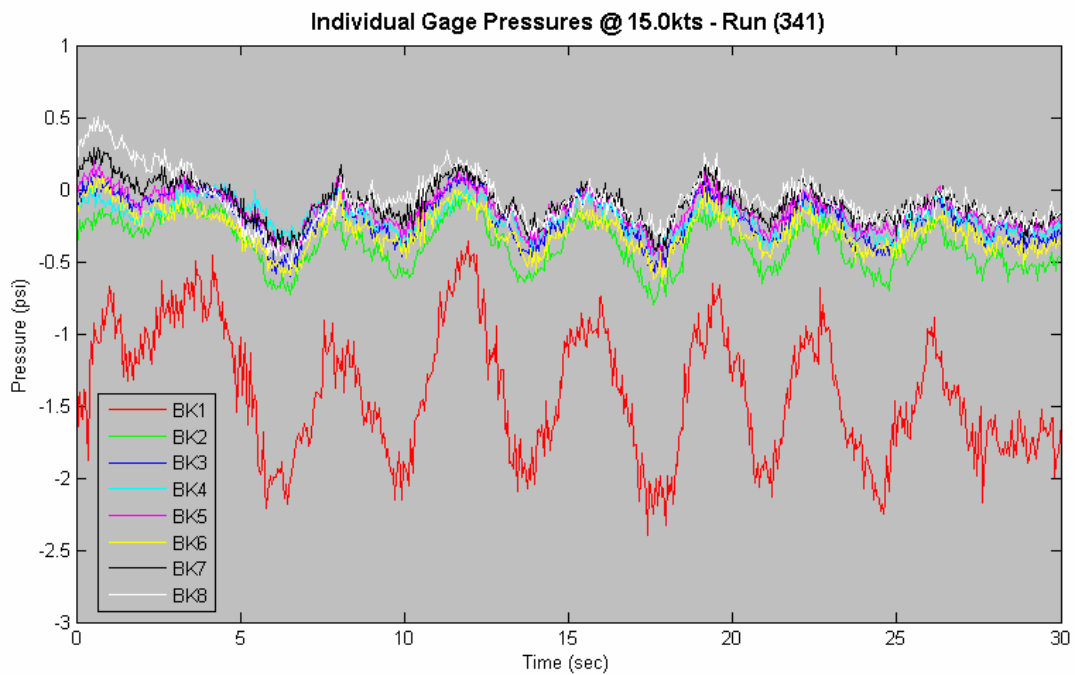


Figure 35 – Individual Gage Pressures at 15.0kts

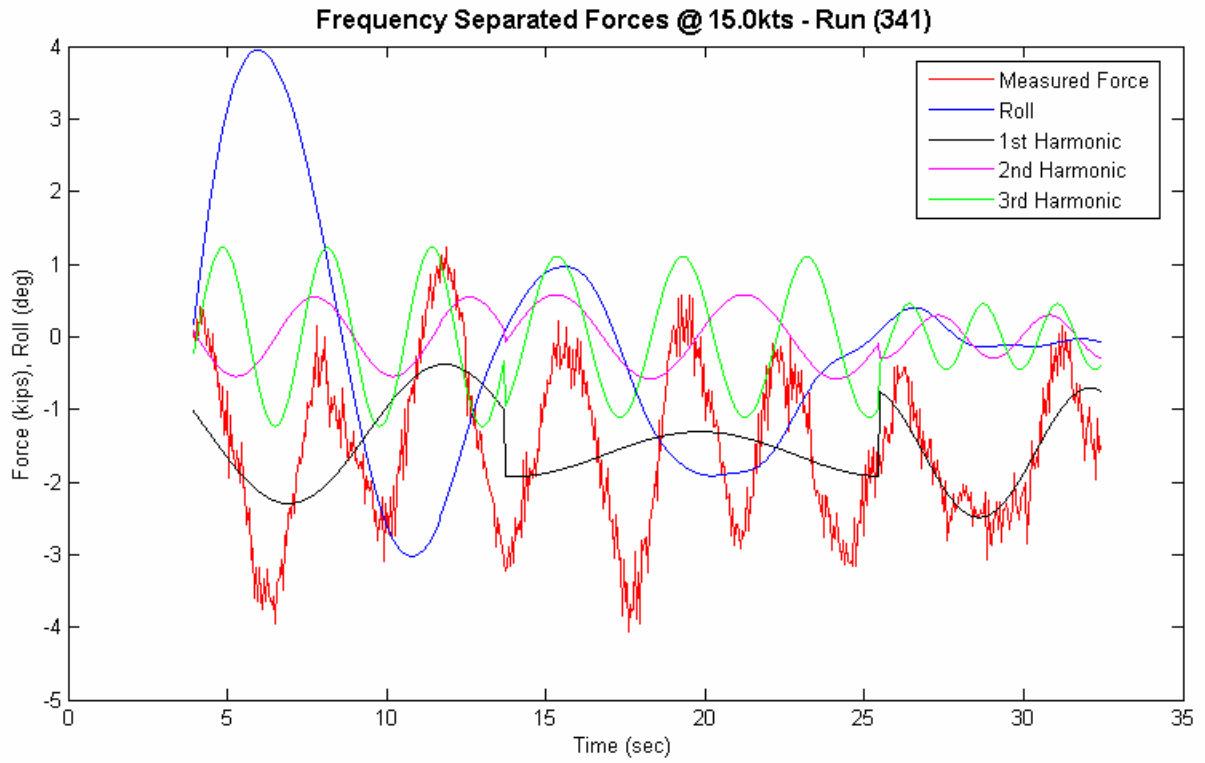


Figure 36 – Frequency Separated Forces at 15kts

5.3 Center of Pressure

Figure 37 shows a negative roll image (pressure side) for 5 knots during run 291 (Frame 53). The hull of the ship is shown at the top of the image, and the bilge keel is shown at the left side. Figure 38 shows the relative pressures along both sides of the bilge keel. The pressures were independently normalized to a magnitude of one and set to a P_0 at the tip where they should be the same value. Suction side pressures are obtained by looking at a positive roll image (Frame 22) at a similar roll velocity. Since the assumed P_0 for each frame is different, they cannot be directly summed to give the total pressure and are instead normalized to the maximum pressure for each frame.

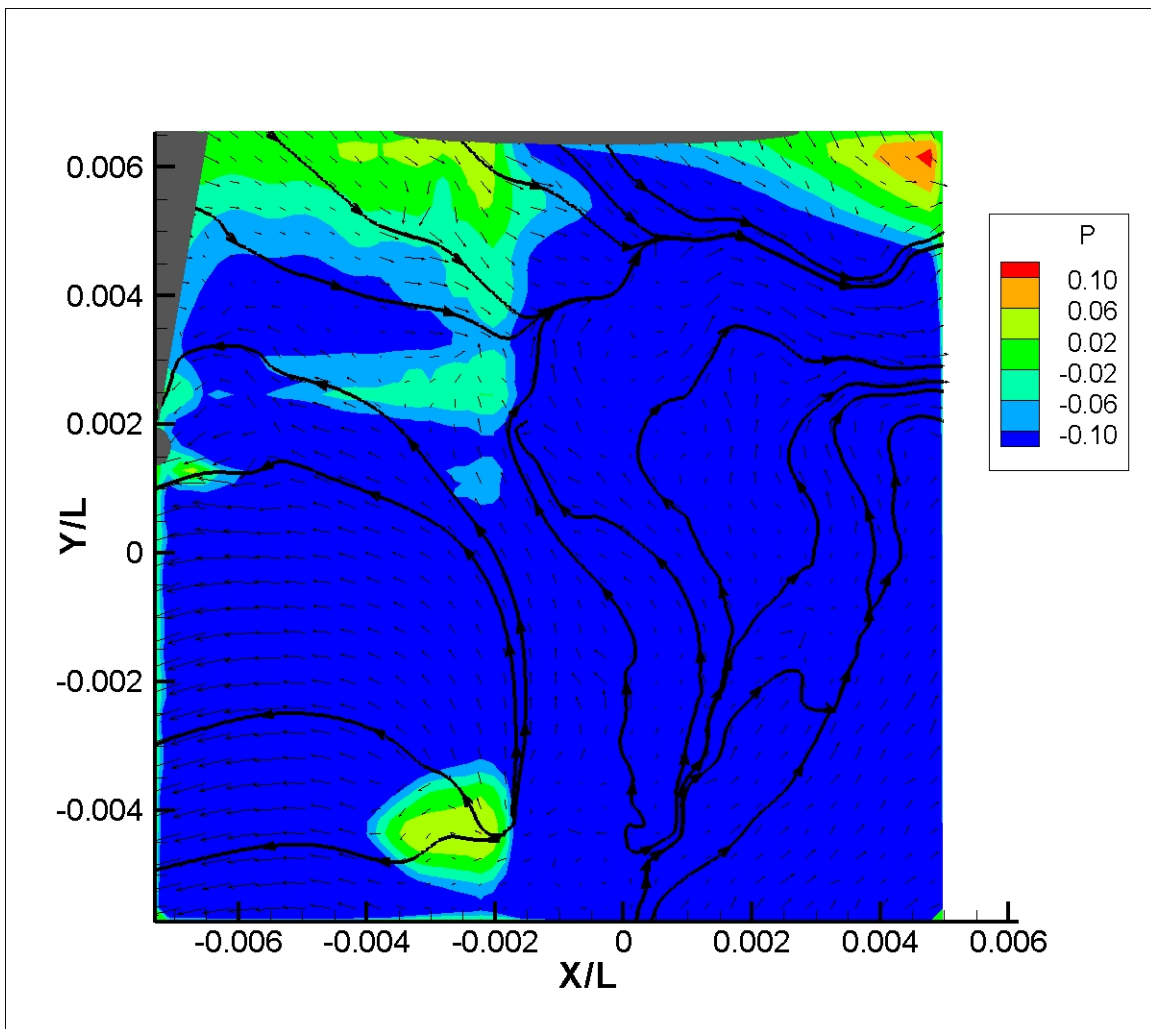


Figure 37 – Pressure Contours in Negative Roll at 5.0kts

Center of Pressure - 5kts (Run 291)

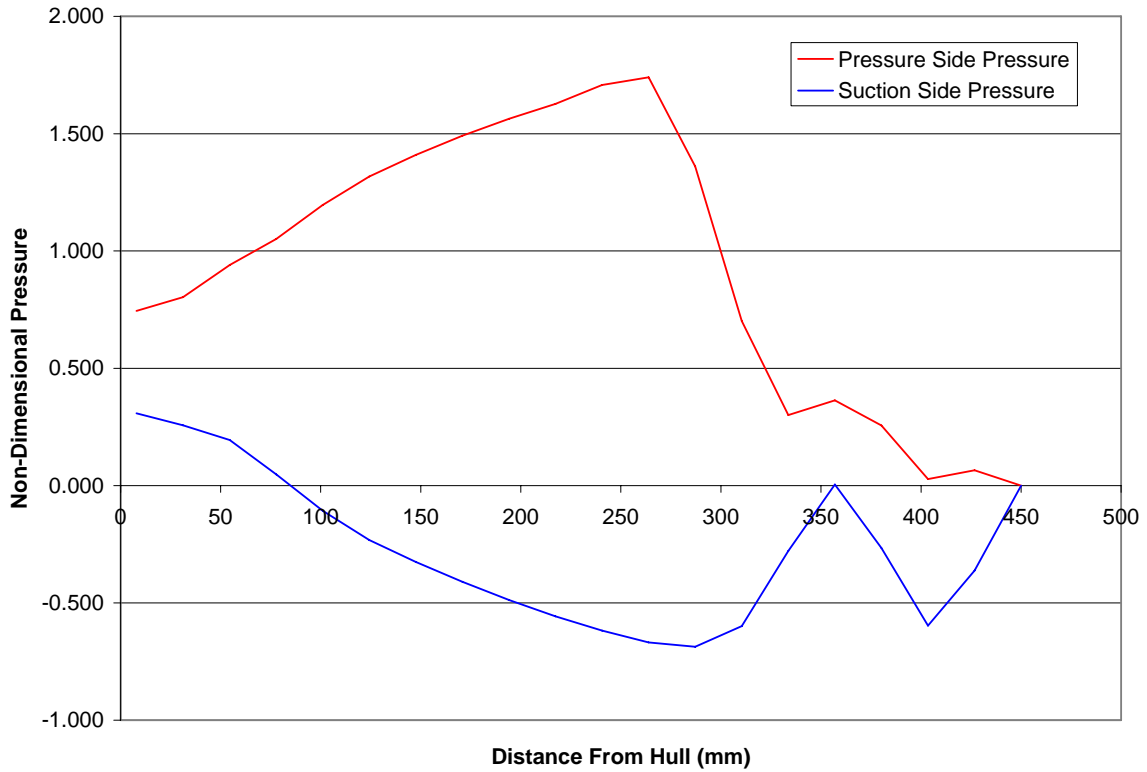


Figure 38 – Pressure Distribution Across Bilge Keel Span

5.4 PIV Images

PIV images are shown here for 5.0 (Run 291) and 10.0kts (Run 281). Every 6th frame is shown, corresponding to one frame per second. Contours show vorticity, vectors show the local velocity, and streamlines are also included.

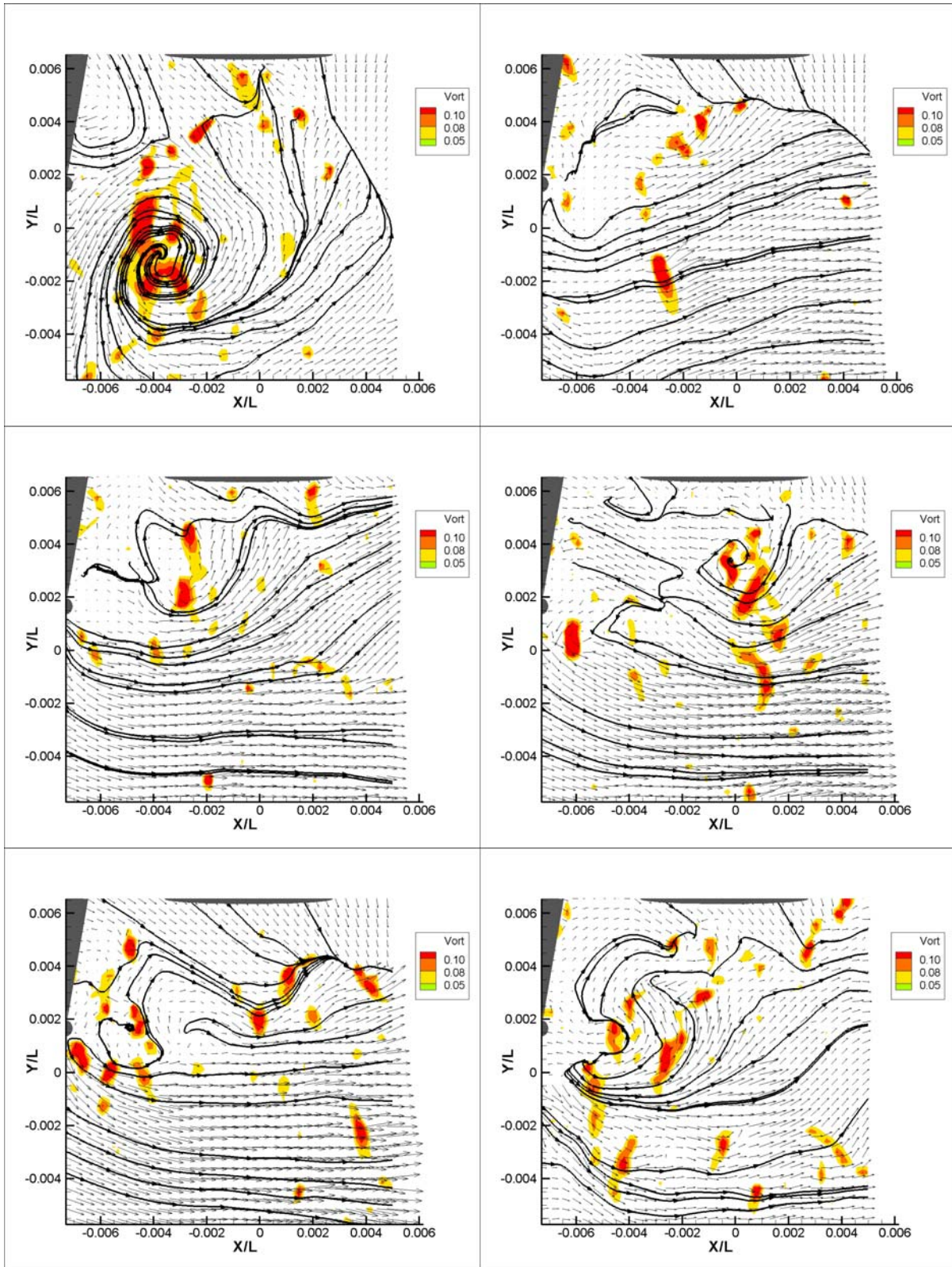


Figure 39 – PIV Images at 5.0kts ($t = 0, 1, 2, 3, 4, 5$ s)

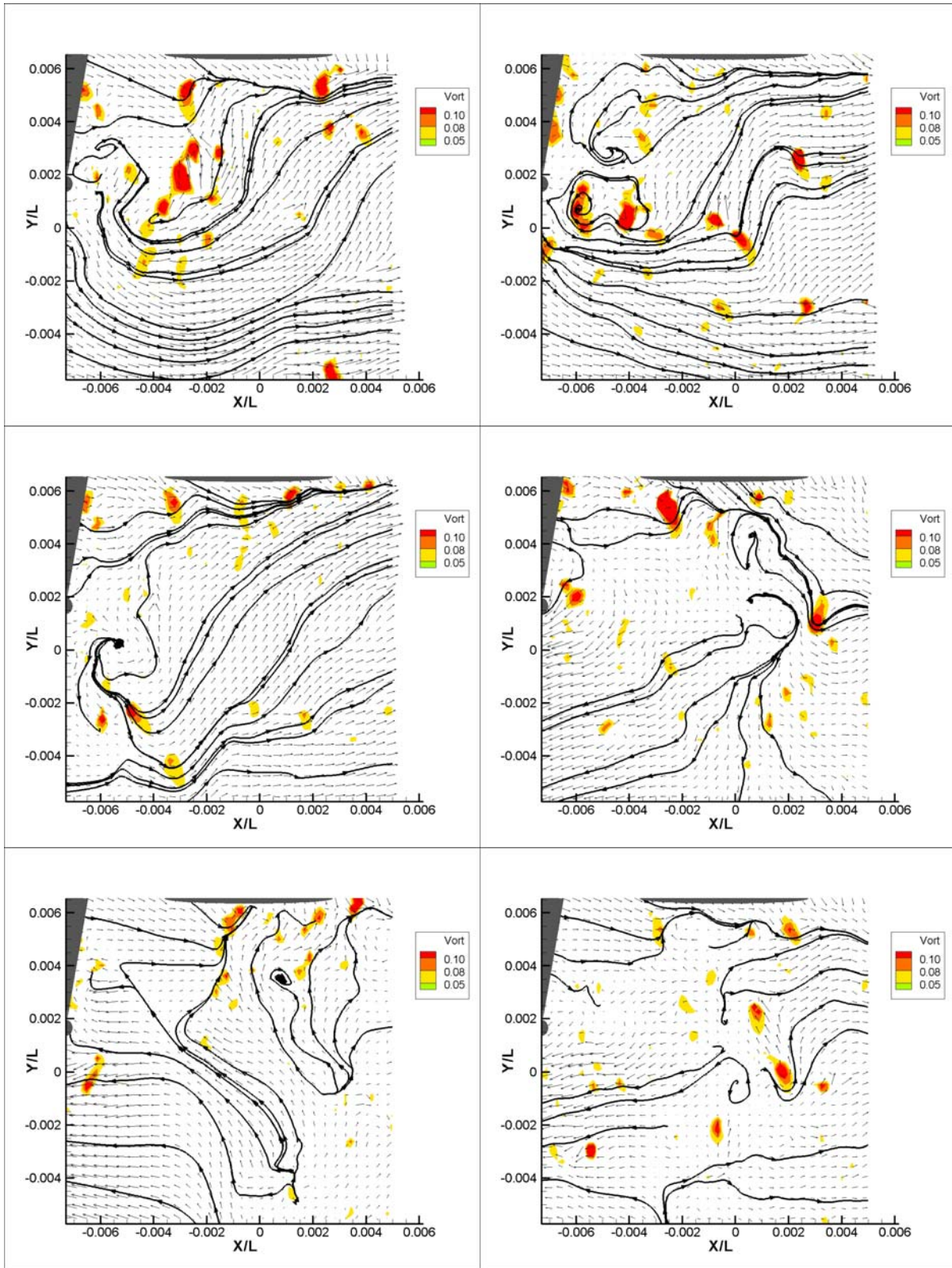


Figure 40 – PIV Images at 5.0kts ($t = 6, 7, 8, 9, 10, 11s$)

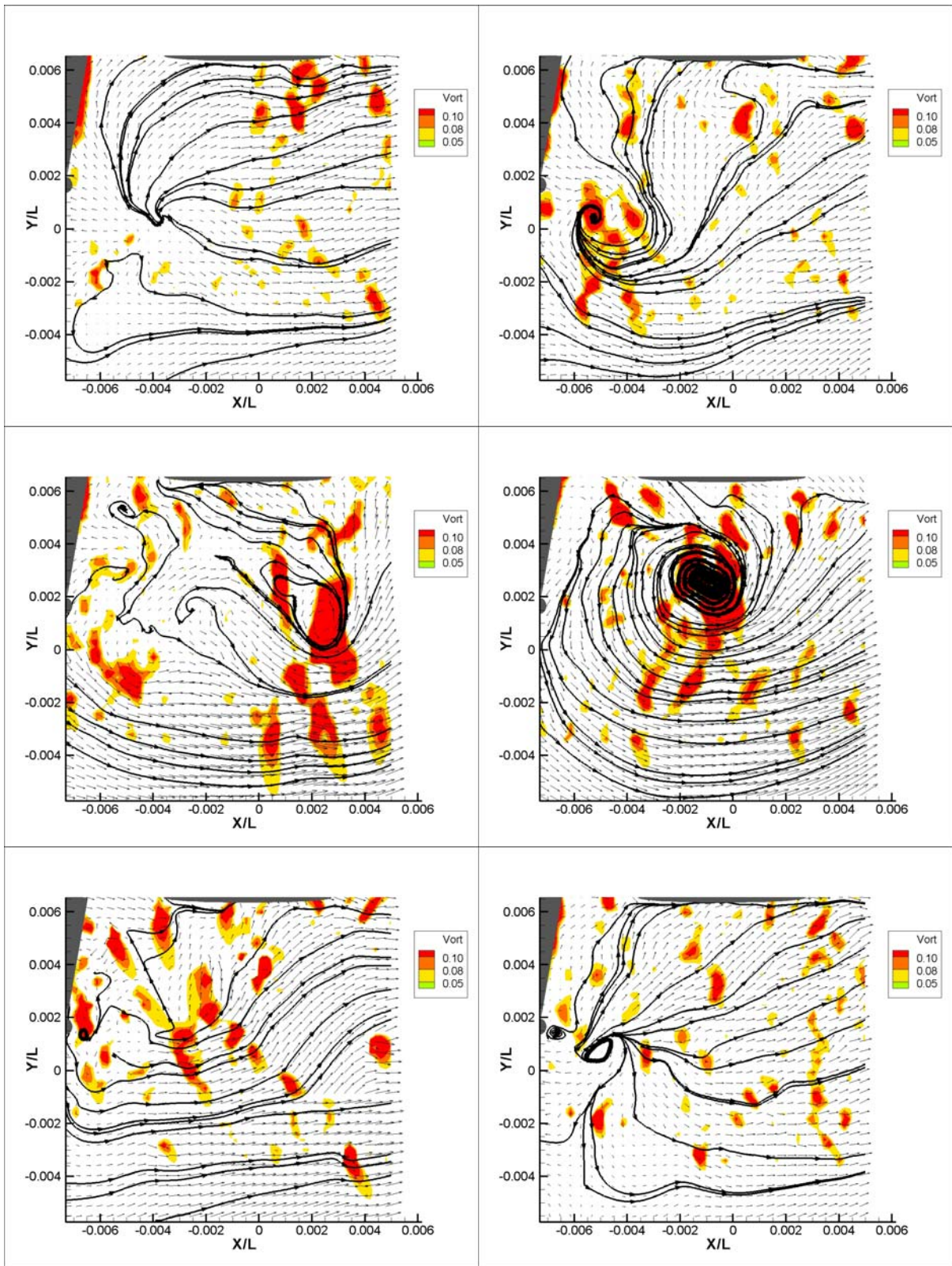


Figure 41 – PIV Images at 10.0kts ($t = 0, 1, 2, 3, 4, 5s$)

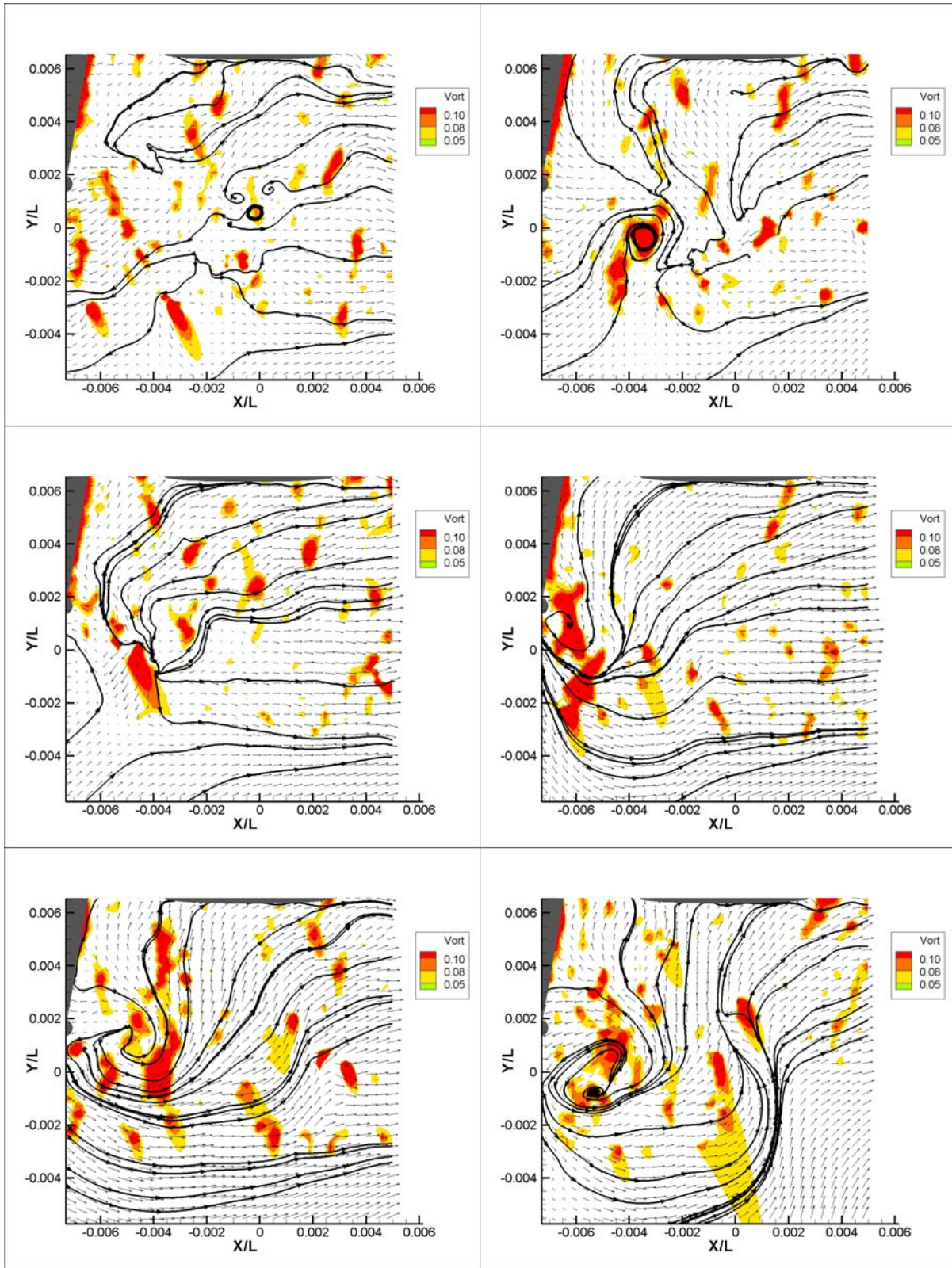


Figure 42 – PIV Images at 10.0kts ($t = 6, 7, 8, 9, 10, 11s$)

CHAPTER 6 CONCLUSIONS & DISCUSSION

6.1 Bilge Keel Forces

In two dimensional roll, the force on the bilge keel can be separated into viscous and added mass components. The drag force due to viscous effects is at a maximum when the roll velocity peaks, or as the ship rolls through its equilibrium position. The added mass will reach a maximum value when roll acceleration is greatest or as the ship reaches maximum roll amplitude. When forward speed is introduced, a third component due to lift must also be considered. If the bilge keel is aligned to the steady state flow along the hull, the lift term will be zero at even heel and vary as the flow around hull changes with roll angle. Generally there is also a steady lift offset as the bilge keel is not aligned to the flow at every, or sometimes any, forward speed. The coefficients for these three force terms can be written as:

$$C_L = -\left(\frac{U_m}{U_\infty}\right)^2 a_0$$
$$C_m = -\frac{4}{\pi} \frac{U_m}{D\omega} \left(b_1 + b_2 \frac{\sin(2\omega t)}{\sin(\omega t)} + b_3 \frac{\sin(3\omega t)}{\sin(\omega t)} + \dots \right)$$
$$C_D = \frac{2}{|\cos(\omega t)|} \left(\frac{\pi}{4} \frac{C_m D \alpha}{U_m} + a_1 + a_2 \frac{\cos(2\omega t)}{\cos(\omega t)} + \dots \right)$$

The bilge keels on this vessel were not aligned to the flow around the hull, and the steady state lift can be seen to increase with the square of forward speed in Figure 18. Looking at the pressure distribution along the hull in Figure 19, the greatest lift forces are occurring at the leading edge of the bilge keel. The flow appears to be hitting this leading edge with significant angle of attack which diminishes as the flow aligns itself with the bilge keel as it proceeds aft.

The steady state lift can also be seen in the roll decay runs, with the total force developing an offset in the up direction (negative z). Individual pressure plots for the roll decay runs also show the greatest lifting forces at the leading edge. However, unlike the steady state runs there is often a corrective downward force at the trailing edge.

The total force in the zero speed plot (Figure 20) gives some insight as to what was occurring while zeros were collected. There is some small roll motion due to the test conditions. It would make sense that any roll at zero speed might yield more sinusoidal force data on the bilge. It should be noted that the even while at zero speed, the ship's controllable pitch propellers did not stop rotating. Additionally the ship's crew was making use of the propellers to try and maintain heading at zero speed, causing water movement around the aft end of the ship even when technically at zero speed. It can be seen that the aft end of the bilge keel at BK8 did see higher pressures than the rest of the gages by looking at Figure 21.

Forward speed roll damping runs do not show sinusoidal force response at the roll frequency as was originally expected, especially at lower roll amplitudes. However, there does seem to be some correlation for the first one to two roll decay cycles up to 12.5kts. During these periods the total force slightly leads the roll velocity. This trend does break down once the roll amplitude has diminished below approximately plus and minus three degrees, and above 12.5kts.

During the length of the runs it is evident that other frequencies seem to be superimposed on the total force. Breaking out the different harmonics in the frequency separated plots allows one to correlate this to other phenomena. Bilge keel natural frequency was calculated and shown to be orders of magnitude above the frequencies of

interest. Frequency of vortex shedding based on Strouhal number was also calculated using the following equation:

$$S = \frac{nD}{V}$$

where n is the frequency, V is the free stream velocity, D is the diameter, and S is the Strouhal number. This is based upon cylinders, but for foils the value of D can be approximated as $0.26t_{\max}$. At Reynolds numbers above 10^3 , the S remains constant at 0.21. The resulting frequencies range from 7Hz at 5kts to 20Hz at 15kts and are therefore not the cause of the oscillations.

Runs taken during the last three days when ambient waves were more significant show this trend more clearly. Without wave data it can only be conjectured that these higher order frequencies correspond with wave encounter frequencies. An attempt was made to group runs by day and heading to investigate whether an obvious frequency shift could be found that might correspond to head or following seas. There is a difference in these higher frequencies between different days, and also between the opposite directions within the same day. This suggests that the ambient wave field is having an effect on the bilge keel forces, but is difficult if not impossible to account for without more information on the wave field or matching starboard force measurements.

6.2 Center of Pressure

During the processing of different runs for center of pressure, several things became apparent. First, while an actual P_0 is not necessary to calculate the center of pressure on the bilge keel, the full pressure profile around the bilge keel using the same assumed P_0 is required. Since flow field data is only taken on one side of the bilge keel, the best estimate can only be made by comparing an image with opposite roll direction

and equal velocity magnitude and roll angle. Since roll is decaying during the run, such an image is not available.

Additionally, looking at the velocity fields in the PIV images makes it apparent that the out of plane velocities cannot be ignored. Since they are unknown for this data set, realistic centers of pressure cannot be obtained. Looking at the pressure gradient along the bilge keel throughout the roll cycle did show that is possible to have the pressure change from positive to negative along the span. This effectively will yield a smaller force on the bilge keel while increasing the moment, causing erroneous force values with the gage configuration used during this experiment.

6.3 Flow Field Measurement

The bilge keel force data suggest transients, mainly in the flow coming into the bilge keel. This is evident when evaluating the PIV images as repeatable flow structures are difficult to find, especially at the lower roll amplitudes. This is more pronounced at higher forward speeds, especially at 15 knots, where much of the bilge keel and measurement plane are within the boundary layer of the hull.

6.4 Limitations of Current Work

While designed as a calm water experiment, small waves were encountered. These waves were larger on the last three days of testing and it appears that they have an effect on the data – both for force and flow field. However, since detailed wave data was not recorded during this test, correlating with the results directly is not possible, nor are any corrections that might have been made to account for this.

The forces on the bilge keel were not directly measured. Instead, the gage configuration allows only the measurement of bending moment at the gage location. The

force data presented in this paper is based on a uniform pressure distribution assumption. Based on the center of pressure analysis, this assumption is not accurate. When the pressures on both sides of the bilge keel are looked at together, it is possible that there will be an effective pure moment in addition to the moment due to net force on the bilge keel. This results in a large apparent force that has no effect on actual vessel roll damping.

The *Nave Bettica* has a large active fin directly forward of the bilge keel. Even though the fin was not active during the roll decay, this would obviously have a large effect on the flow into the bilge keel area. As the bilge keel rolls to port, the angle of attack increases with roll velocity and the wake of the active fin will pass above the bilge keel. As the roll velocity crosses zero and reverses, the angle of attack also reverses causing the wake of the active fin to pass under the bilge keel. As a result, twice during the roll cycle the wake from the active fin passes over the bilge keel and affects the forces along the bilge keel and the total moment measured.

6.5 Recommendations for Future Work

The effects of the active fin and the roll motion's effect on the overall flow around the hull due to forward speed could be modeled using CFD. This would offer an estimation of the actual flow field around the bilge keel, enabling a much better understanding of what is happening, and a basis for calculating the lift component.

The highest measured loads occurred at the leading edge of the bilge keel. Taking PIV measurements at the forward end of the bilge keel would yield flow measurements where it has the most effect. Additionally, if the flow field measurement was expanded to a SPIV configuration, the out of plane velocities would be directly measured. This

would improve upon the assumption that this velocity is constant across the span of the bilge keel. If performed it would also help to quantify the force on the bilge keel due to lift during the roll cycle.

Only the port bilge keel was gauged. The installed acquisition system could have handled the extra channels, meaning only the cost of installing the gages and running wire would be necessary. Understanding some of the unexpected force oscillations would be aided by having matching data from the starboard bilge keel as well to compare with.

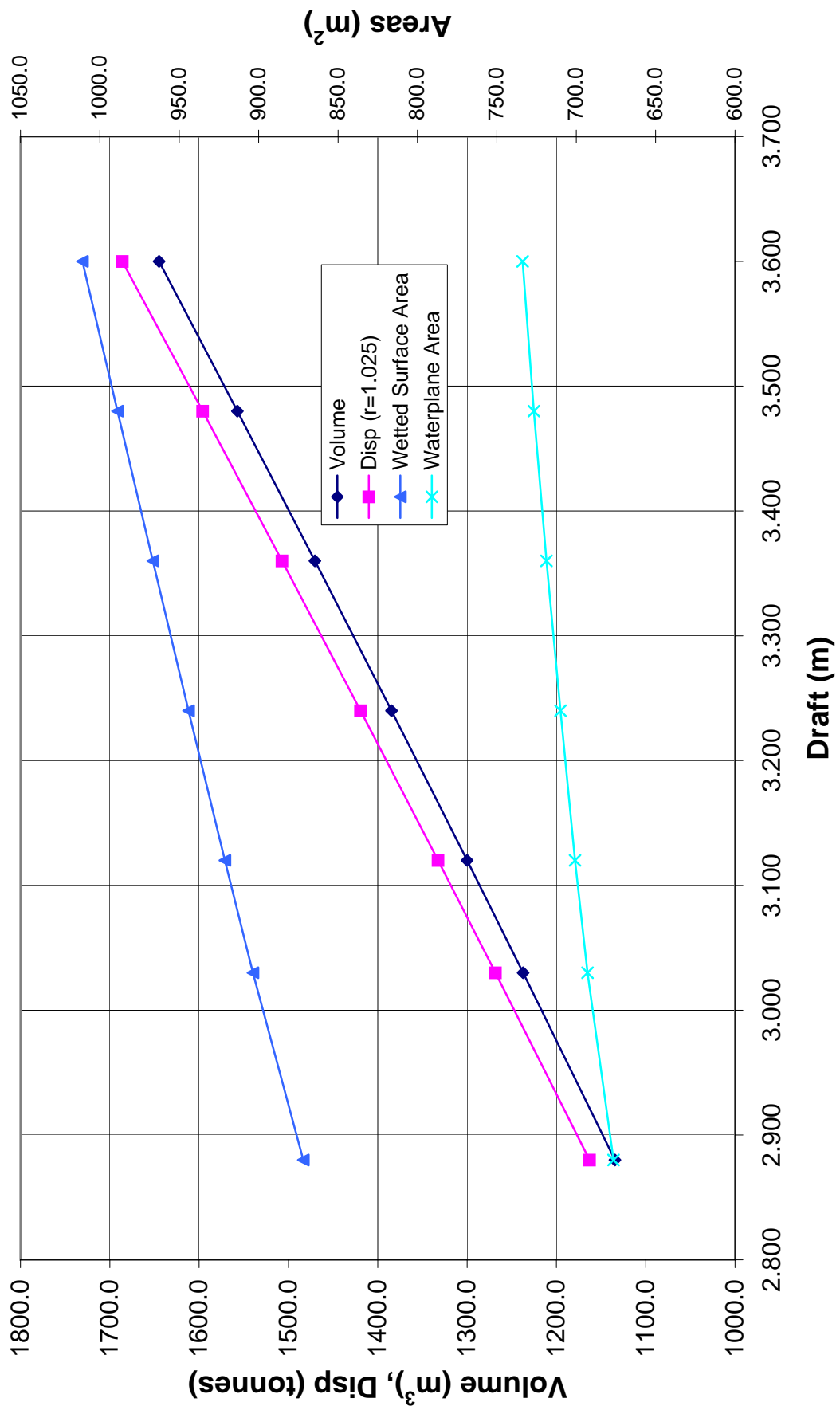
Multiple options are available to help quantify the effects of the incoming wave field on the bilge keel. A wave buoy collecting data in the test area would offer data on the local wave heights and frequencies during the test. Multiple wave buoys would also allow for the direction of the incoming waves. It would also be possible to measure the wave field immediately in front of the vessel using optical and/or acoustic wave height instrumentation currently in use at NSWCCD. If correlating to CFD models, free surface height measurement directly above the bilge keel could be collected in the same manner.

LIST OF REFERENCES

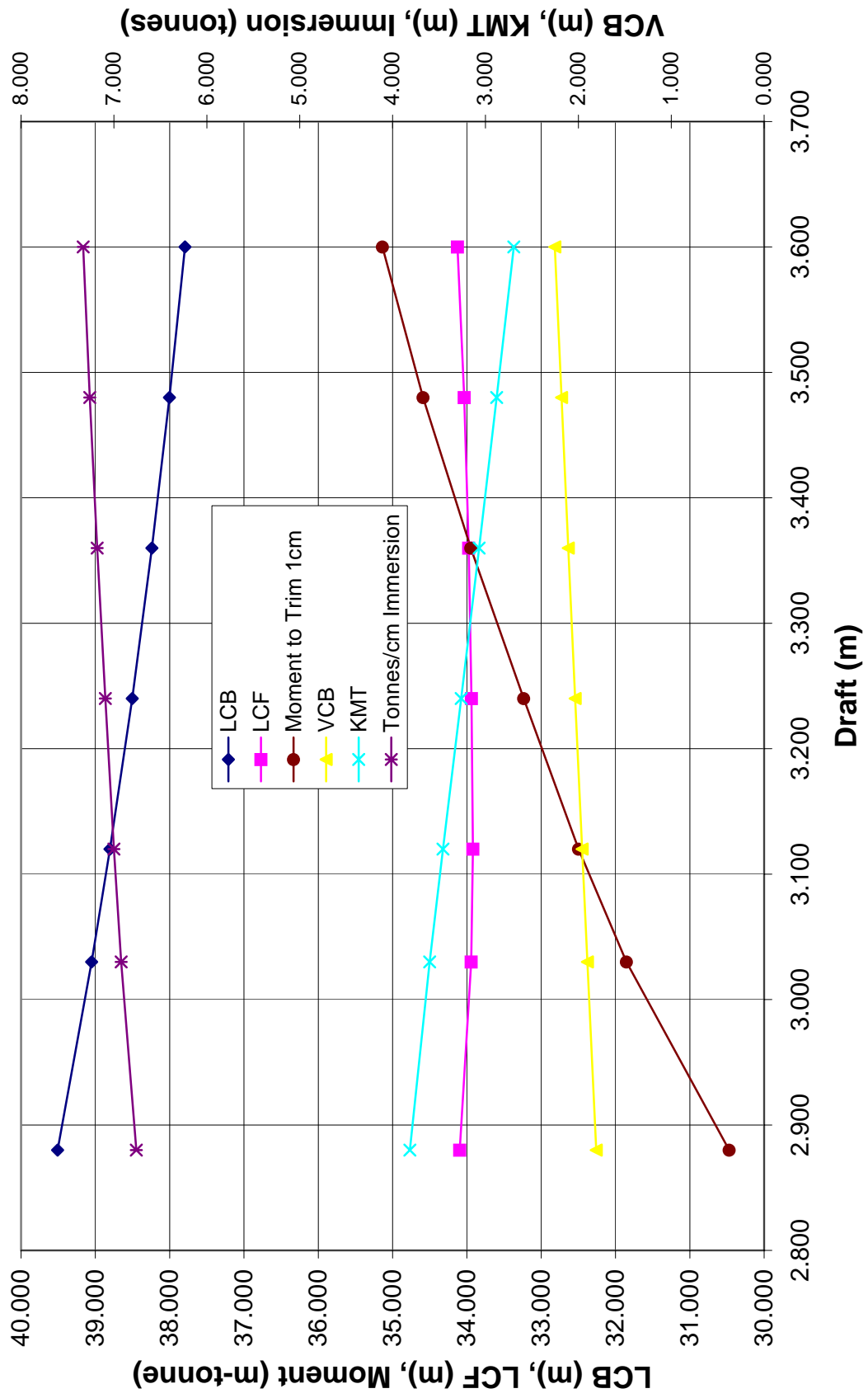
- Atsavapranee, P., Carneal, J., Grant, D., Percival, A.S., "Experimental Investigation of Viscous Roll Damping on the DTMB Model 5617 Hull Form," *OMAE 2007-29324*.
- Grant, D., Etebari, A., Atsavapranee P., "Experimental Investigation of Roll and Heave Excitation and Dampin in Beam Wave Fields," *OMAE 2007-29318*.
- Silva, S.R., Pascoal, R., Rodrigues, B., Soares, C.G., "Forced Rolling Trials on Board a Portuguese Navy Frigate," *Marine Technology*, Vol. 43, No. 3, July 2006.
- DeFatta, D. J., Lucas, J.G., Hodgkiss, W.S., **Digital Signal Processing: A System Design Approach.** John Wiley and Sons, New York, 1988.
- Haddara, M.R., Zhang, S., "Effect of Forward Speed on the Roll Damping of Three Small Fishing Vessels," *Transactions of ASME*, Vol. 116, May 1994.
- Himeno, Y., "Prediction of Ship Roll Damping-State of the Art," Report 239, Department of Naval Architecture and Marine Engineering, University of Michigan, 1981.
- Ikeda, Y., Himeno, Y., Tanaka, N., "A Prediction Method for Ship Roll Damping," Report 00405, Department of Naval Architecture, University of Osaka Prefecture, 1978.
- Keulegan, G.M. and Carpenter, L.H., "Forces on Cylinders and Plates in an Oscillating Fluid," *Journal of Research of the National Bureau of Standards*, Vol. 60, 1958.
- Lloyd, A.R.J.M., **Seakeeping: Ship Behaviour in Rough Weather**, ARJM Lloyd, 1998.
- Lewandowski, E., **The Dynamics of Marine Craft**, World Scientific Publishing Company, 2004
- Dalzell, J.F., "A Note on the Form of Ship Roll Damping," *Journal of Ship Research*, Vol. 22, No. 3, Sept. 1978.
- Schmitke, R.T., "Ship Sway, Roll, and Yaw Motions in Oblique Seas," *SNAME Transactions*, Vol. 86, 1978.

APPENDIX A – SHIP CHARACTERISTICS

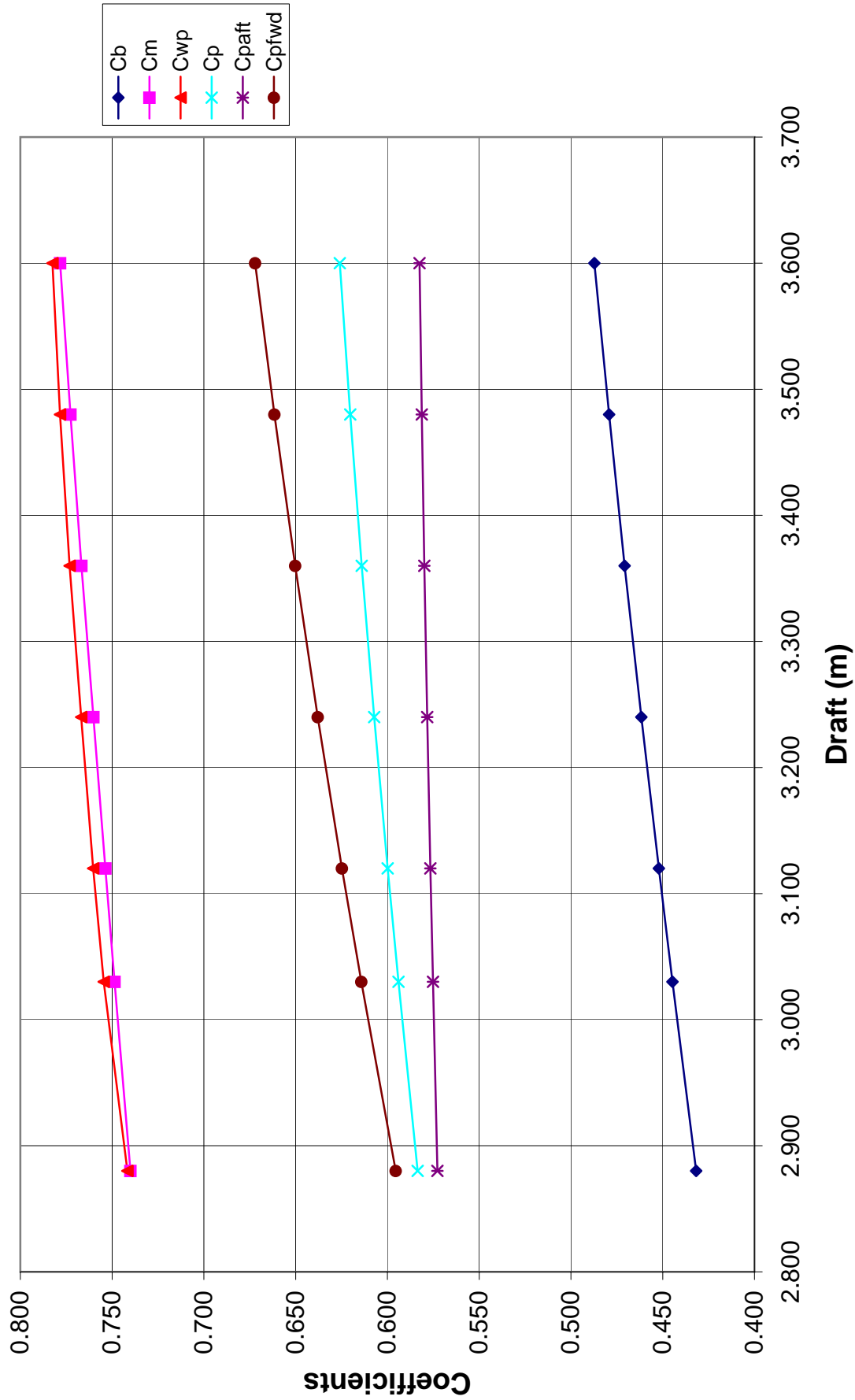
Curves of Form



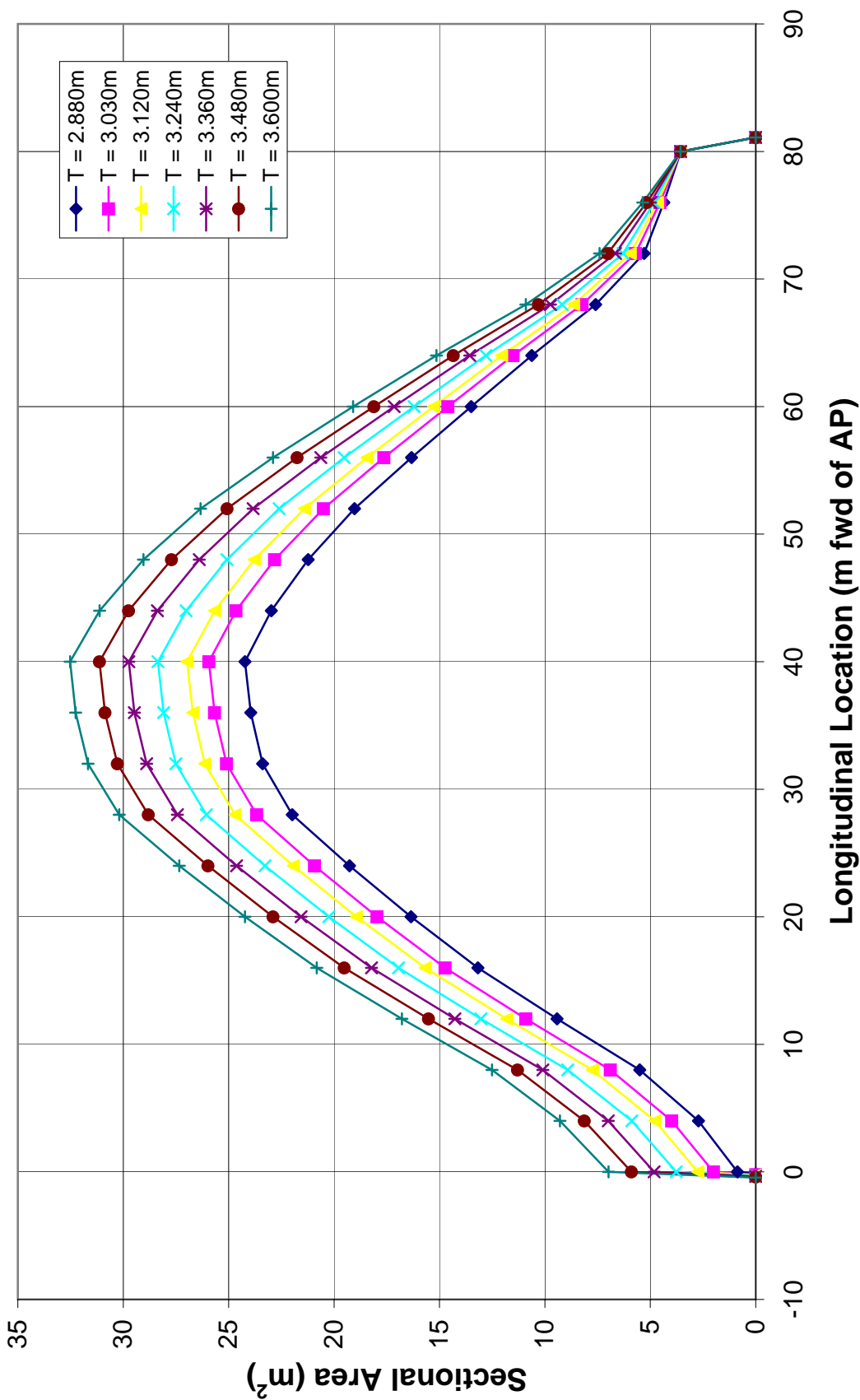
Curves of Form - Continued



Curves of Form - Continued



Sectional Area Curve



APPENDIX B – RUN LOGS & CHANNEL ZEROS

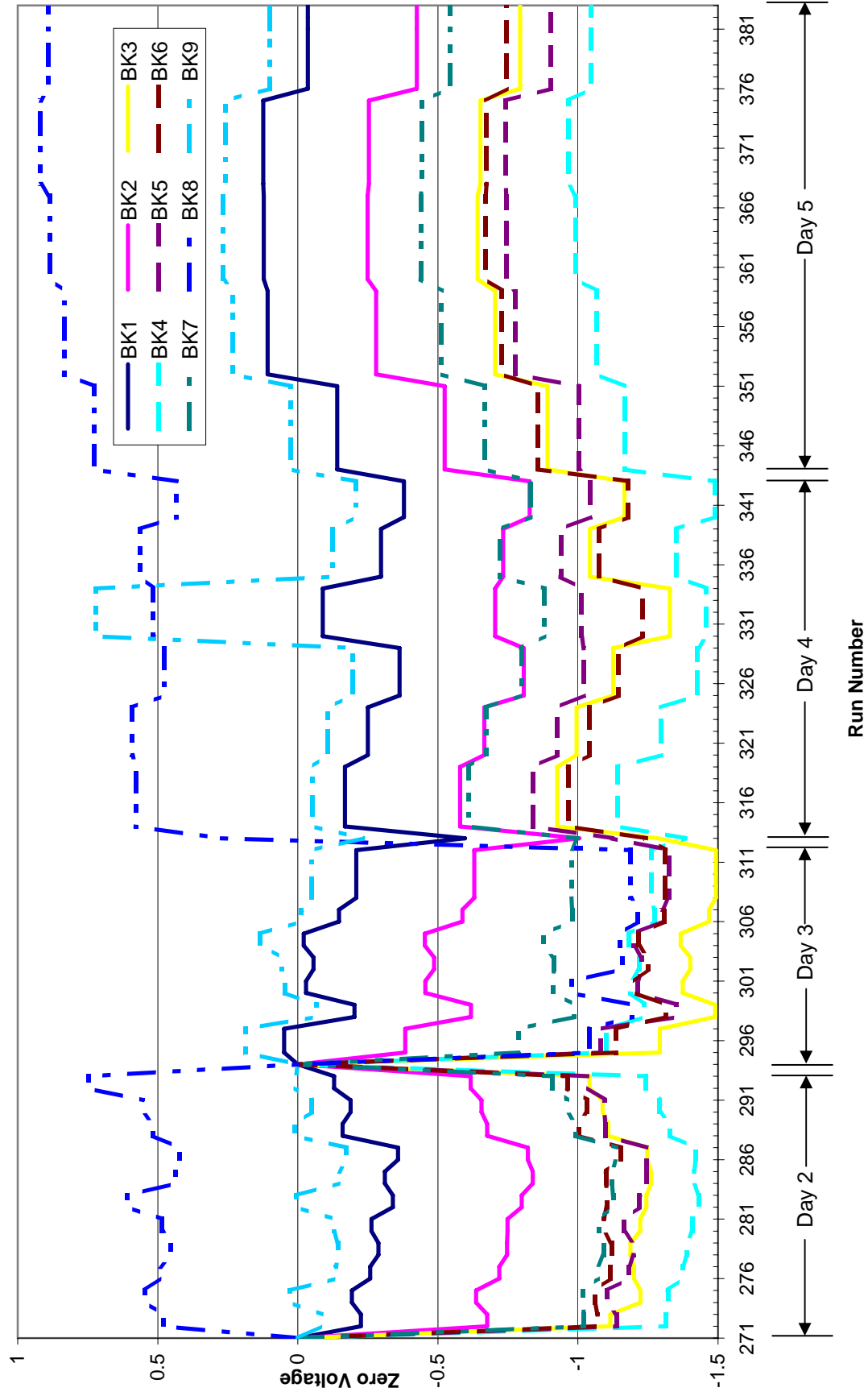
TRIAL LOG FOR BETTICA ROLL-DECAY TEST

Run #	Speed over ground (kts)	Froude #	Dt (ms)	Date/Time	Ship Heading	Wind Speed and Direction (kts, degrees)	Roll Period (sec)	Seeding	Water Temp (deg C)	Fins Control Release (sec)	Note	# of frames
252	0.0	0.000	N/A	10/03/07, 2141HR	20						Zero run for boresight, roll boresight set at -0.353	
253	7.5	0.138	2.0	10/03/07, 2204HR	20						Steady state	2000
256	7.5	0.138	1.5	10/03/07, 2218HR	20						Roll decay, data collect after release of fins control	2000
257	7.5	0.138	1.5	10/03/07, 2307HR	20						Steady state	2000
258	7.5	0.138	1.5	10/03/07, 2313HR	20						Roll decay, data collect after release of fins control	2000
260	7.5	0.138	1.5	10/03/07, 2355HR	20					24	Steady state	2000
261	7.5	0.138	1.5		20						Roll decay, data collect before release of fins control	2000
262	10.0	0.184	1.0	10/04/07, 0054HR	20					3	Steady state	2000
263	10.0	0.184	1.0	10/04/07, 0100HR	20						Roll decay	2000
264	10.0	0.184	1.0	10/04/07, 0134HR	20						Steady state	2000
265	10.0	0.184	1.0	10/04/07, 0138HR	20					31	Roll decay	2000
266	10.0	0.184	1.0	10/04/07, 0210HR	20						Steady state	2000
267	10.0	0.184	1.0	10/04/07, 0215HR	20					37	Roll decay	2000
268	10.0	0.184	1.0	10/04/07, 0245HR	20						Steady state	2000
269	10.0	0.184	1.0	10/04/07, 0250HR	20						Forced roll only, fins control was not released	2000
270	10.0	0.184	1.0	10/04/07, 0305HR	20						Roll Decay	2000
271	0.3	0.006	N/A	10/04/07, 2100HR	165	1, 13		no	22			
272	7.5	0.138	1.3	10/04/07, 2116HR	165	2, 302		no	22		Zero run for roll/pitch boresight, set at 0.7, -0.551	
273	7.5	0.138	1.3	10/04/07, 2122HR	165	2, 302	9.55	no	22	88	Steady state, control fins on auto	1000
274	7.4	0.136	1.3	10/04/07, 2155HR	165	4, 103		no	22		Roll decay (first 320 frames blank), visual sea state 0	2000
275	7.4	0.136	1.3	10/04/07, 2201HR	165	4, 103	9.75	no	22	40	Steady state, auto fins, manual triggered, zero at 1.2 kts	1000
276	10.5	0.193	1.0	10/04/07, 2237HR	166	2, 105		no	22		Roll decay	2000
277	10.5	0.193	1.0	10/04/07, 2242HR	166	2, 105	9.65	no	22	16	Steady state, control fins on auto, zero taken at 0.8 kts	1000
278	10.0	0.184	1.0	10/04/07, 2309HR	166	0, 26		no	22		Roll decay	2000
279	10.0	0.184	1.0	10/04/07, 2317HR	166	0, 26	9.55	no	22	20	Steady state, control fins on auto, zero taken at 0.7 kts	1000
280	10.7	0.197	1.0	10/04/07, 2343HR	166	2, 63		no	22		Roll decay, frames 85-124 missing	2000
281	10.7	0.197	1.0	10/04/07, 2349HR	166	2, 63	9.55	no	22	14	Steady state, control fins on auto, zero taken at 0.8 kts	1000
282	10.0	0.184	1.0	10/05/07, 0015HR	166	4, 326		no	22		Roll decay	2000
283	10.0	0.184	1.0	10/05/07, 0020HR	166	4, 326	9.44	no	22	43	Steady state, control fins on auto, zero taken at 0.6 kts	1000
284	7.0	0.129	1.3	10/05/07, 0103HR	166	6, 320		yes	22		Roll decay	2000
285	7.0	0.129	1.3	10/05/07, 0107HR	166	6, 320	9.90	yes	22	142	Steady state, control fins on auto, zero taken at 0.6 kts	2000
286	7.4	0.136	1.3	10/05/07, 0135HR	166	9, 328		yes	22		Roll decay	2000
287	7.4	0.136	1.3	10/05/07, 0140HR	166	9, 328	9.70	yes	22	40	Steady state, auto fins, vis sea state 0.1, zero at 1.0 kt	1000
288	5.0	0.092	2.0	10/05/07, 0208HR	165	4, 345		yes	22		Roll decay	2000
290	5.1	0.094	2.0	10/05/07, 0237HR	166	4, 312		yes	22		Steady state, control fins on auto, zero taken at 0.4 kt	1000
291	5.1	0.094	2.0	10/05/07, 0242HR	166	4, 312	9.25	yes	22	25	Steady state, control fins on auto, zero taken at 1.0 kt	1000
292	5.0	0.092	2.0	10/05/07, 0309HR	166	10, 345		yes	22		Roll decay	2000
293	5.0	0.092	2.0	10/05/07, 0315HR	166	10, 345	8.90	yes	22	41	Steady state, control fins on auto, zero taken at 0.6 kt	1000

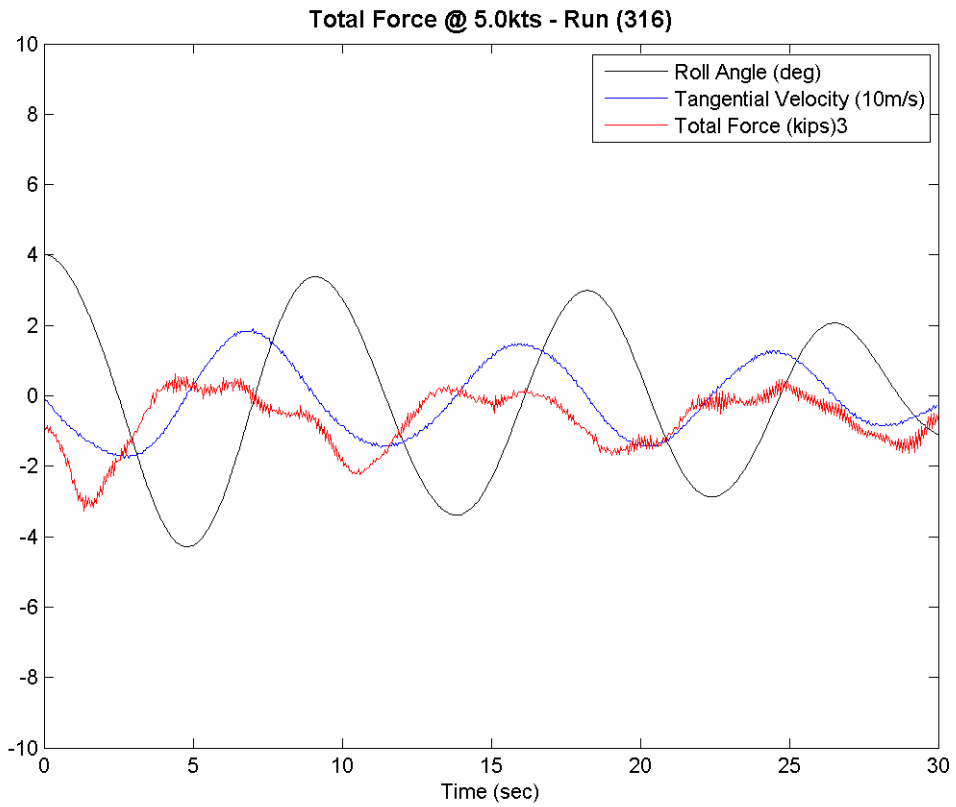
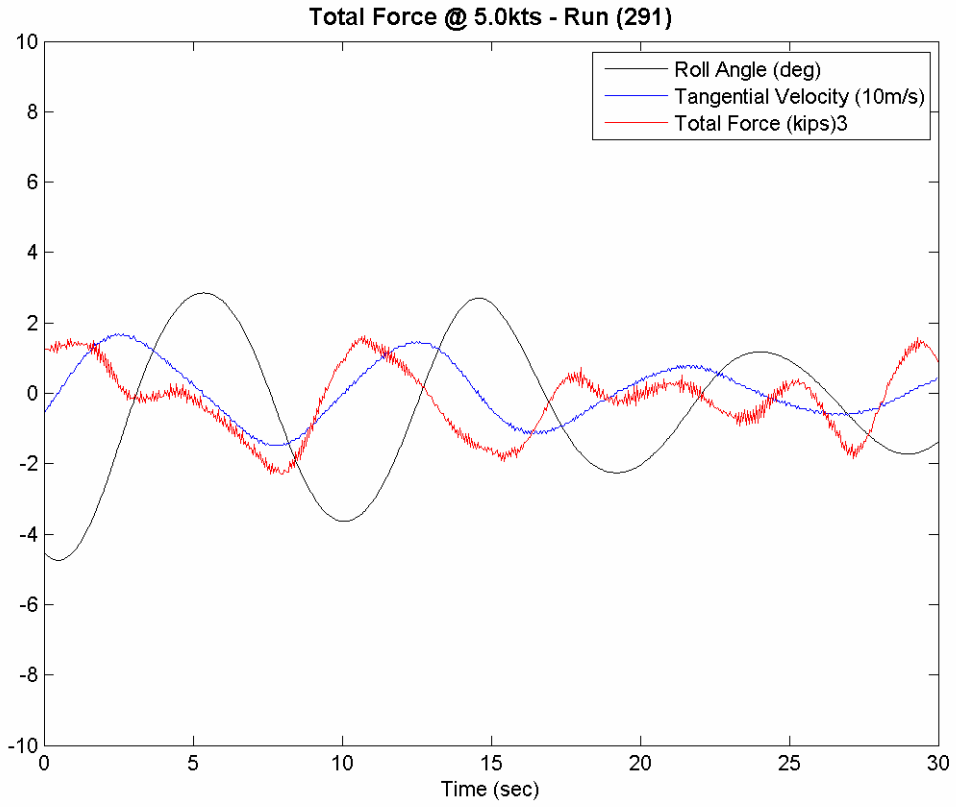
Run #	Speed thru water (kts)	Froude #	Dt (ms)	Date/Time	Ship Heading	Wind Speed and Direction (kts, degrees)	Roll Period (sec)	Seeding	Water Temp (deg C)	Fins Control Release (sec)	Note	# of frames	sig. wave height (cm)
294	0.0	0.000	2.0	10/08/07, 2200HR	150	18, 18		no	21		Zero run, boresight set at 0.7, -0.551		
295	4.8	0.088	2.0	10/08/07, 2205HR	150	18, 18		yes	21		Steady state, control fins on auto, zero taken at 1.2 kt	1000	13
296	4.8	0.088	2.0	10/08/07, 2212HR	150	18, 18		yes	21		Roll decay	2000	13
297	4.8	0.088	2.0	10/08/07, 2216HR	150	18, 18		yes	21		Roll decay, tried again	2000	13
298	10.2	0.187	2.0	10/08/07, 2245HR	331	16, 12		no	21		Steady state, control fins on auto, zero taken at 1.0 kt	1000	23
299	10.2	0.187	2.0	10/08/07, 2250HR	331	16, 12		no	21	14	Roll decay, head sea	2000	23
300	10.3	0.189	2.0	10/08/07, 2321HR	150	11, 355		no	21		Steady state, control fins on auto, zero taken at 1.0 kt	1000	22
301	10.3	0.189	1.0	10/08/07, 2325HR	150	11, 351	9.40	no	21	21	Roll decay	2000	22
302	10.1	0.186	1.0	10/08/07, 2348HR	150	13, 349		no	21		Steady state, control fins on auto, zero taken at 1.1 kt	1000	18
303	10.1	0.186	1.0	10/08/07, 2353HR	150	13, 349		no	21	23	Roll decay, really good images	2000	18
304	8.3	0.152	1.0	10/08/07, 0035HR	152	8, 359		no	21		Steady state, control fins on auto, zero taken at 1.0 kt	1000	15
305	8.3	0.152	1.0	10/09/07, 0041HR	152	8, 359		no	21	43	Roll decay	2000	15
306	7.3	0.134	1.3	10/09/07, 0102HR	152	6, 347		no	21		Steady state, control fins on auto, zero taken at 0.9 kt	1000	20
307	7.3	0.134	1.3	10/09/07, 0107HR	152	6, 347		no	21	105	Roll decay	2000	20
308	7.0	0.129	1.3	10/09/07, 0133HR	330	12, 332		no	21		Steady state, control fins on auto, zero taken at 0.7 kt	1000	20
309	7.0	0.129	1.3	10/09/07, 0139HR	330	12, 332		no	21	47	Roll decay	2000	20
310	7.0	0.129	1.3	10/09/07, 0143HR	330	12, 332		no	21	130	Roll decay	1000	20
311	10.1	0.186	1.0	10/09/07, 0148HR	332	12, 317		no	21		Steady state	2000	20
312	10.1	0.186	1.0	10/09/07, 0154HR	332	12, 317		no	21		Roll decay	1000	20
Run #	Speed thru water (kts)	Froude #	Dt (ms)	Date/Time	Ship Heading	Wind Speed and Direction (kts, degrees)	Roll Period (sec)	Seeding	Water Temp (deg C)	Fins Control Release (sec)	Note	# of frames	sig. wave height (cm)
313	0.0	0.000	N/A					N/A			playing around	N/A	
314	0.0	0.000	N/A	10/09/07, 1809HR	280	9, 178		N/A	18		Zero run, boresight set at 0.7, -0.551	N/A	10
315	4.8	0.088	N/A	10/09/07, 1817HR	280	9, 178		N/A	18		Steady state, control fins on auto, zero taken at 1.0 kt	N/A	10
316	4.8	0.088	N/A	10/09/07, 1821HR	280	9, 178		N/A	18	8	Roll decay	N/A	10
317	4.8	0.088	N/A	10/09/07, 1825HR	280	9, 178		N/A	18	50	Roll decay	N/A	10
318	4.8	0.088	N/A	10/09/07, 1829HR	280	9, 178		N/A	18	43	Roll decay	N/A	10
319	4.8	0.088	N/A	10/09/07, 1836HR	280	9, 178		N/A	18	43	Roll decay	N/A	10
320	7.5	0.138	1.3	10/09/07, 2112HR	211	14, 216		no	19		Steady state, control fins on auto, zero taken at 0.5 kt	1000	11
321	7.5	0.138	1.3	10/09/07, 2119HR	211	14, 216		no	19	86	Roll decay	2000	11
322	7.5	0.138	1.3	10/09/07, 2123HR	211	14, 216		no	19	67	Roll decay	2000	11
323	7.5	0.138	1.3	10/09/07, 2127HR	211	14, 216		no	19	47	Roll decay	2000	11
324	7.5	0.138	1.3	10/09/07, 2131HR	211	14, 216		no	19	31	Roll decay	2000	11
325	10.3	0.189	1.0	10/09/07, 2155HR	272	6, 270		no	19		Steady state, control fins on auto, zero taken at 0.4 kt	1000	20
326	10.3	0.189	1.0	10/09/07, 2201HR	272	6, 270		no	19	13	Roll decay	2000	20
327	10.3	0.189	1.0	10/09/07, 2204HR	272	6, 270		no	19	19	Roll decay	2000	20
328	10.3	0.189	1.0	10/09/07, 2208HR	272	6, 270		no	19	19	Roll decay	2000	20
329	10.3	0.189	1.0	10/09/07, 2212HR	272	6, 270		no	19	20	Roll decay	2000	20
330	12.6	0.231	0.8	10/09/07, 2227HR	292	6, 327		no	19		Steady state, control fins on auto, zero taken at 0.3 kt	1000	24
331	12.6	0.231	0.8	10/09/07, 2233HR	292	6, 327		no	19	5	Roll decay	2000	24
332	12.6	0.231	0.8	10/09/07, 2237HR	292	6, 327		no	19	17	Roll decay	2000	24
333	12.6	0.231	0.8	10/09/07, 2241HR	292	6, 327		no	19	19	Roll decay	2000	24
334	12.6	0.231	0.8	10/09/07, 2245HR	292	6, 327		no	19	20	Roll decay	2000	24
335	12.0	0.220	0.8	10/10/07, 0053HR	180	8, 330		no	19		Steady state, control fins on auto, zero taken at 0.2 kt	2000	9
336	12.0	0.220	0.8	10/10/07, 0059HR	180	8, 330		no	19	18	Roll decay	2000	9
337	12.0	0.220	0.8	10/10/07, 0104HR	180	8, 330		no	19	19	Roll decay	2000	9
338	12.0	0.220	0.8	10/10/07, 0108HR	180	8, 330		no	19	26	Roll decay	2000	9
339	12.0	0.220	0.8	10/10/07, 0112HR	180	8, 330		no	19	48	Roll decay	2000	9
340	15.3	0.281	0.65	10/10/07, 0128HR	0	6, 340		no	19		Steady state, control fins on auto, zero taken at 0.3 kt	1000	9
341	15.3	0.281	0.65	10/10/07, 0134HR	0	6, 340		no	19	33	Roll decay	2000	9
342	15.3	0.281	0.65	10/10/07, 0138HR	0	6, 340		no	19	21	Roll decay	2000	9
343	15.3	0.281	0.65	10/10/07, 0141HR	0	6, 340		no	19	12	Roll decay, camera went dead	2000	9

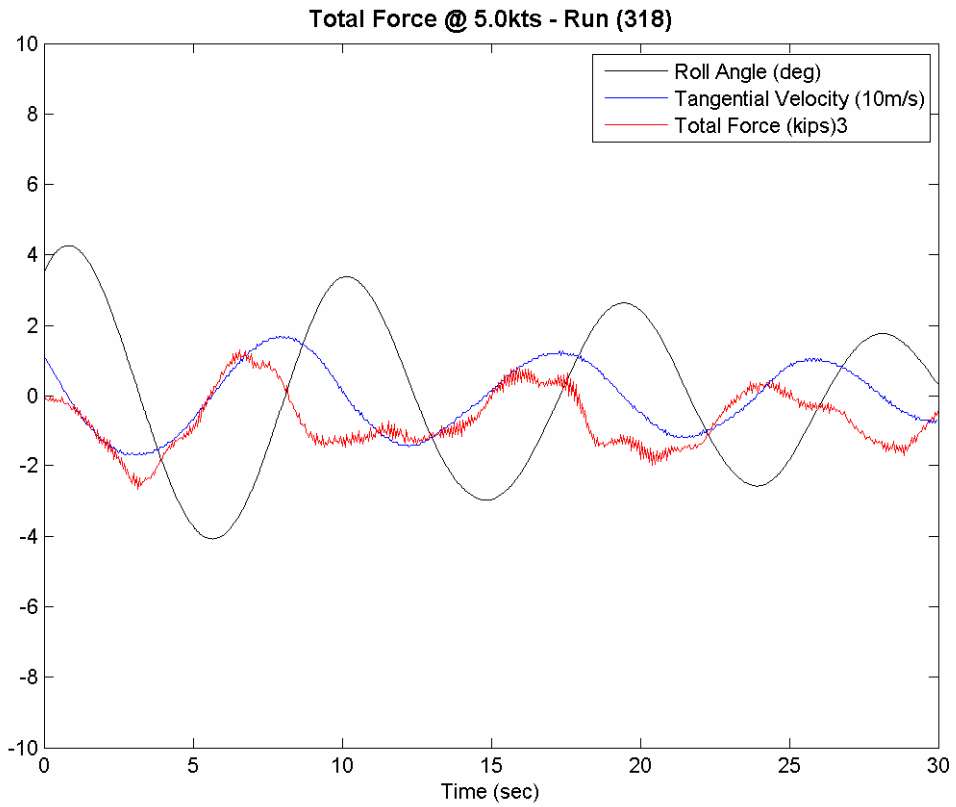
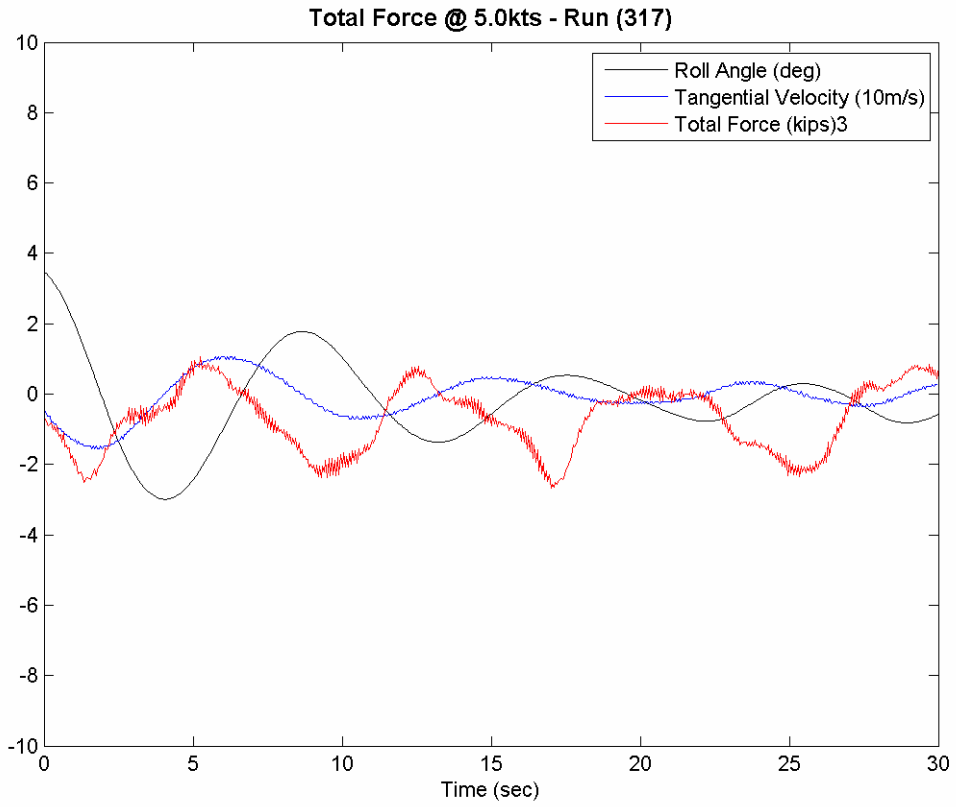
Run #	Speed thru water (kts)	Froude #	Dt (ms)	Date/Time	Ship Heading	Wind Speed and Direction (kts, degrees)	Roll Period (sec)	Seeding	Water Temp (deg C)	Fins Control Release (sec)	Note	# of frames	sig. wave height (cm)
344	0.0	0.000	N/A	10/10/07, 2213HR	166	8, 263		N/A	21		Zero run, boresight set at 0.7, -0.551	N/A	7
345	5.0	0.092	N/A	10/10/07, 2218HR	166	8, 263		N/A	21		Steady state, control fins on auto, zero taken at 0.8 kt	N/A	7
346	5.0	0.092	N/A	10/10/07, 2221HR	166	8, 263		N/A	21	43	Roll decay	N/A	7
347	5.0	0.092	N/A	10/10/07, 2223HR	166	8, 263		N/A	21	54	Roll decay	N/A	7
348	5.0	0.092	N/A	10/10/07, 2226HR	166	8, 263		N/A	21	38	Roll decay	N/A	7
349	5.0	0.092	N/A	10/10/07, 2229HR	166	8, 263		N/A	21	44	Roll decay	N/A	7
350	5.0	0.092	N/A	10/10/07, 2232HR	166	8, 263		N/A	21	32	Roll decay	N/A	7
351	5.0	0.092	N/A	10/10/07, 2235HR	166	8, 263		N/A	21	65	Roll decay	N/A	7
352	0.0	0.000	N/A	10/10/07, 2246HR	0	12, 278		N/A	21		Zero run, boresight set at 0.7, -0.551	N/A	25
353	7.4	0.136	N/A	10/10/07, 2251HR	0	12, 278		N/A	21		Steady state, control fins on auto, zero taken at 0.6 kt	N/A	25
354	7.4	0.136	N/A	10/10/07, 2255HR	0	12, 278		N/A	21	25	Roll decay	N/A	25
355	7.4	0.136	N/A	10/10/07, 2258HR	0	12, 278		N/A	21	57	Roll decay	N/A	25
356	7.4	0.136	N/A	10/10/07, 2301HR	0	12, 278		N/A	21	44	Roll decay	N/A	25
357	7.4	0.136	N/A	10/10/07, 2303HR	0	12, 278		N/A	21	40	Roll decay	N/A	25
358	7.4	0.136	N/A	10/10/07, 2306HR	0	12, 278		N/A	21	62	Roll decay	N/A	25
359	7.4	0.136	N/A	10/10/07, 2308HR	0	12, 278		N/A	21	27	Roll decay	N/A	25
360	0.0	0.000	N/A	10/10/07, 2319HR	0	10, 260		N/A	21		Zero run, boresight set at 0.7, -0.551	N/A	25
361	10.2	0.187	N/A	10/10/07, 2324HR	0	10, 260		N/A	21		Steady state, control fins on auto, zero taken at 1.2 kt	N/A	25
362	10.2	0.187	N/A	10/10/07, 2328HR	0	10, 260		N/A	21	26	Roll decay	N/A	25
363	10.2	0.187	N/A	10/10/07, 2330HR	0	10, 260		N/A	21	18	Roll decay	N/A	25
364	10.2	0.187	N/A	10/10/07, 2333HR	0	10, 260		N/A	21	16	Roll decay	N/A	25
365	10.2	0.187	N/A	10/10/07, 2336HR	0	10, 260		N/A	21	20	Roll decay	N/A	25
366	10.2	0.187	N/A	10/10/07, 2339HR	0	10, 260		N/A	21	8	Roll decay	N/A	25
367	10.2	0.187	N/A	10/10/07, 2341HR	0	10, 260		N/A	21	19	Roll decay	N/A	25
368	0.0	0.000	N/A	10/10/07, 2350HR	0	14, 290		N/A	21		Zero run, boresight set at 0.7, -0.551	N/A	25
369	12.5	0.230	N/A	10/10/07, 2358HR	0	14, 290		N/A	21		Steady state, control fins on auto, zero taken at 0.3 kt	N/A	25
370	12.5	0.230	N/A	10/11/07, 0001HR	0	14, 290		N/A	21	17	Roll decay	N/A	25
371	12.5	0.230	N/A	10/11/07, 0004HR	0	14, 290		N/A	21	16	Roll decay	N/A	25
372	12.5	0.230	N/A	10/11/07, 0007HR	0	14, 290		N/A	21	11	Roll decay	N/A	25
373	12.5	0.230	N/A	10/11/07, 0009HR	0	14, 290		N/A	21	12	Roll decay	N/A	25
374	12.5	0.230	N/A	10/11/07, 0012HR	0	14, 290		N/A	21	9	Roll decay	N/A	25
375	12.5	0.230	N/A	10/11/07, 0015HR	0	14, 290		N/A	21	36	Roll decay	N/A	25
376	0.0	0.000	N/A	10/11/07, 0055HR	180	11, 283		N/A	21		Zero run, boresight set at 0.7, -0.551	N/A	8
377	15.2	0.279	N/A	10/11/07, 0101HR	180	11, 283		N/A	21		Steady state, control fins on auto, zero taken at 1.1 kt	N/A	8
378	15.2	0.279	N/A	10/11/07, 0104HR	180	11, 283		N/A	21	61	Roll decay	N/A	8
379	15.2	0.279	N/A	10/11/07, 0107HR	180	11, 283		N/A	21	13	Roll decay	N/A	8
380	15.2	0.279	N/A	10/11/07, 0109HR	180	11, 283		N/A	21	13	Roll decay	N/A	8
381	15.2	0.279	N/A	10/11/07, 0110HR	180	11, 283		N/A	21	15	Roll decay	N/A	8
382	15.2	0.279	N/A	10/11/07, 0112HR	180	11, 283		N/A	21	13	Roll decay	N/A	8
383	15.2	0.279	N/A	10/11/07, 0114HR	180	11, 283		N/A	21	13	Roll decay	N/A	8

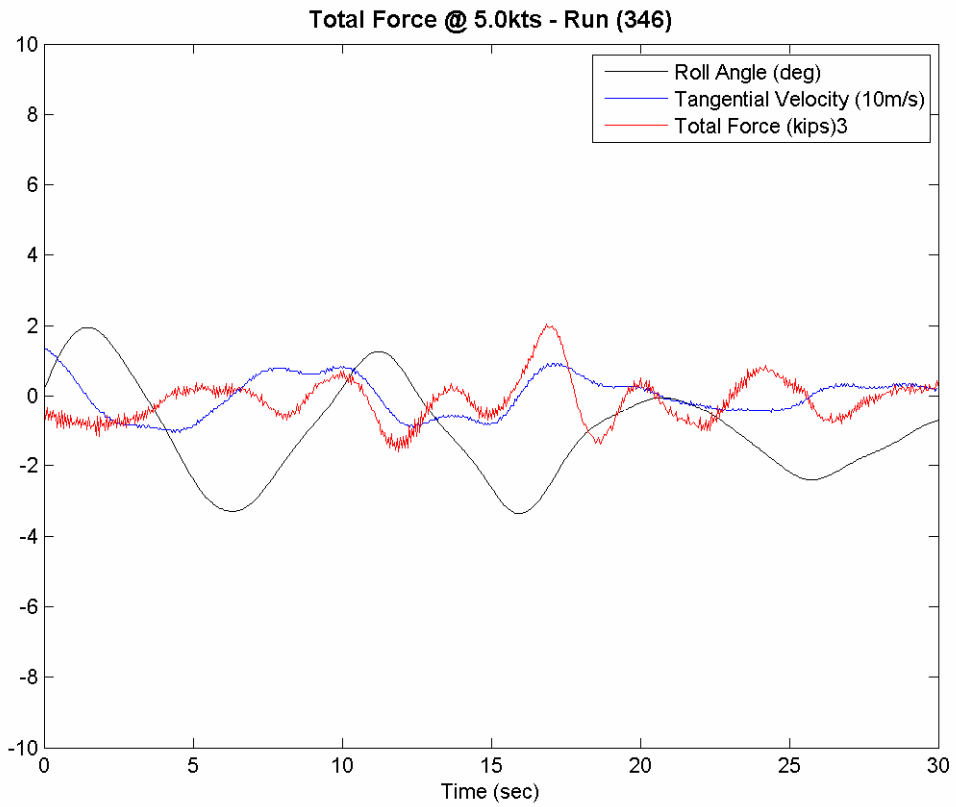
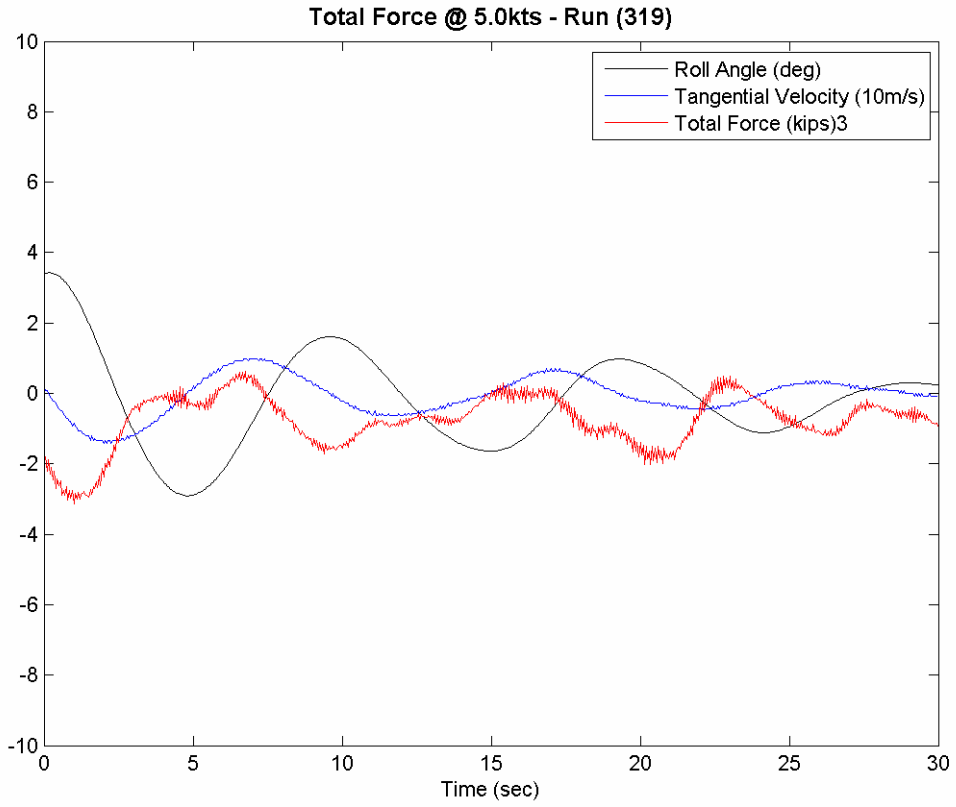
Strain Gage Zeros

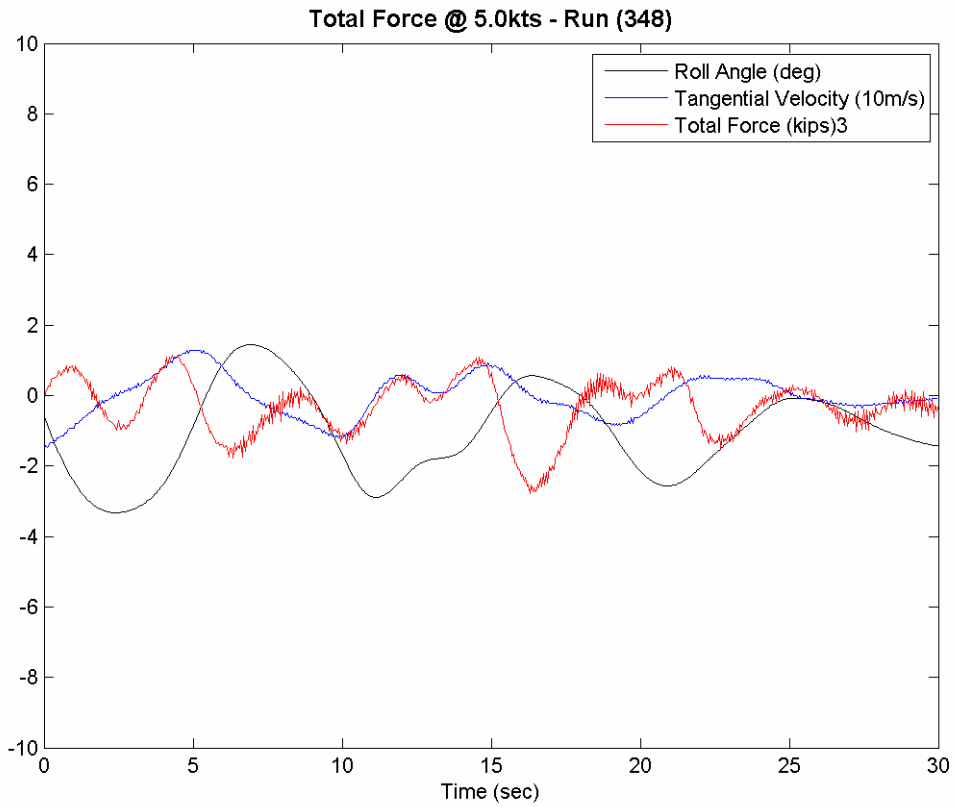
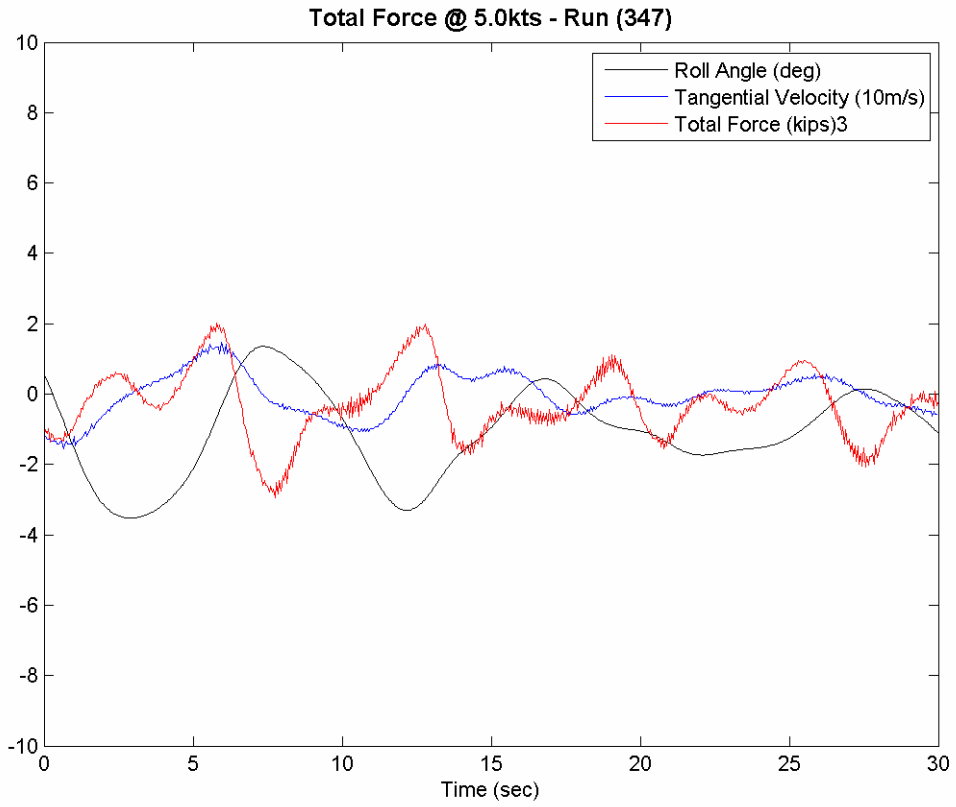


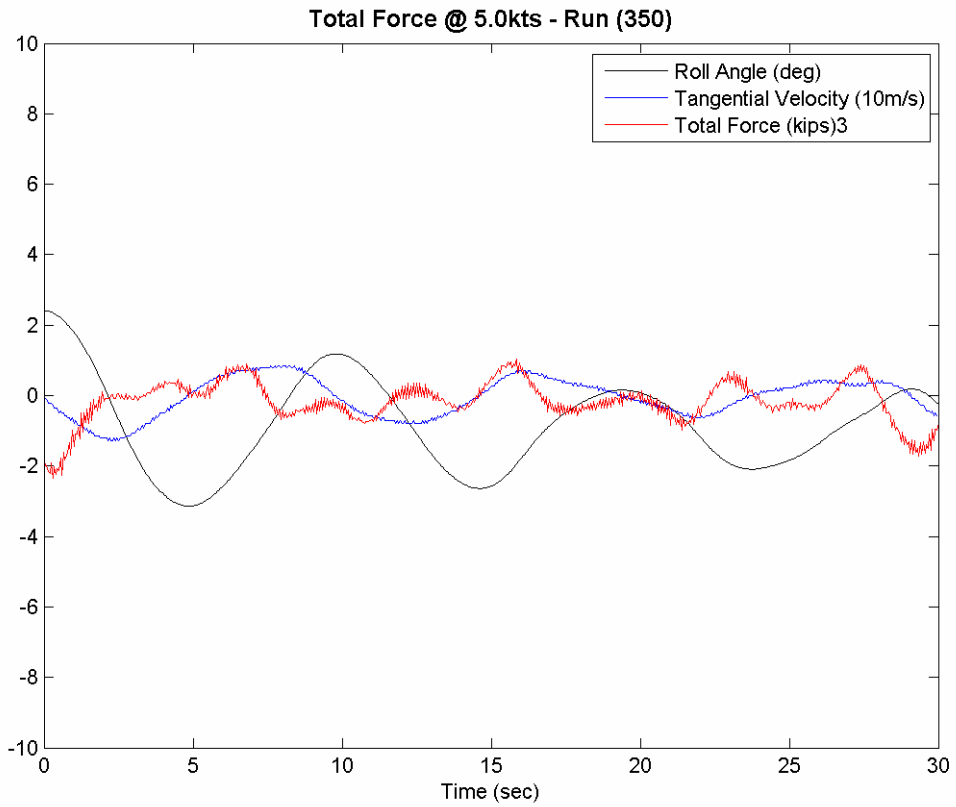
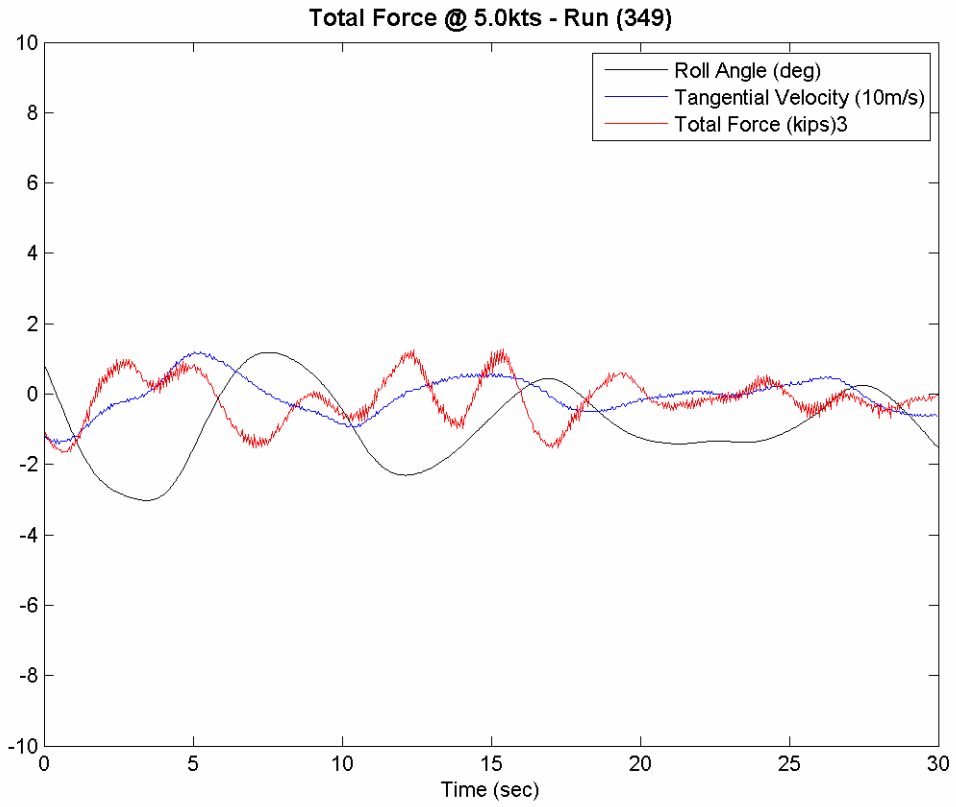
APPENDIX C – COMPLETE ROLL DAMPING FORCE PLOTS

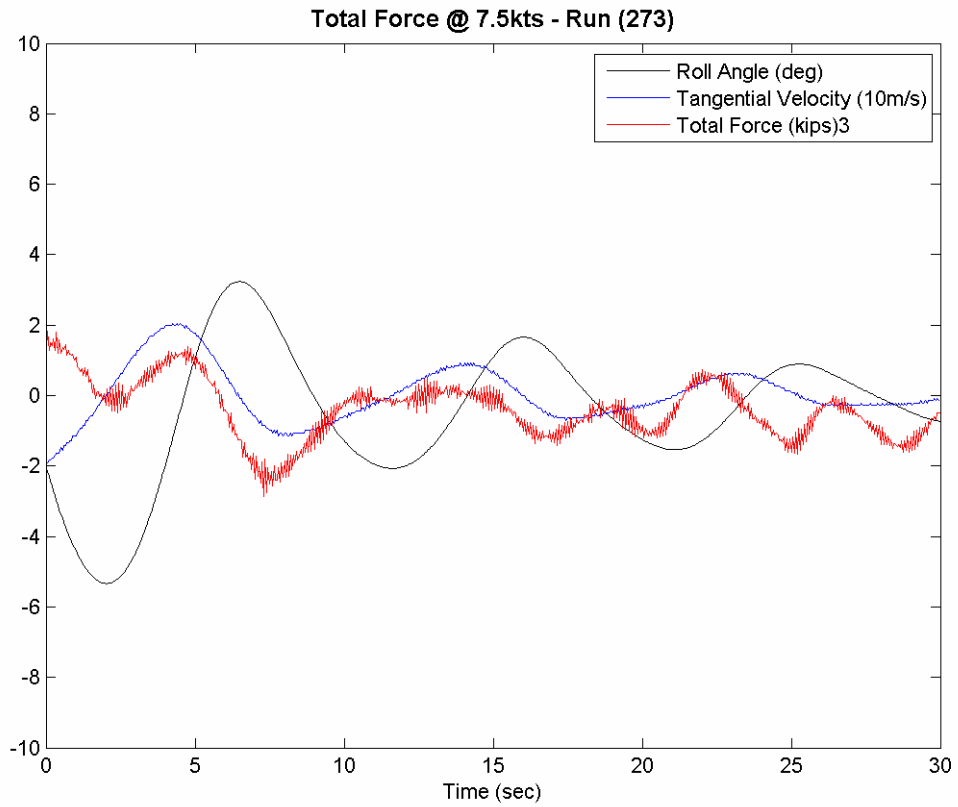
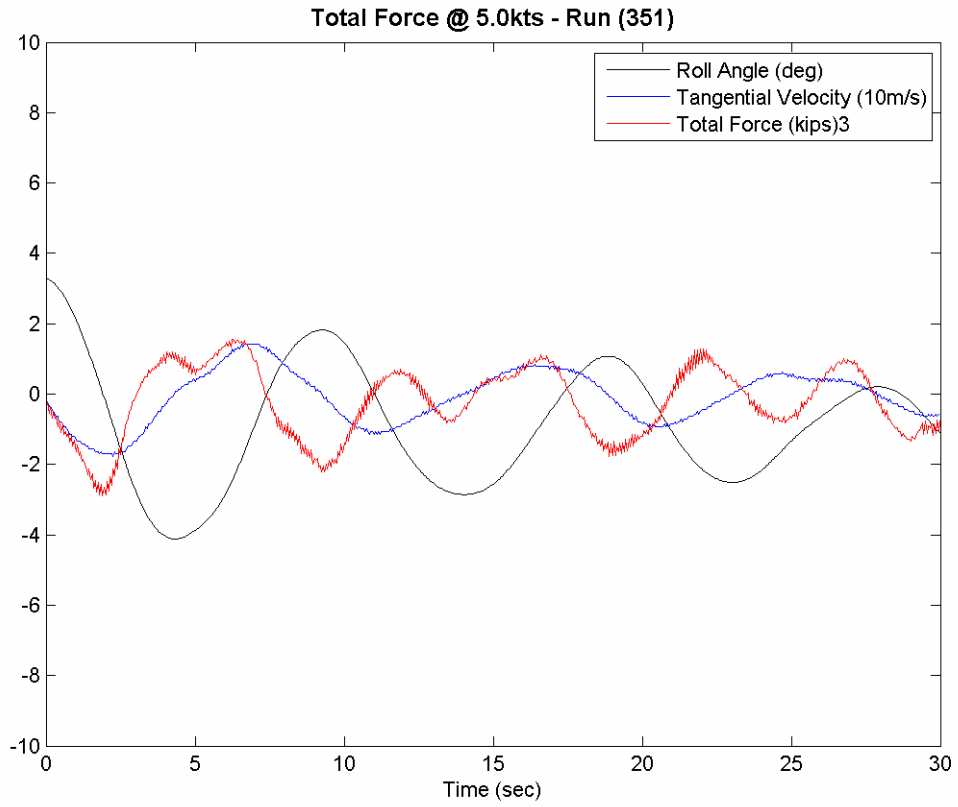


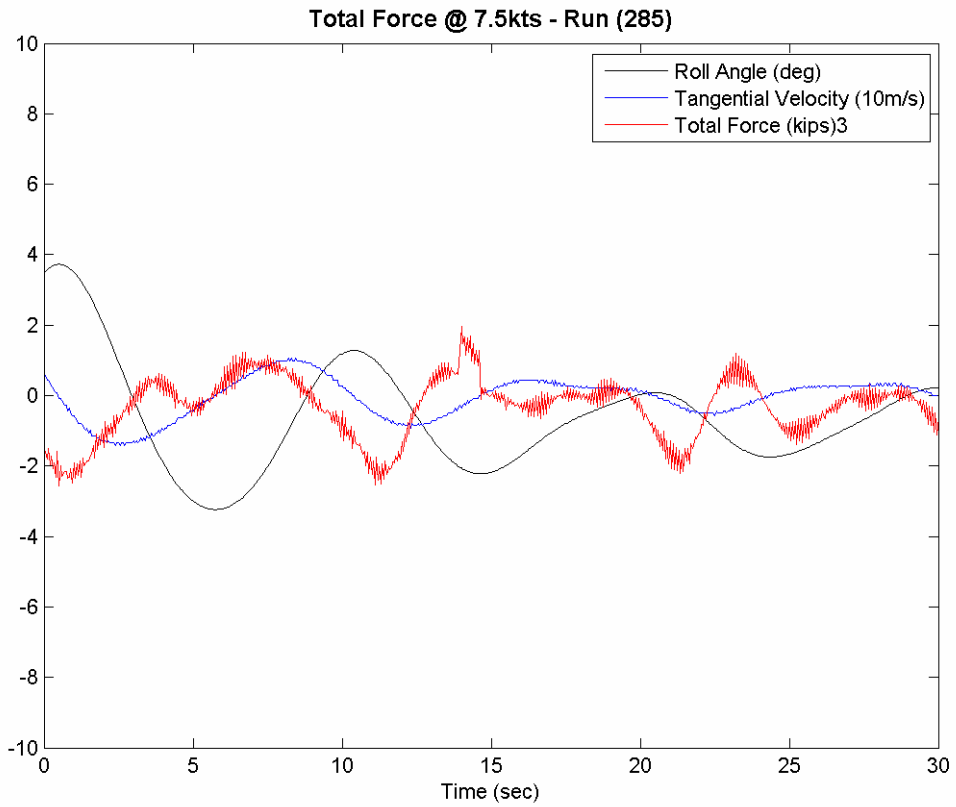
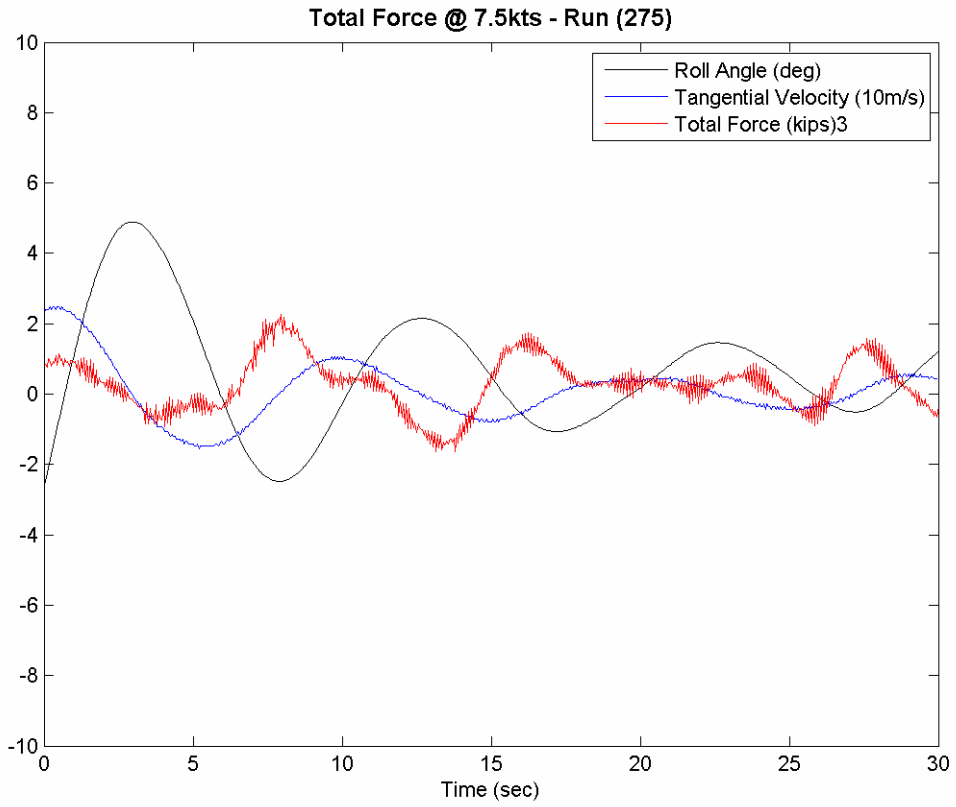


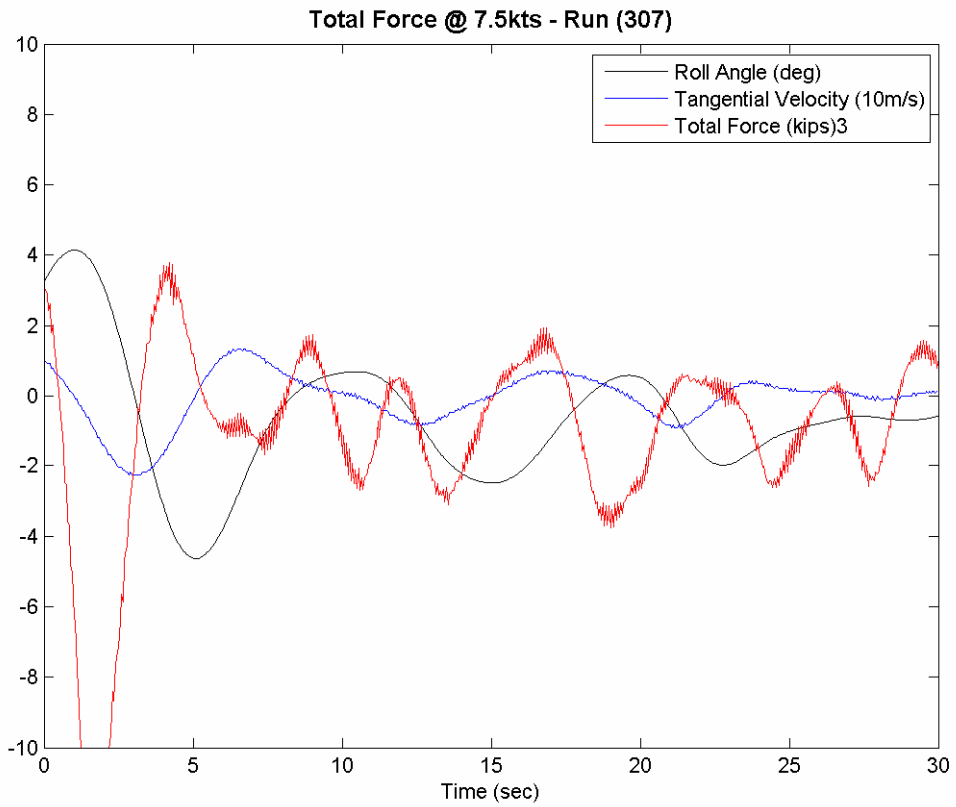
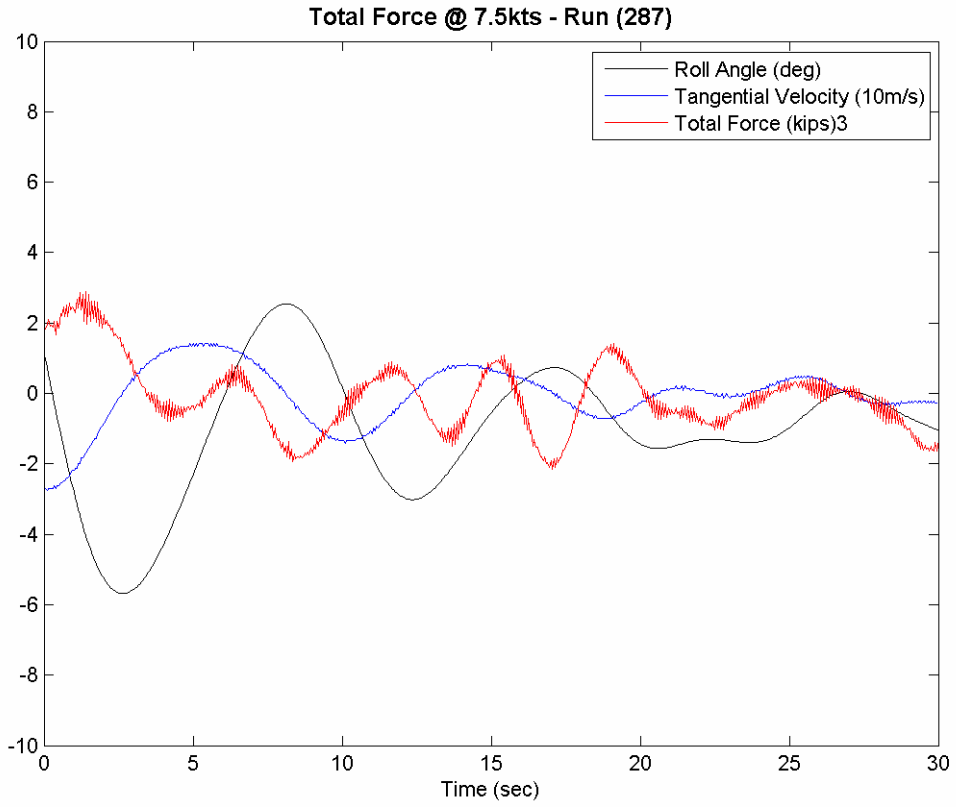


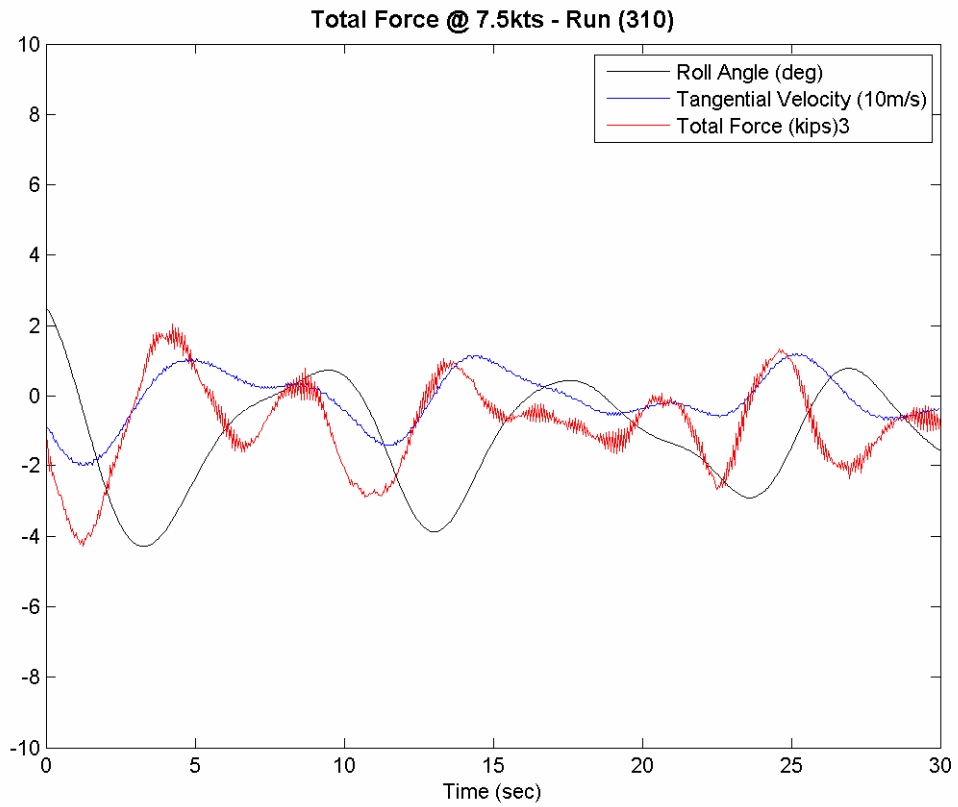
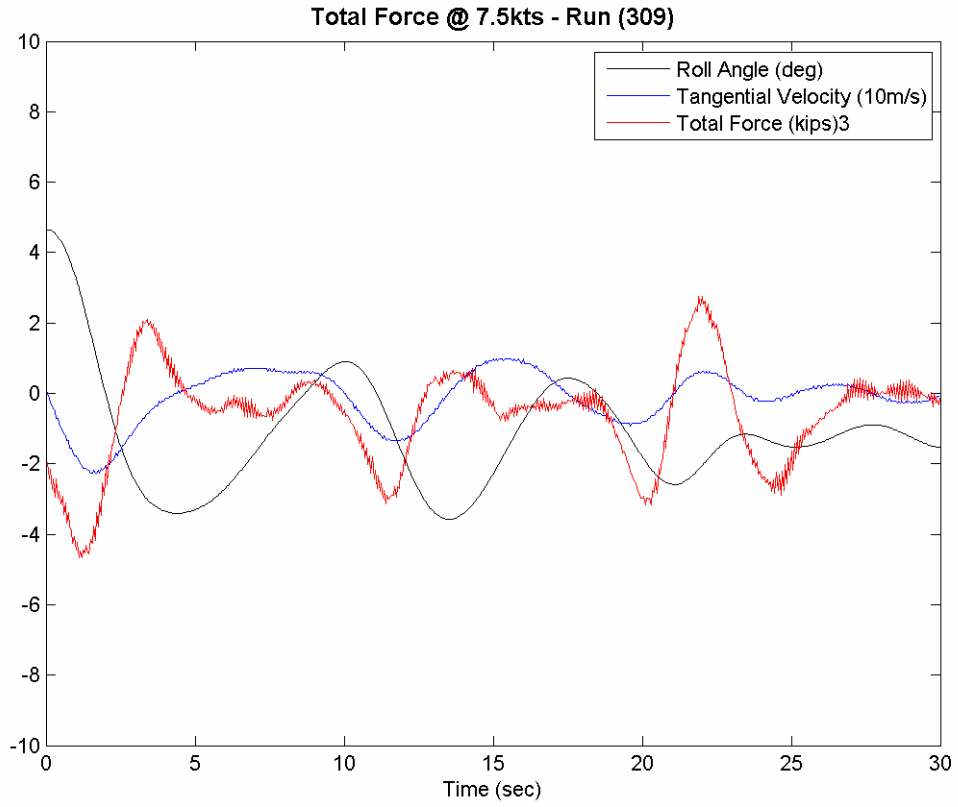


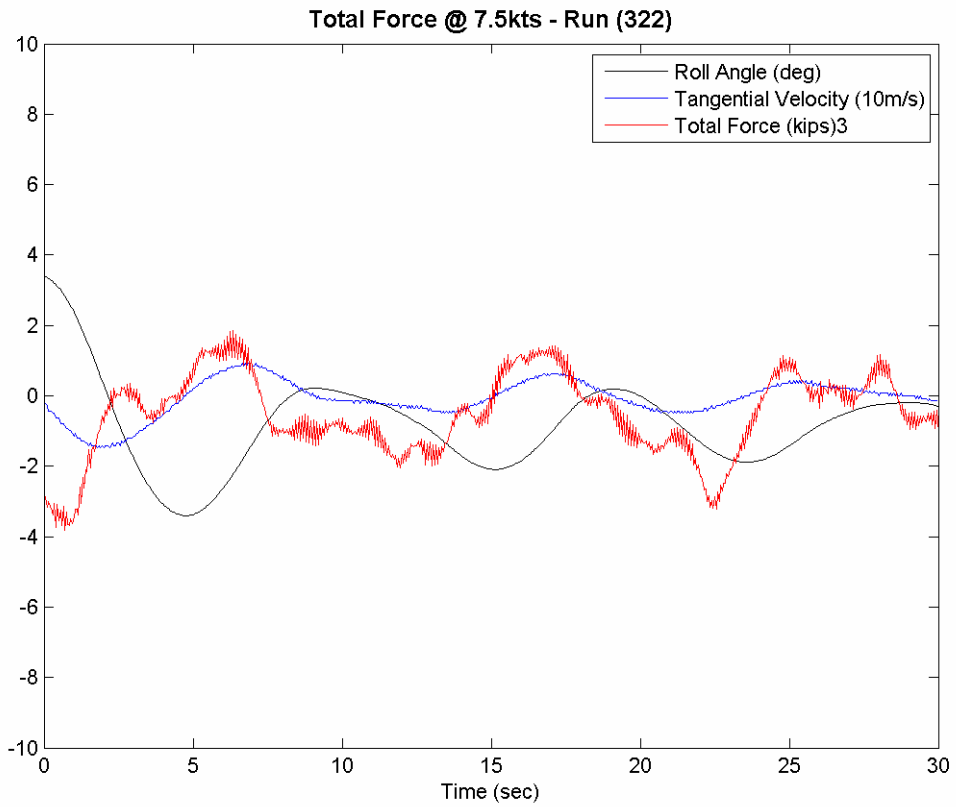
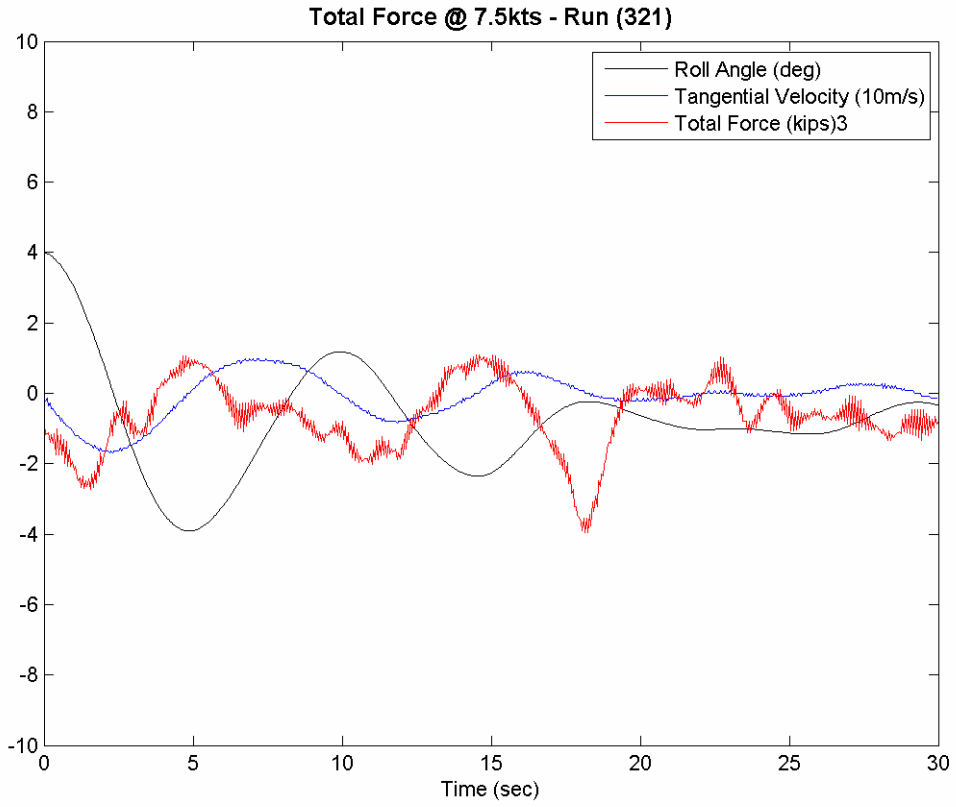


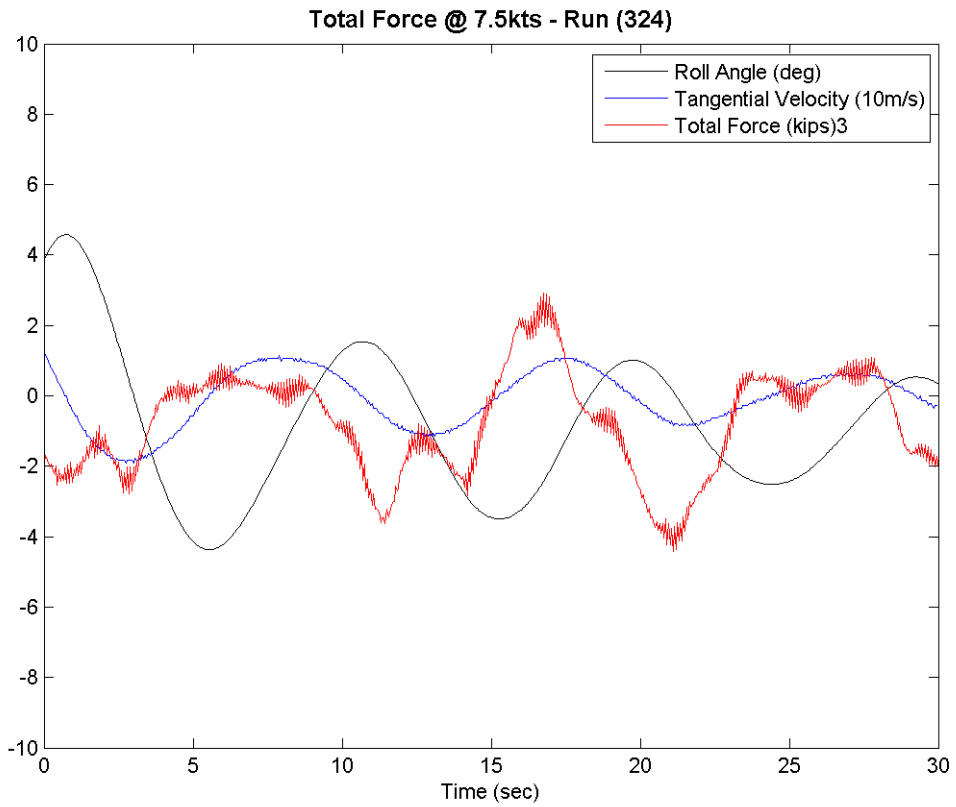
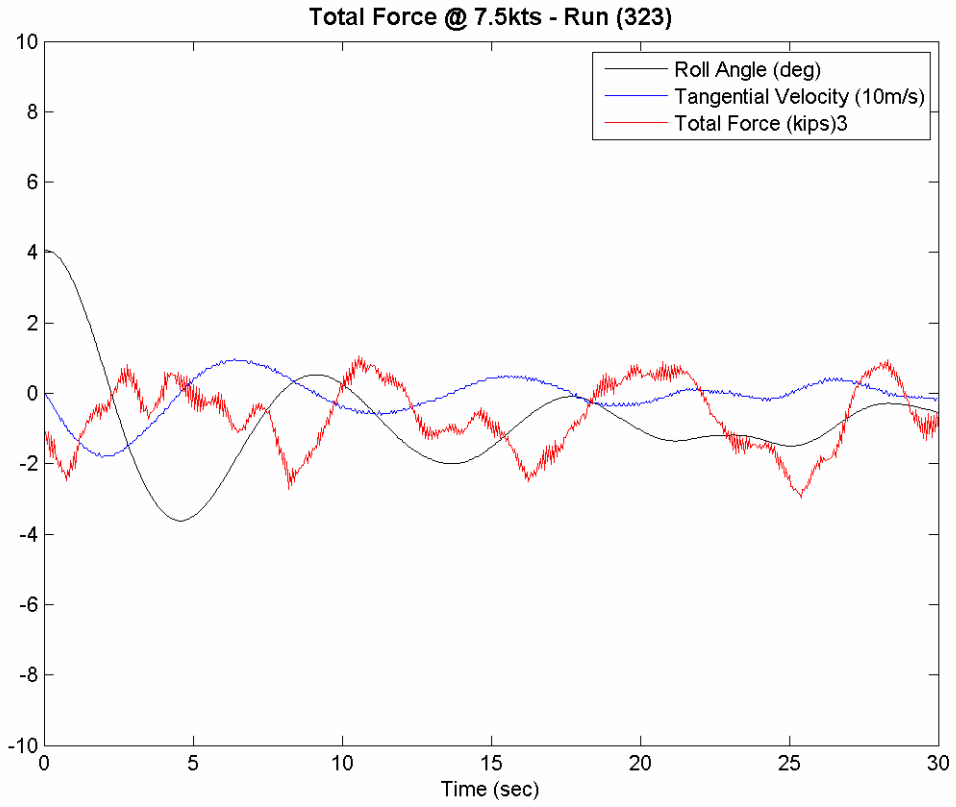


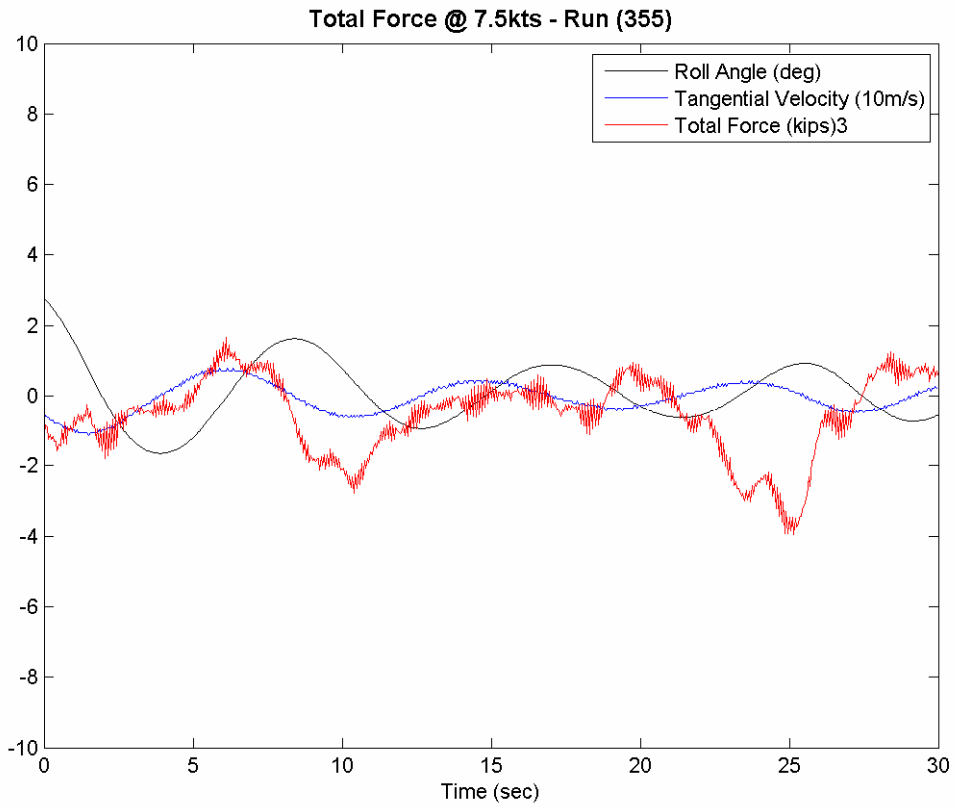
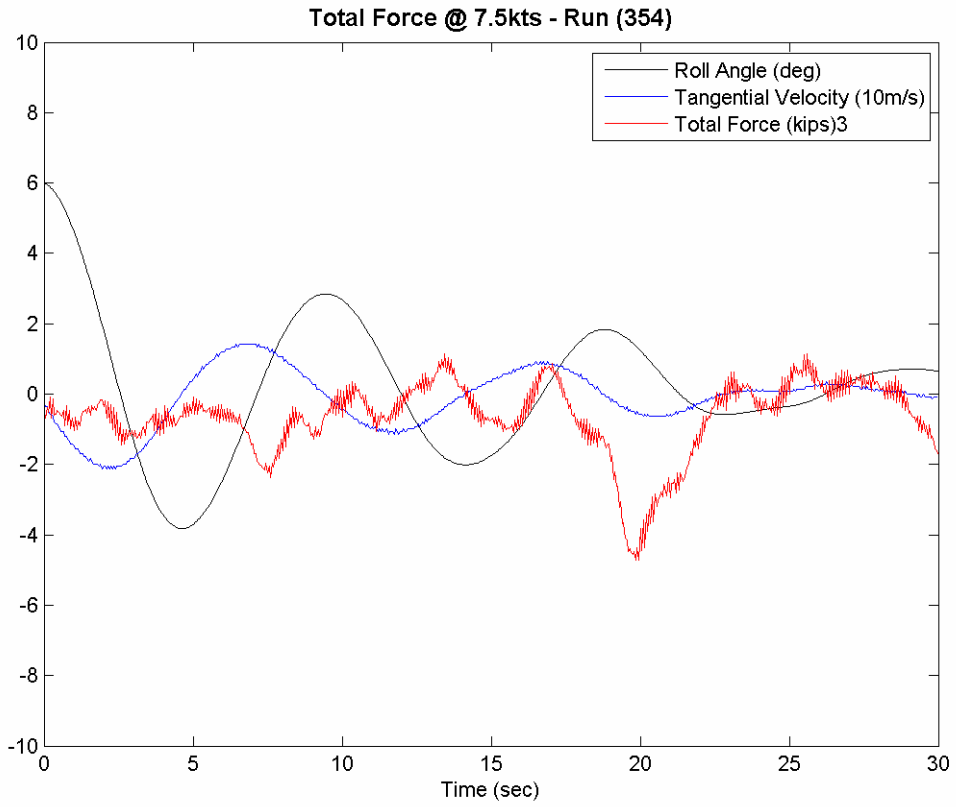


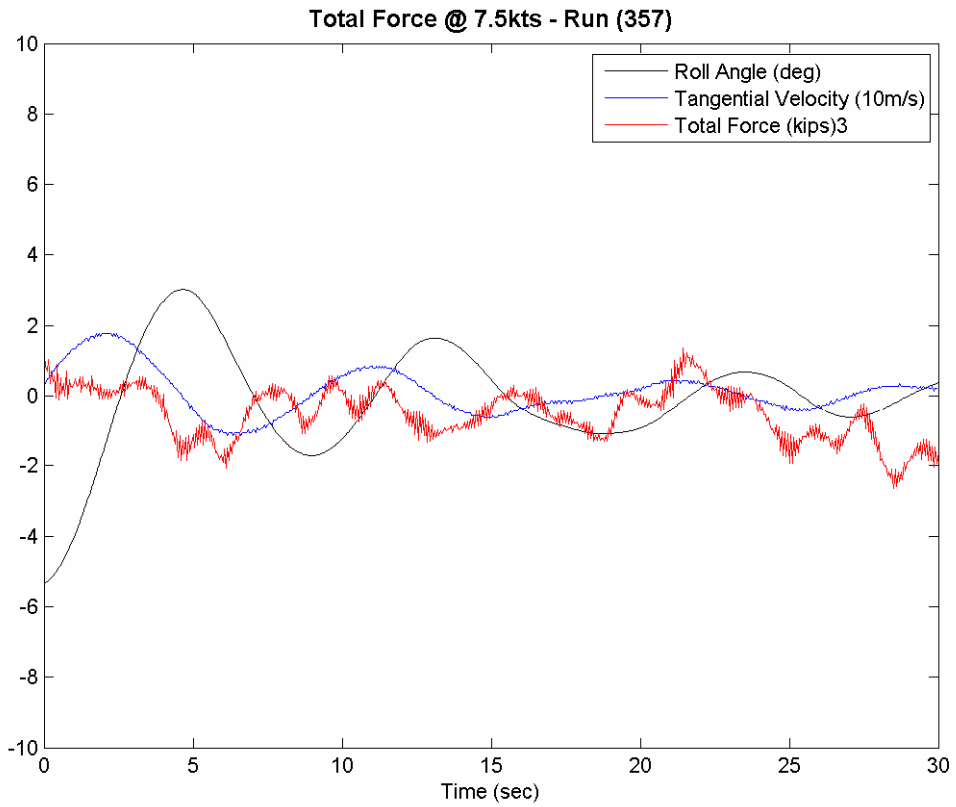
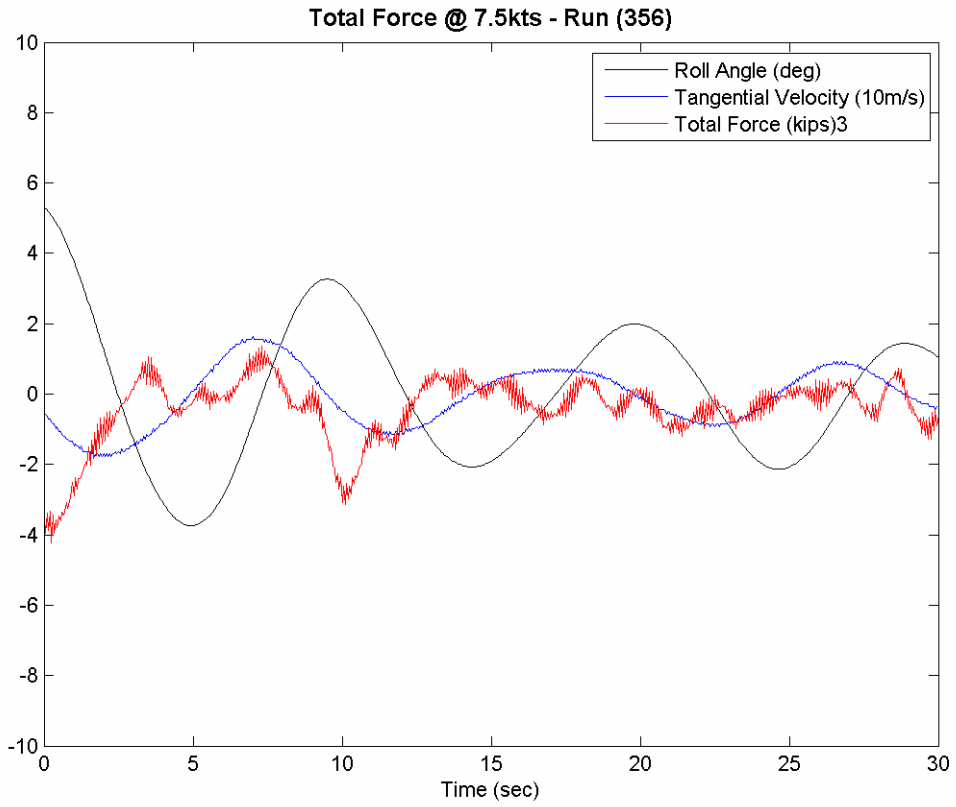


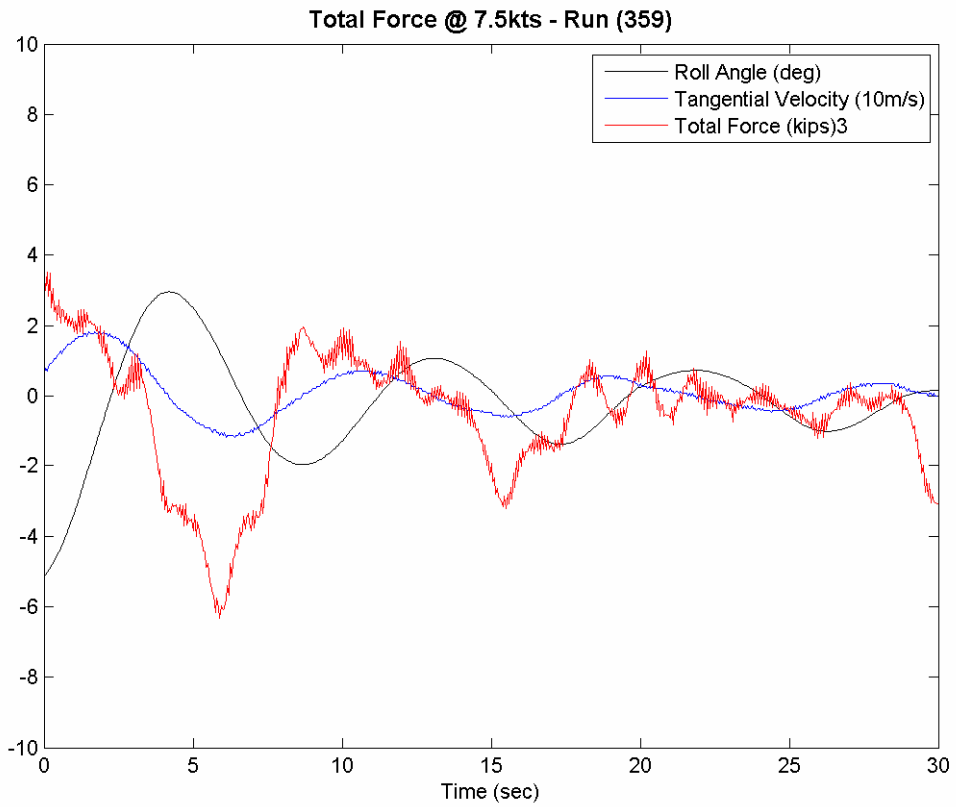


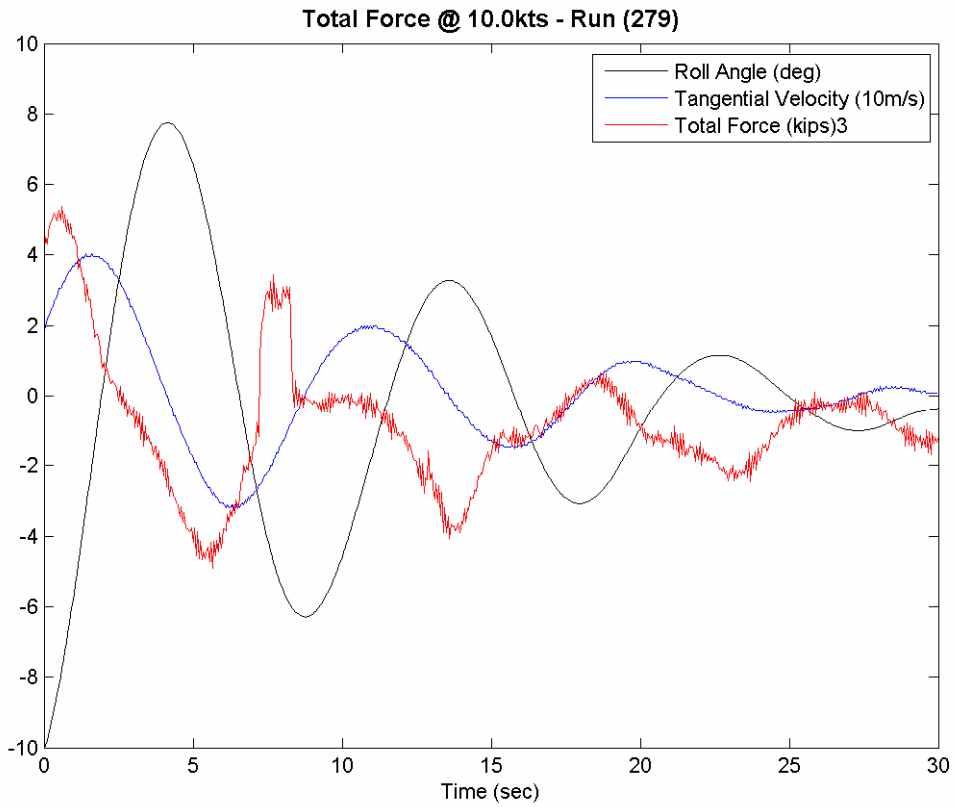
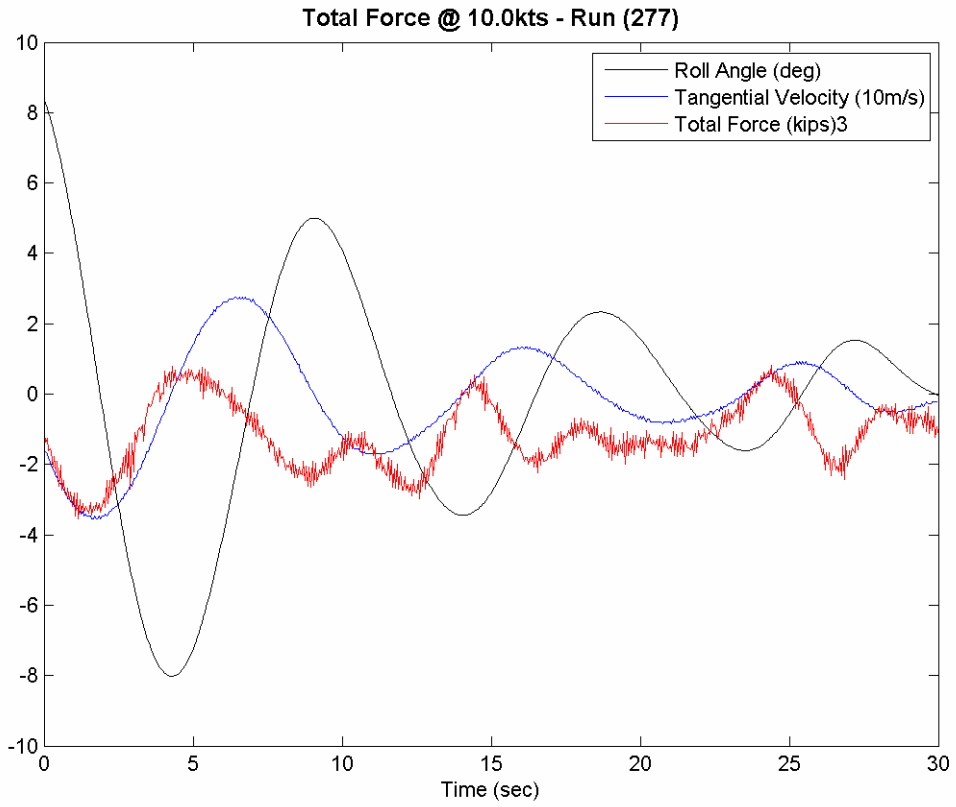


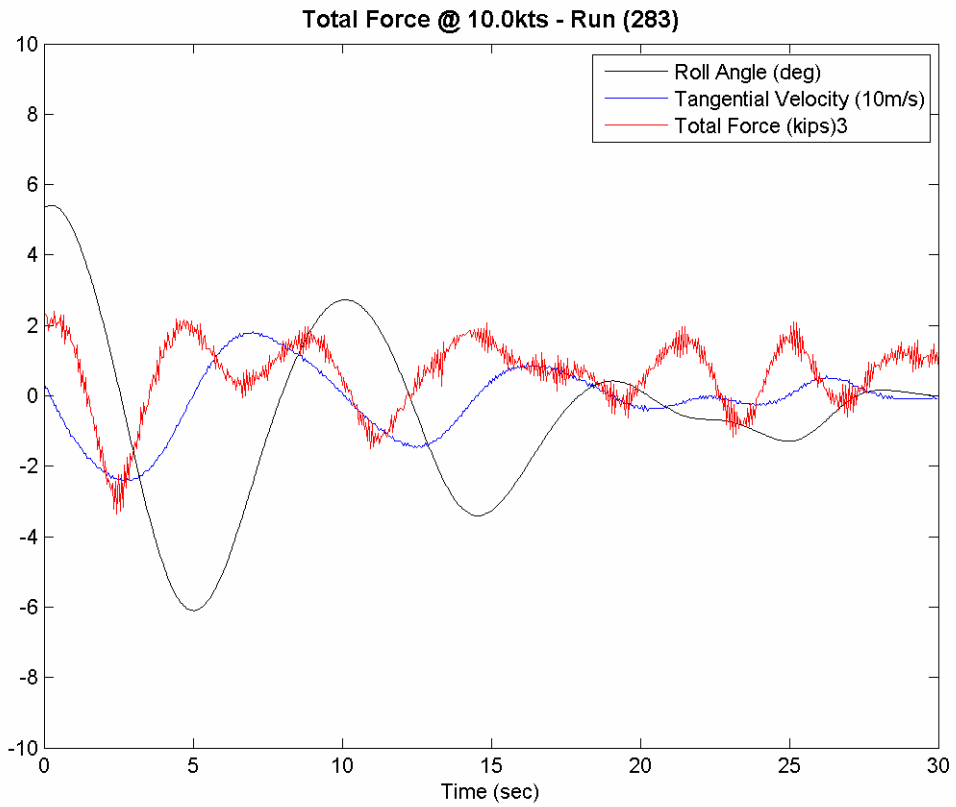
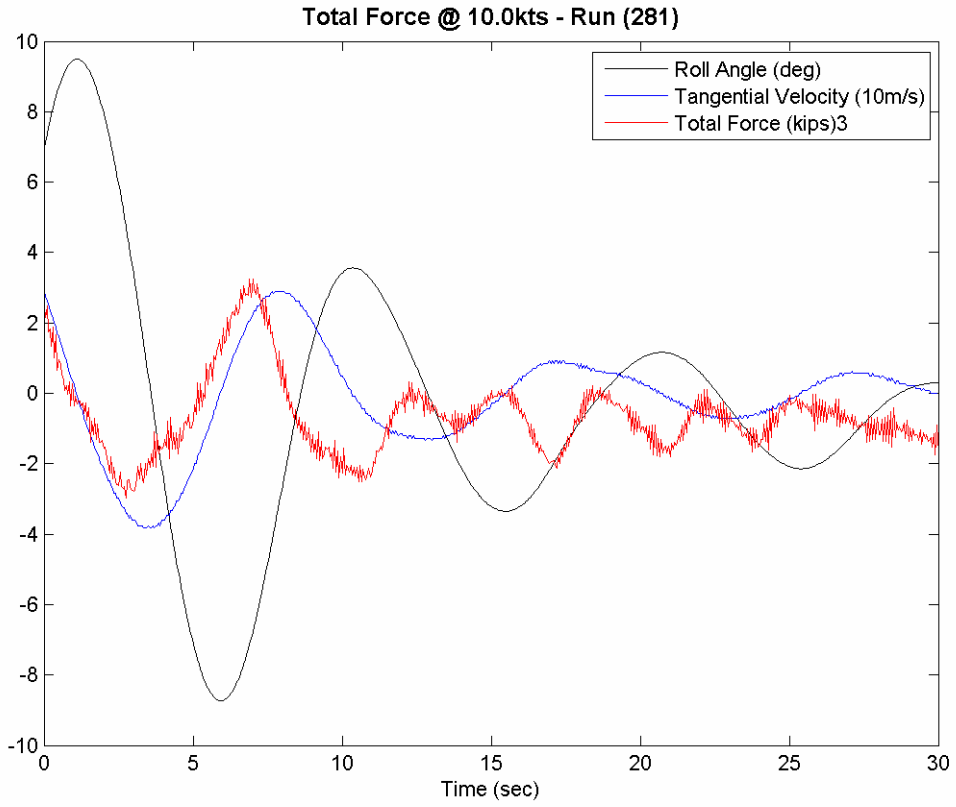


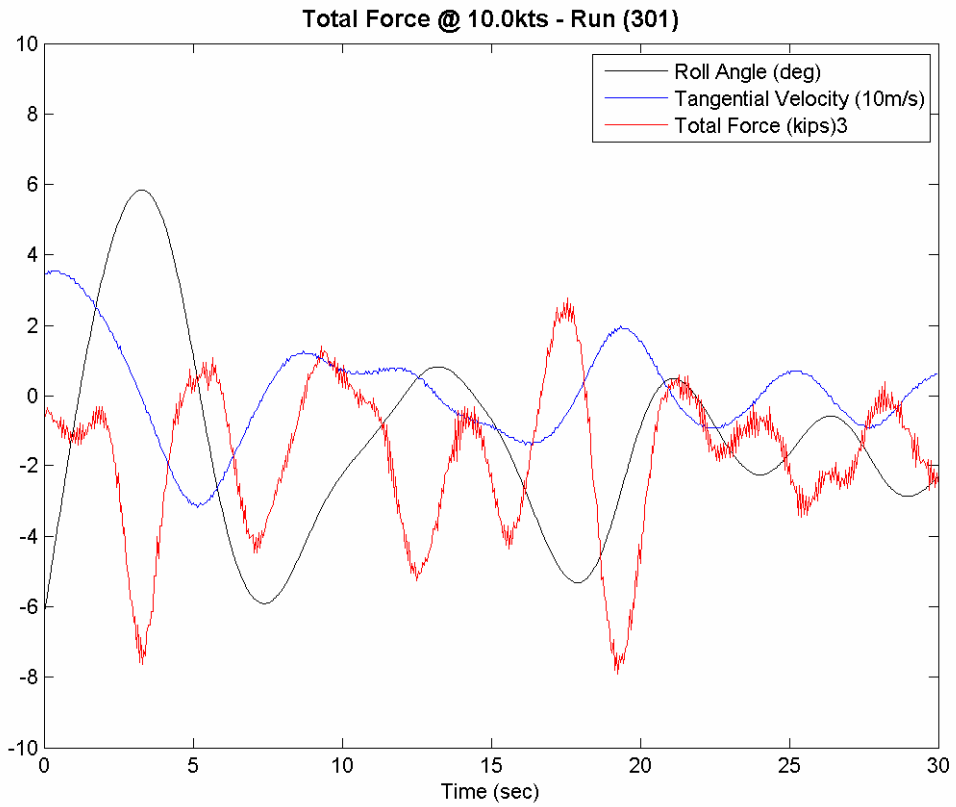
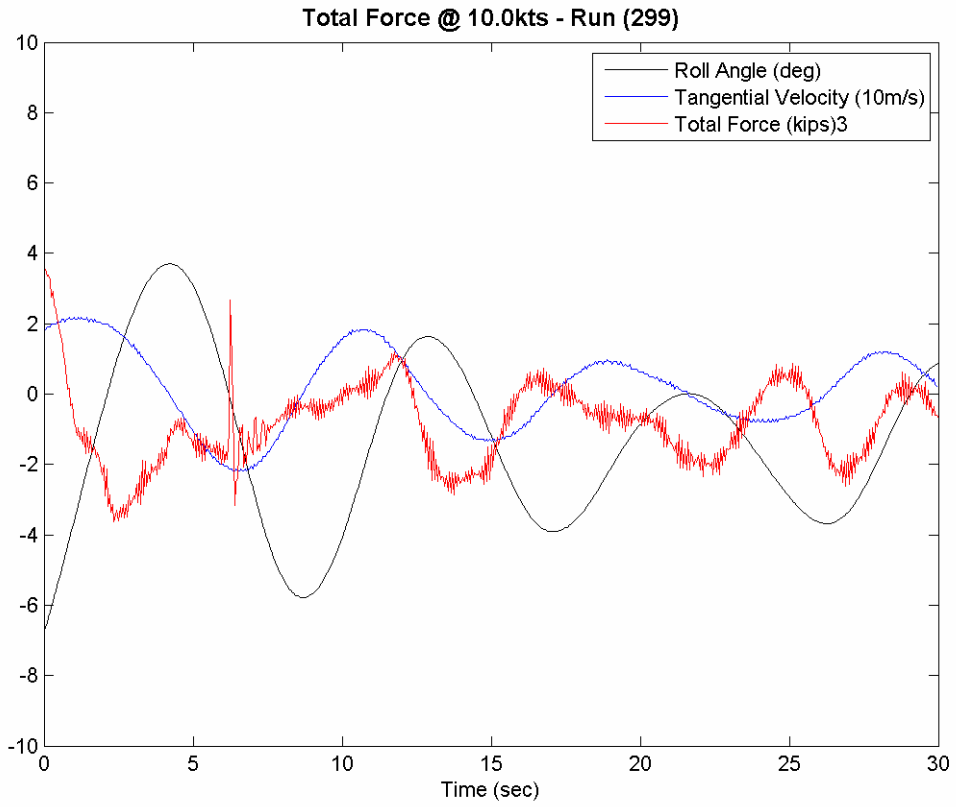


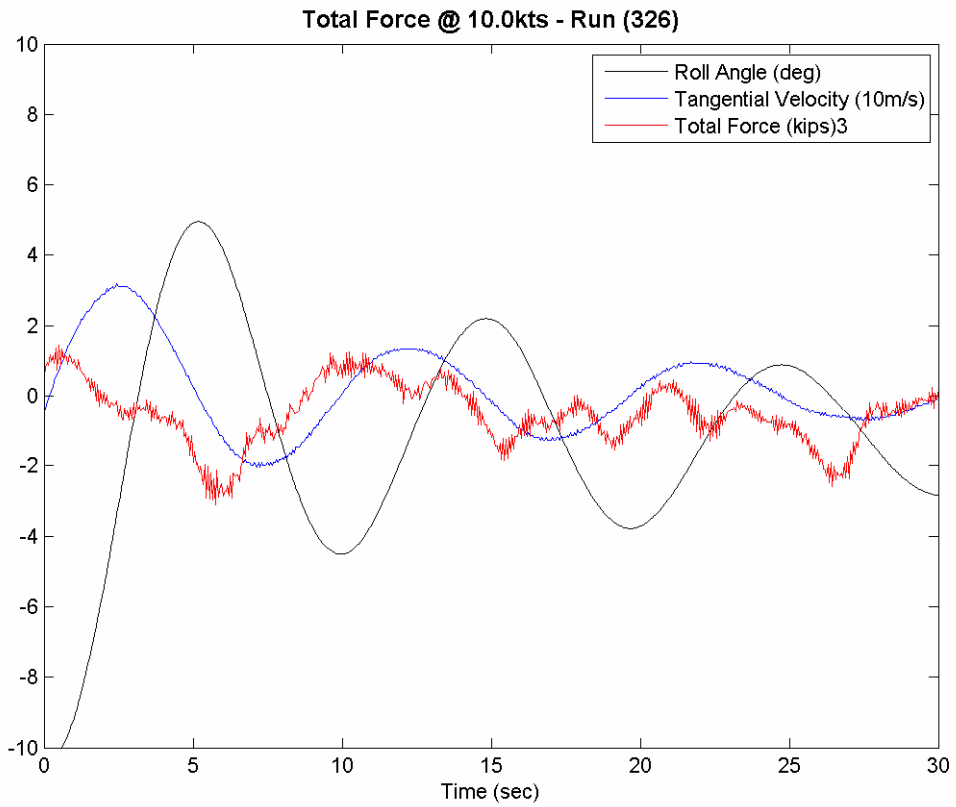
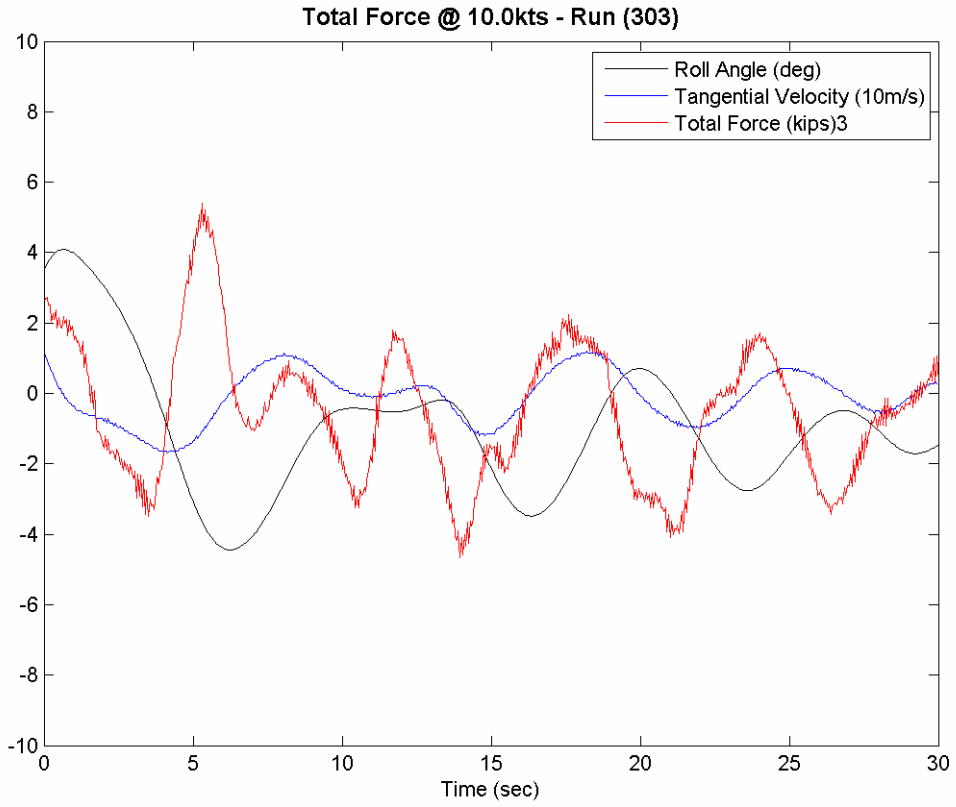


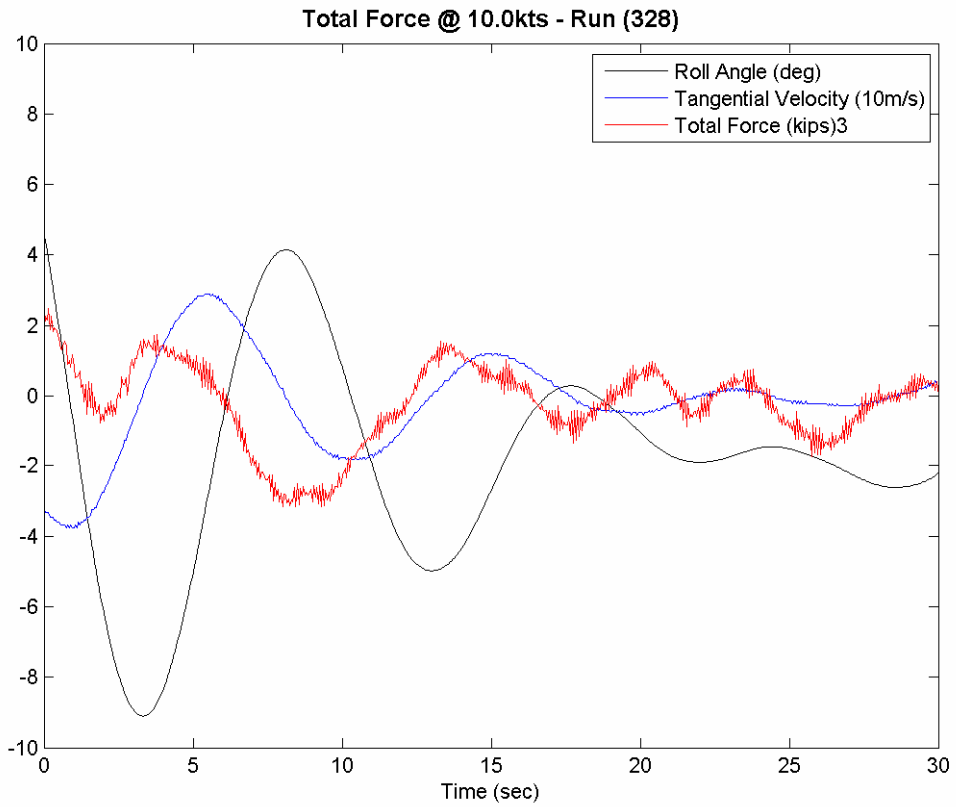
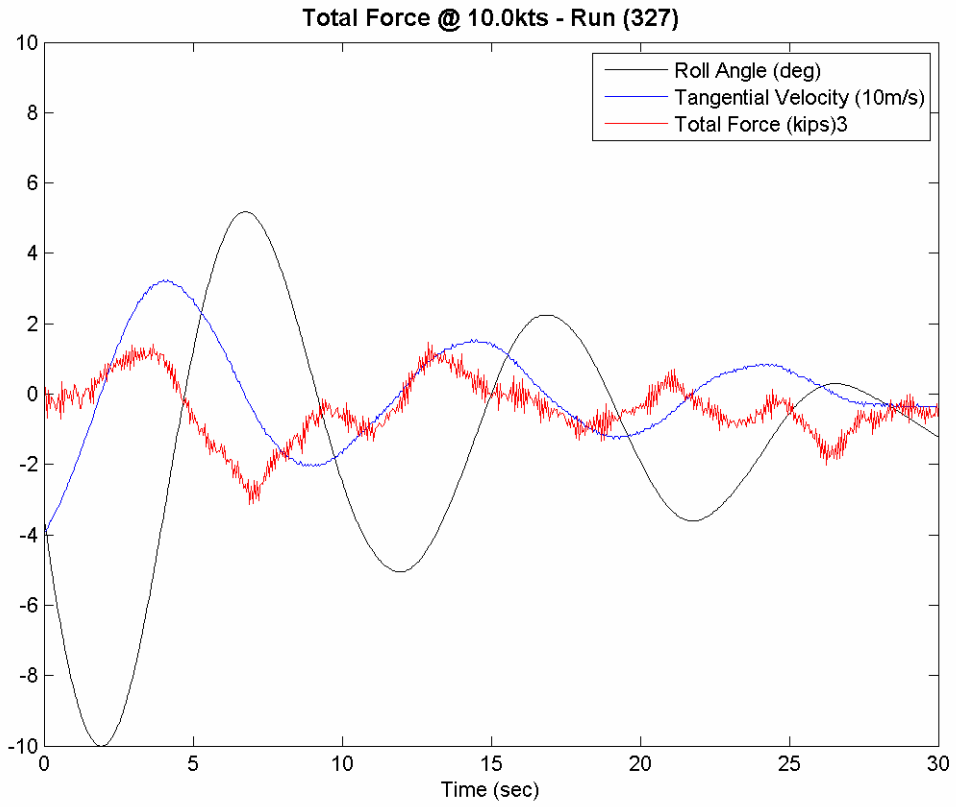


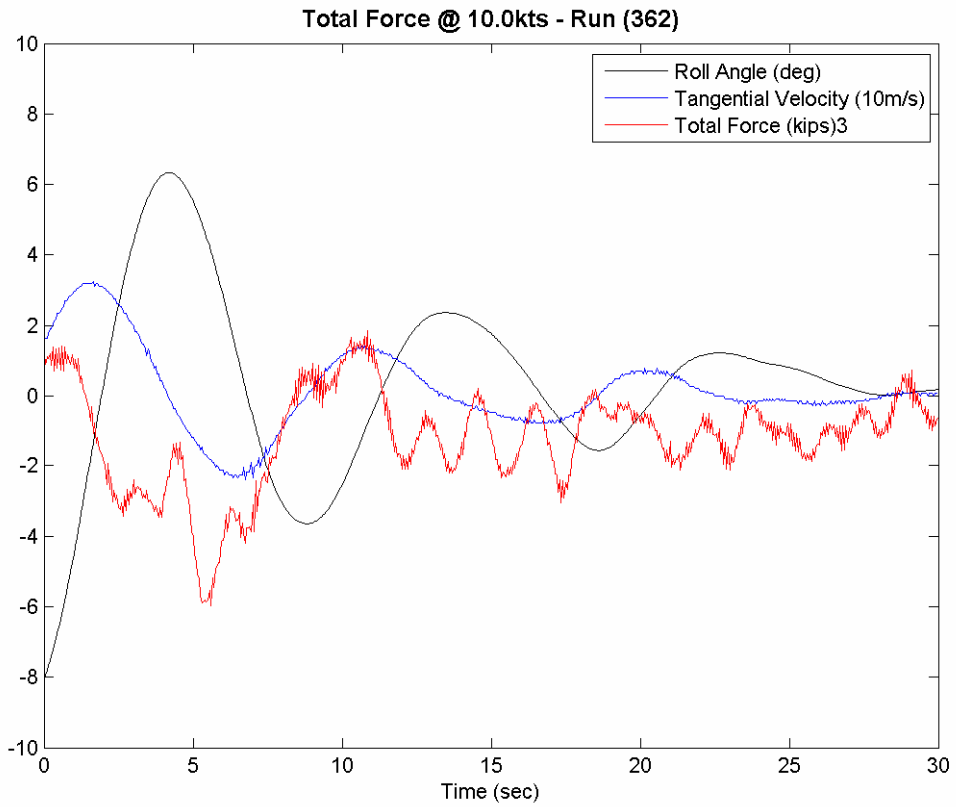
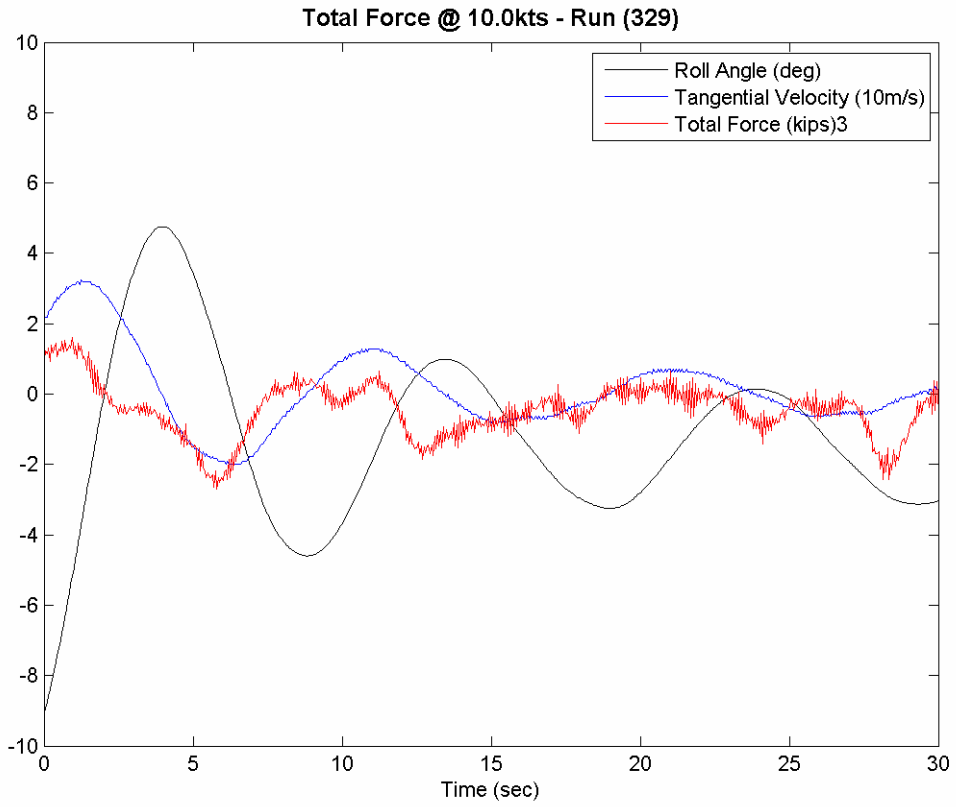


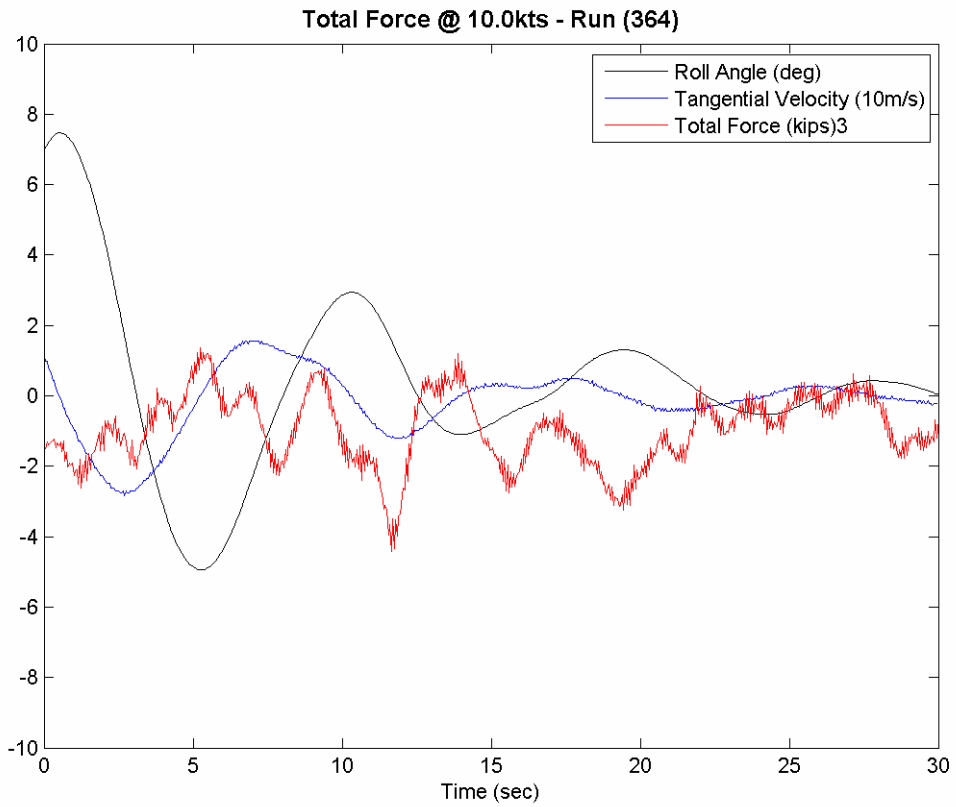
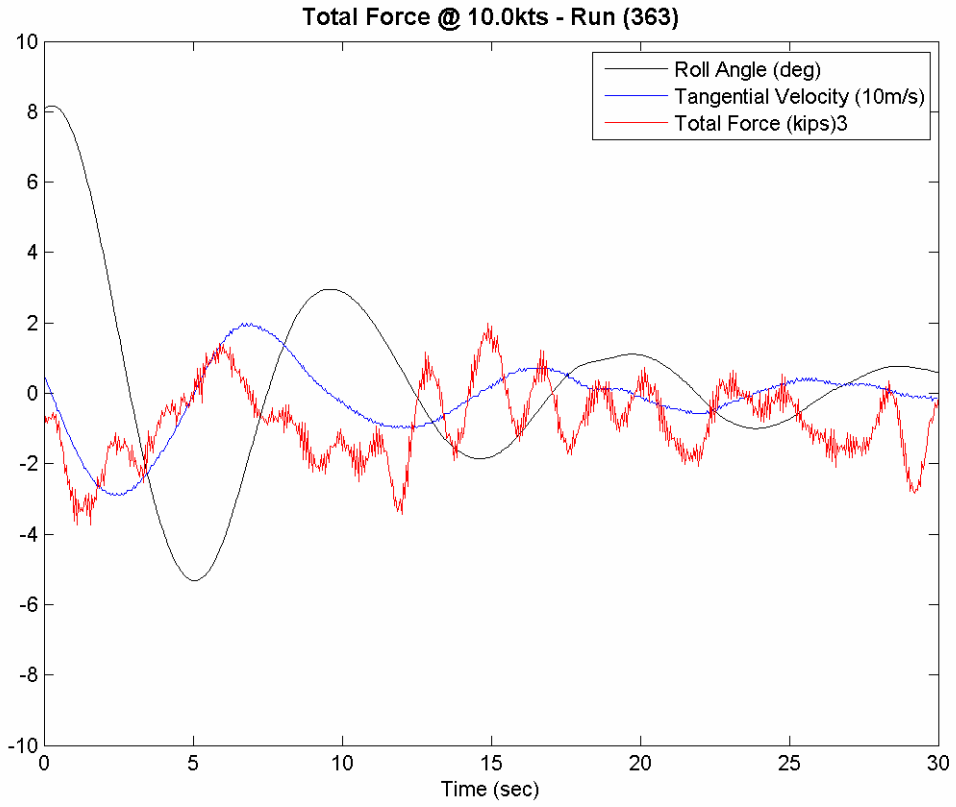


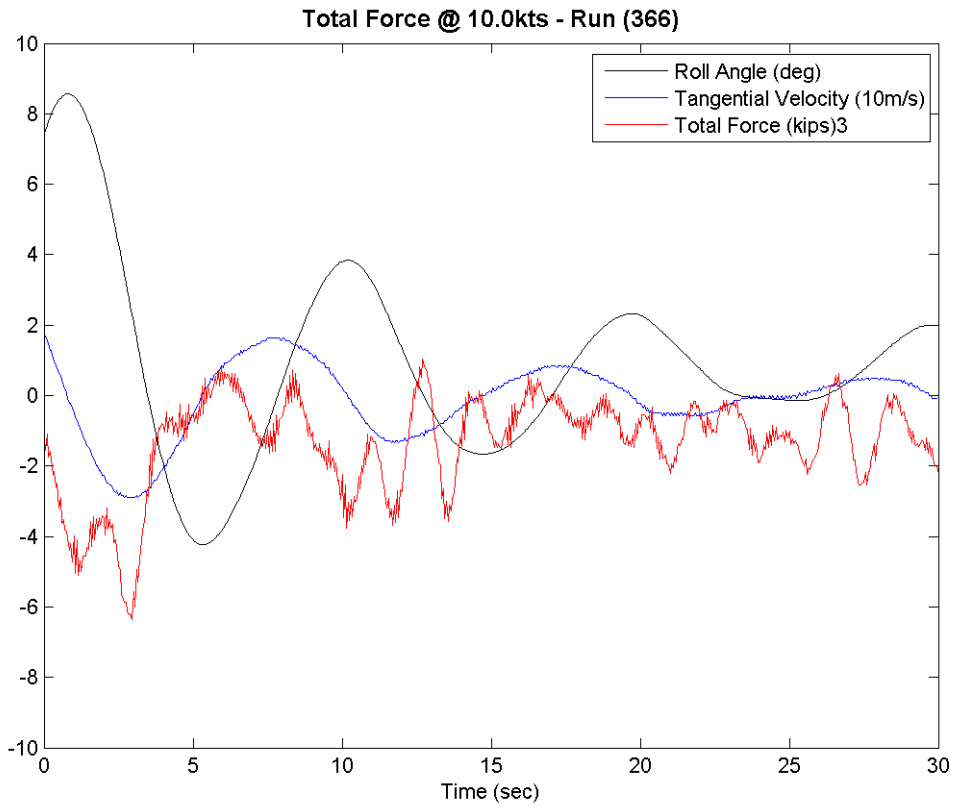
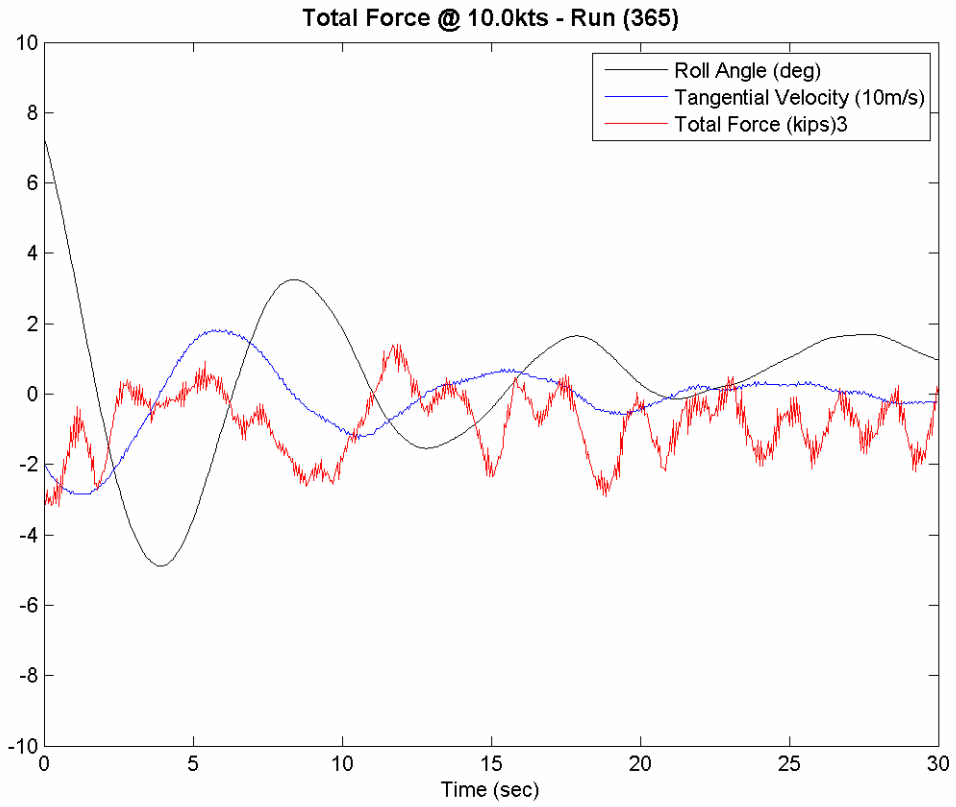


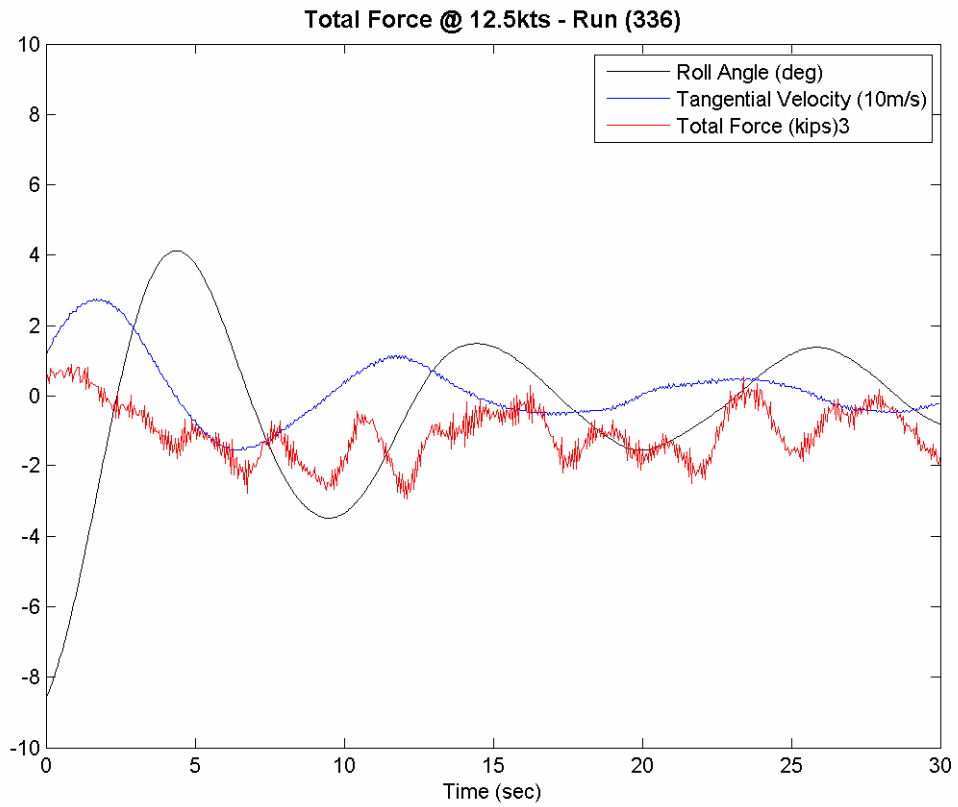
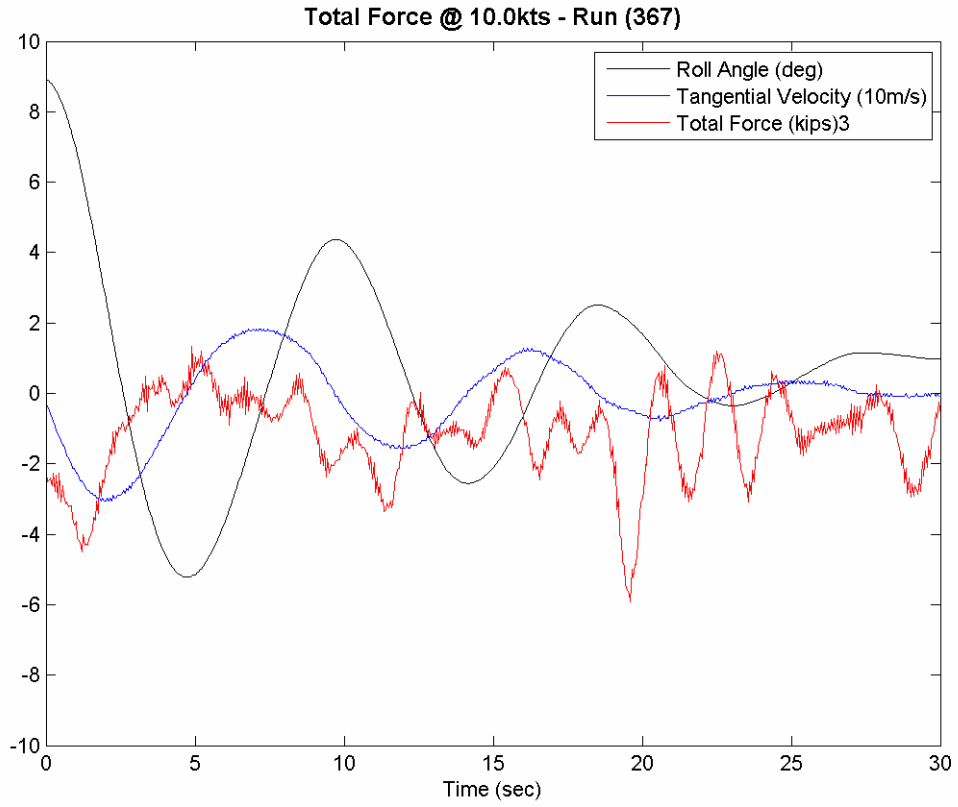


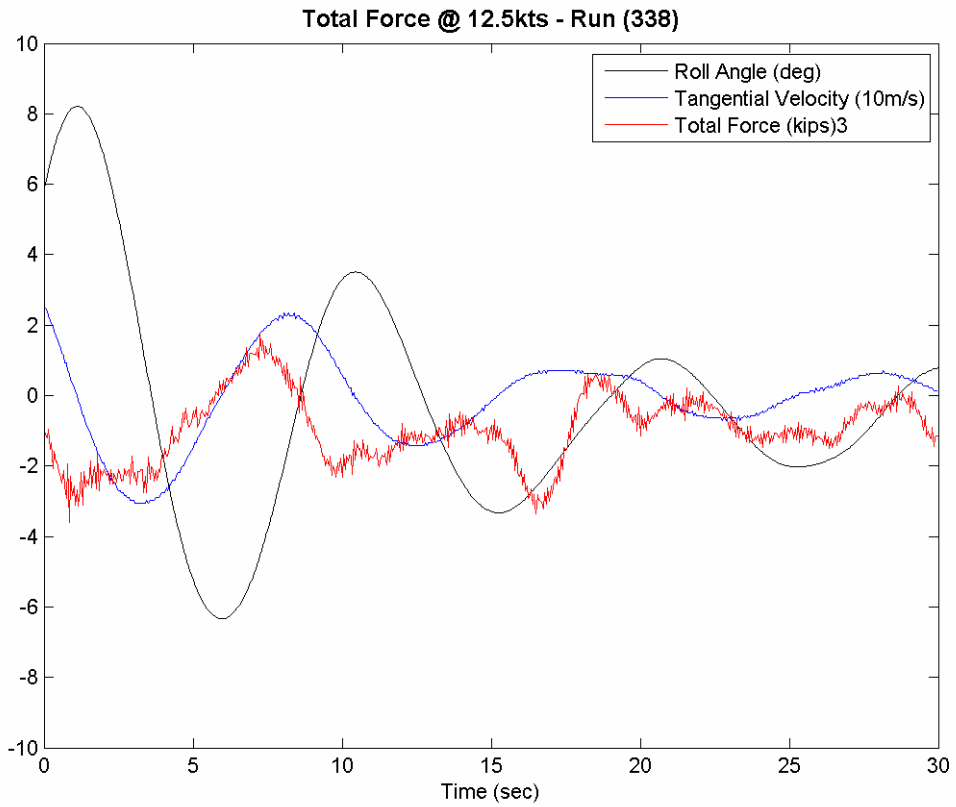
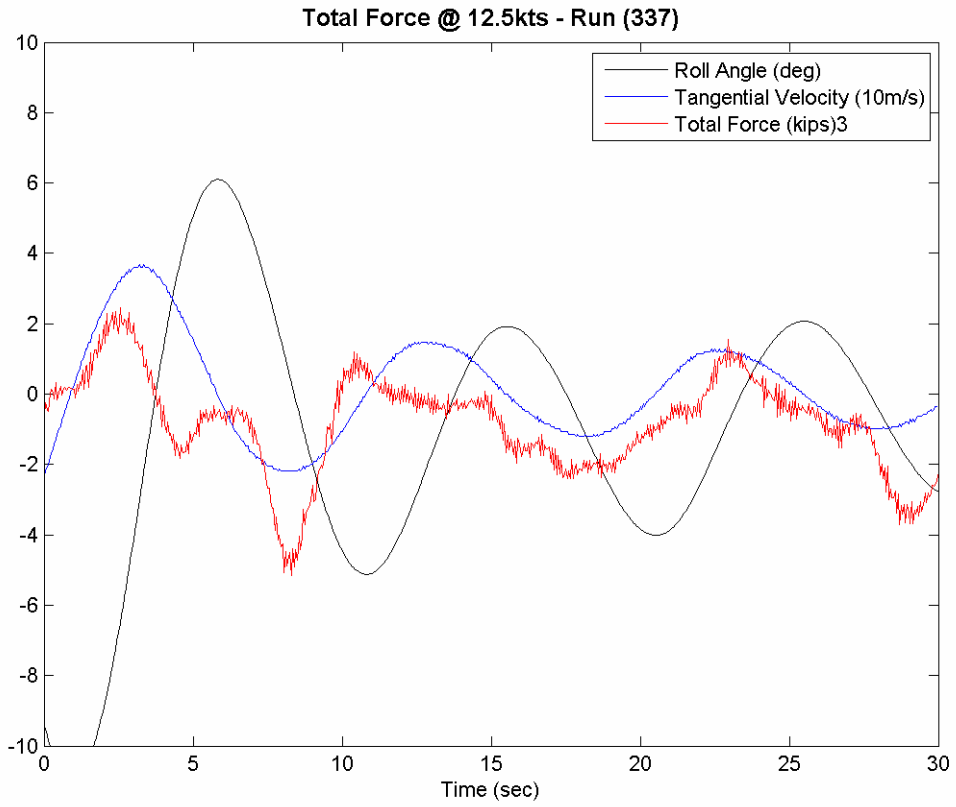




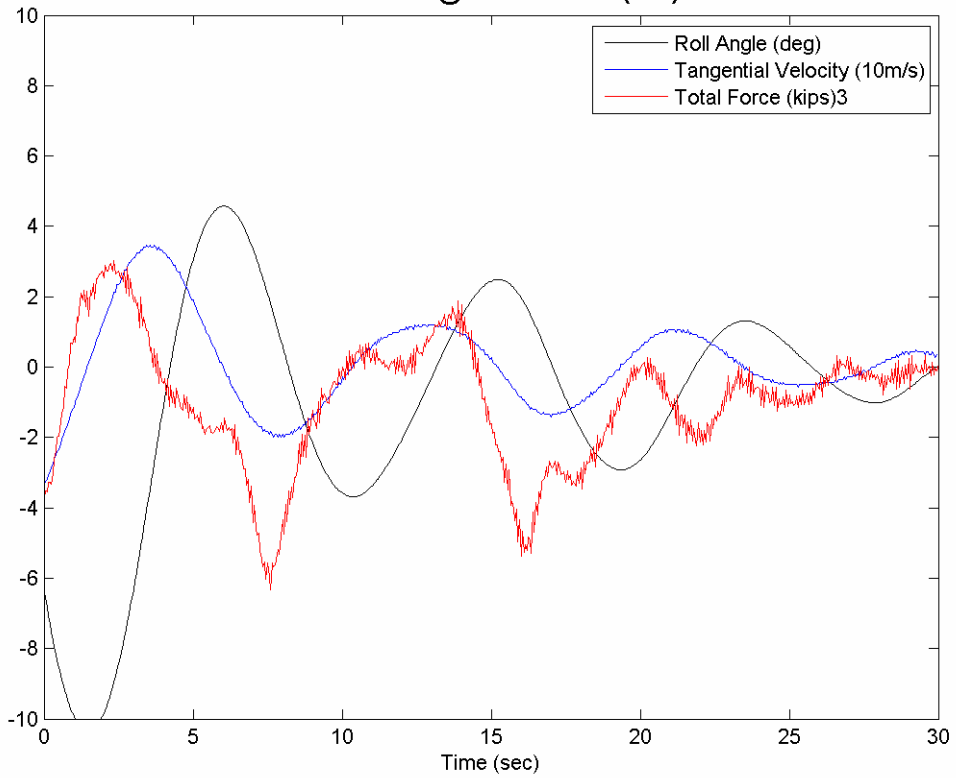




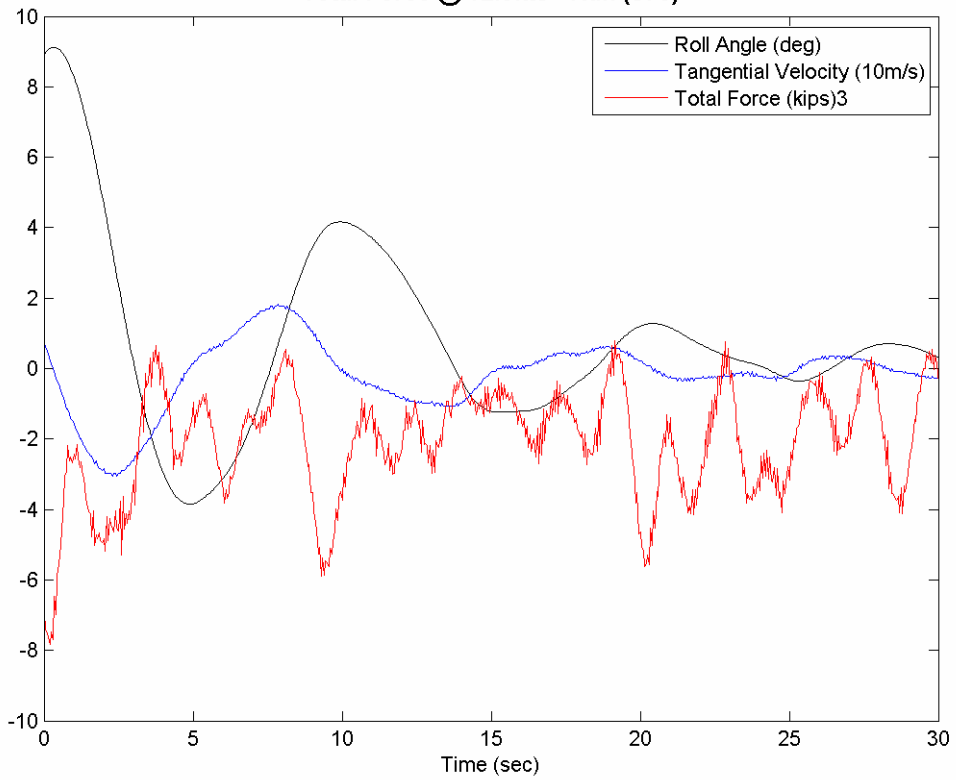


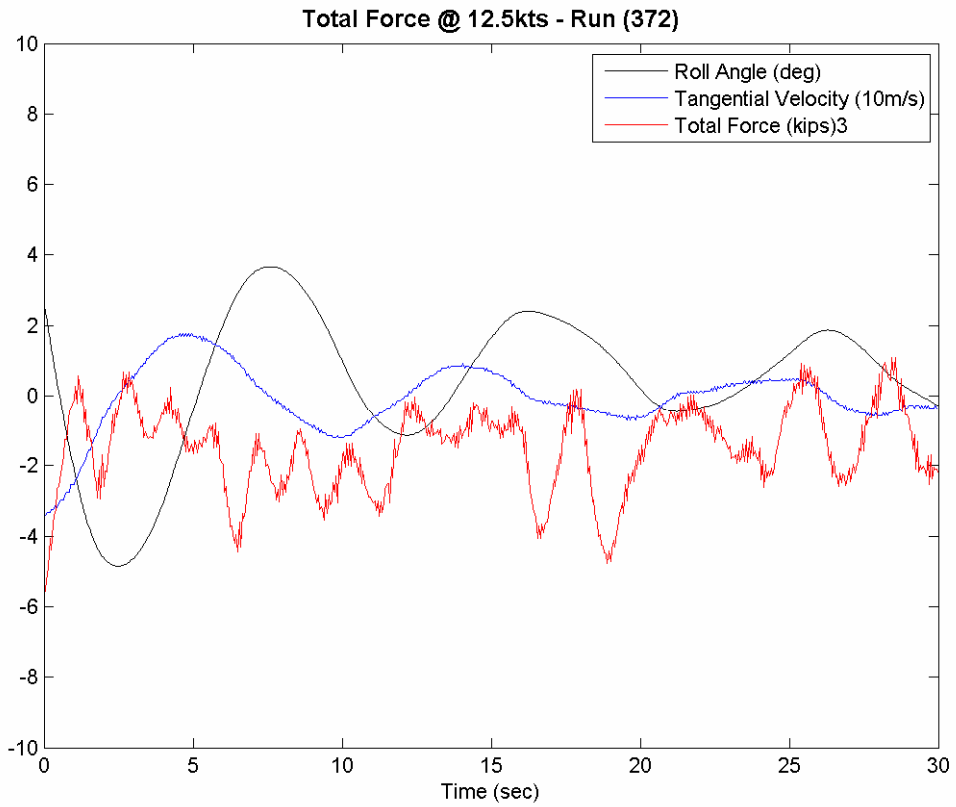
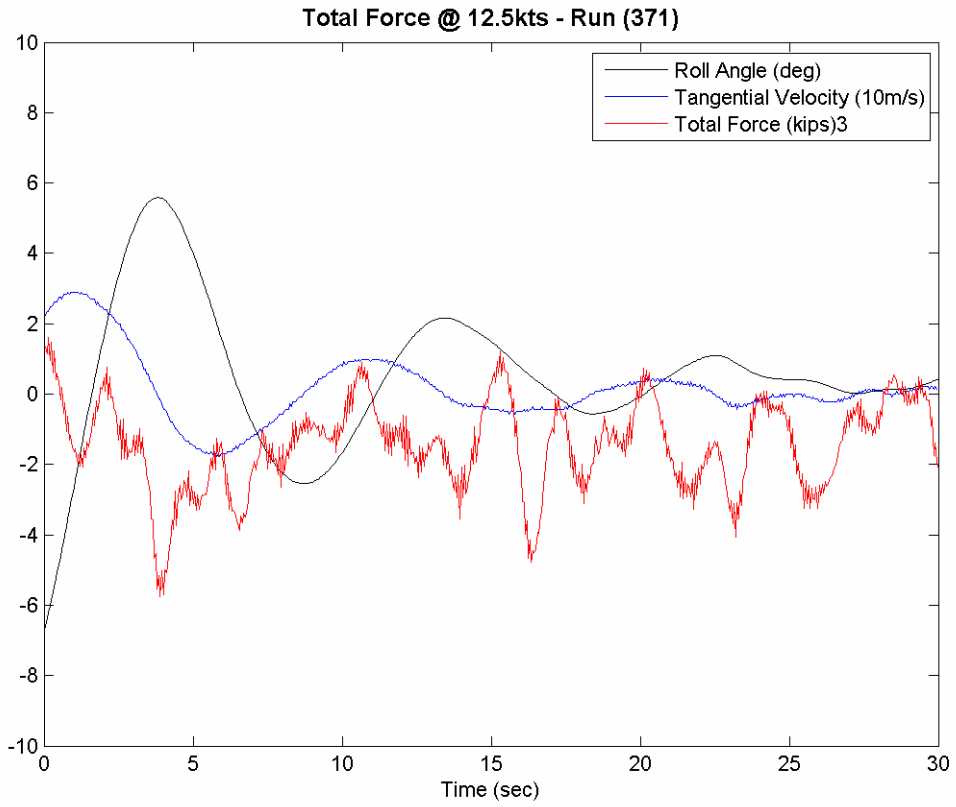


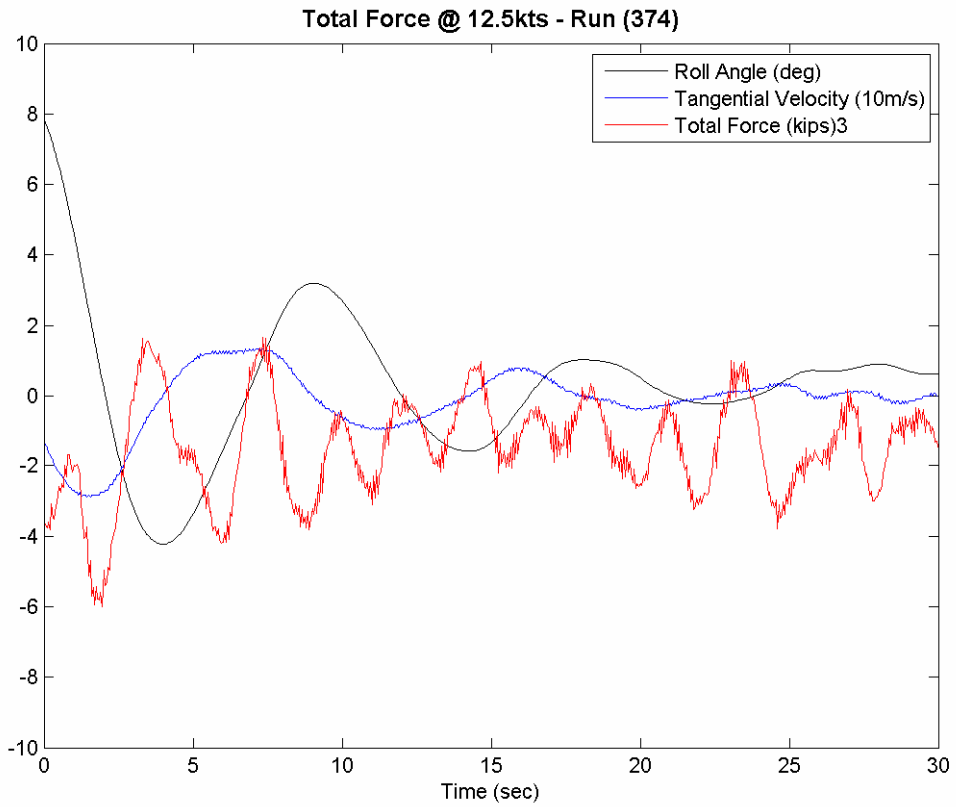
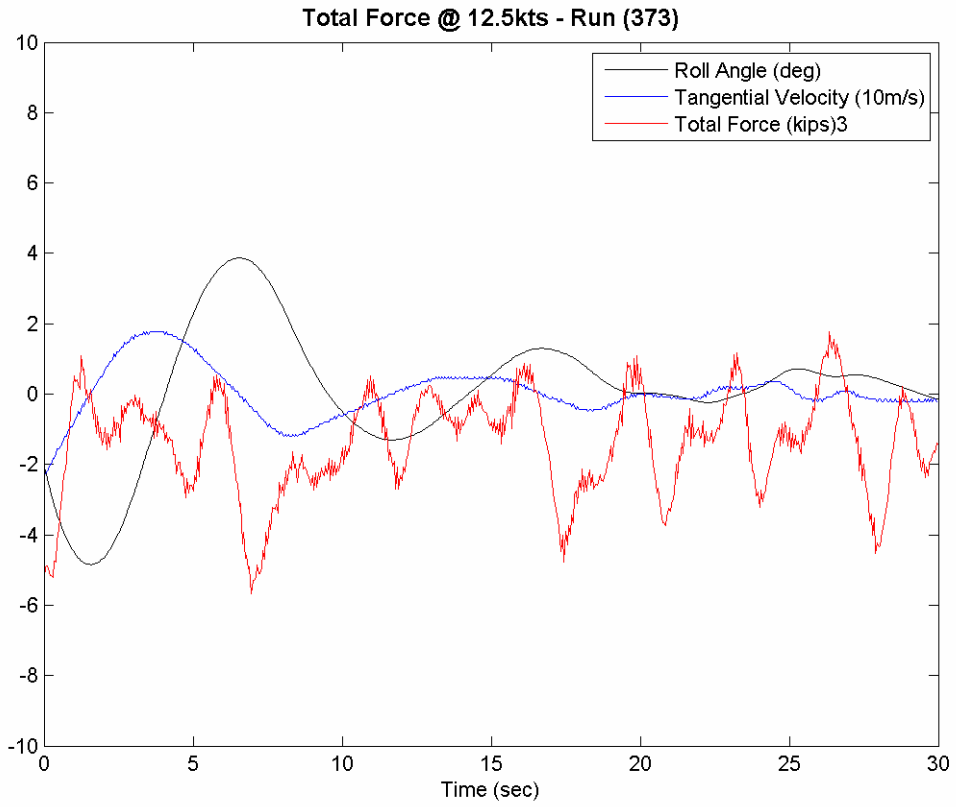
Total Force @ 12.5kts - Run (339)

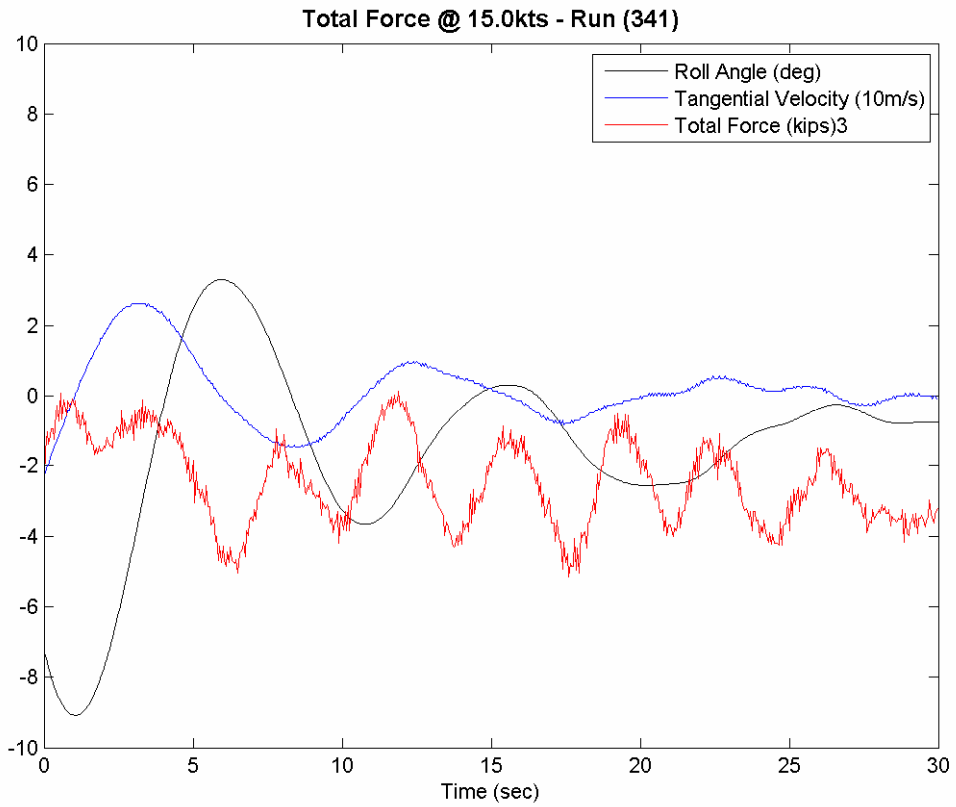
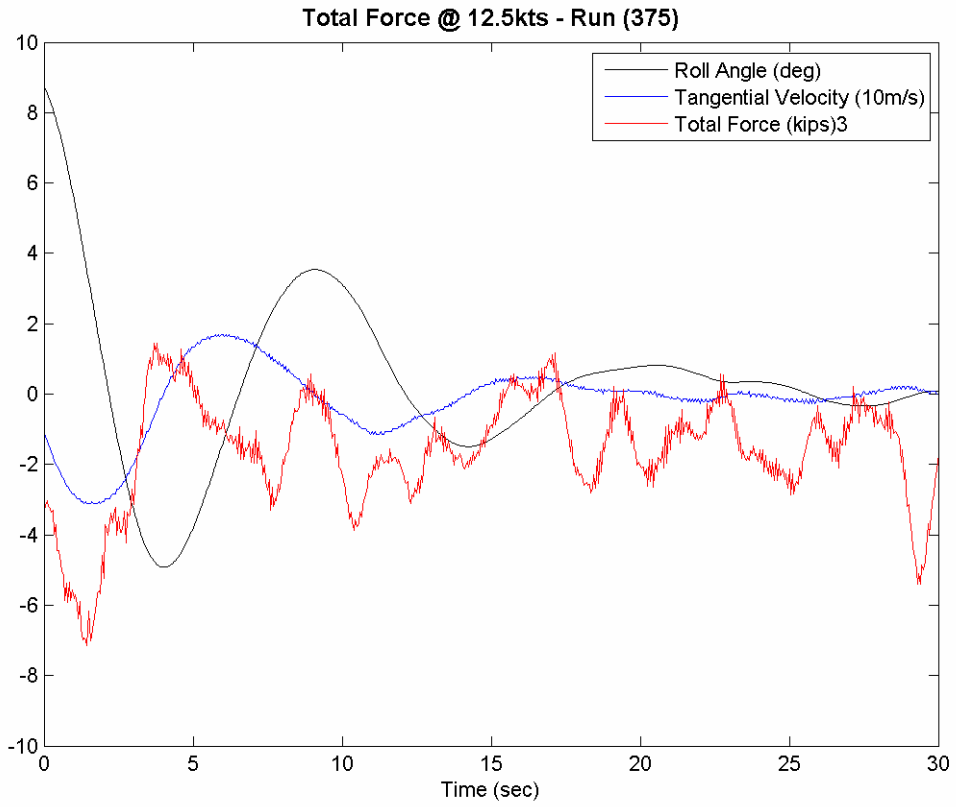


Total Force @ 12.5kts - Run (370)

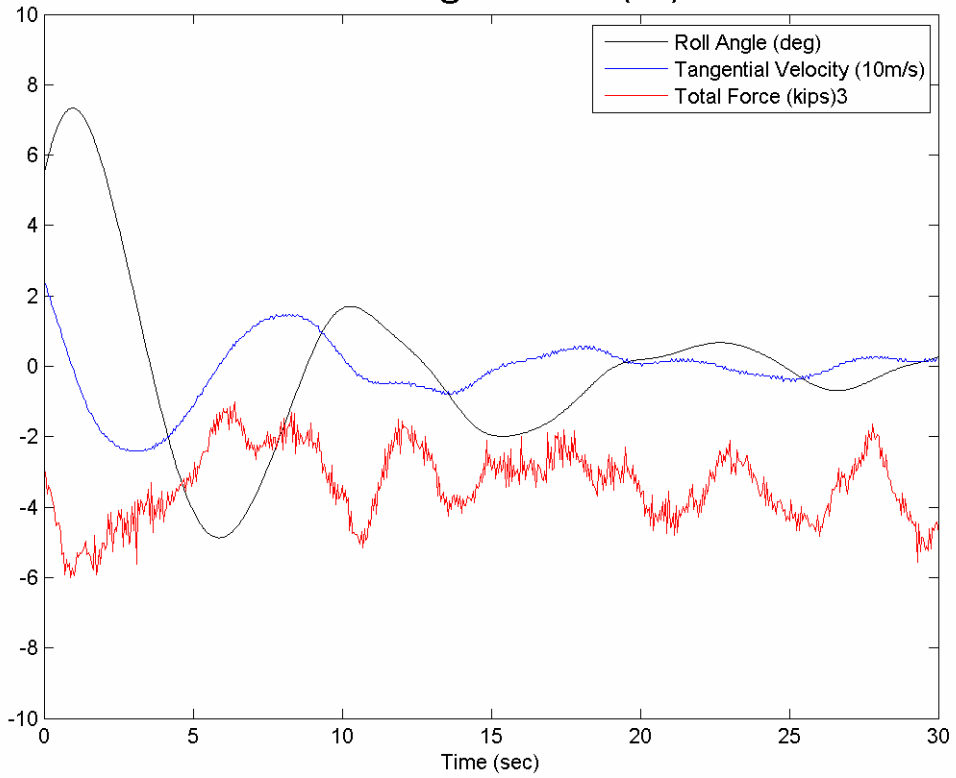




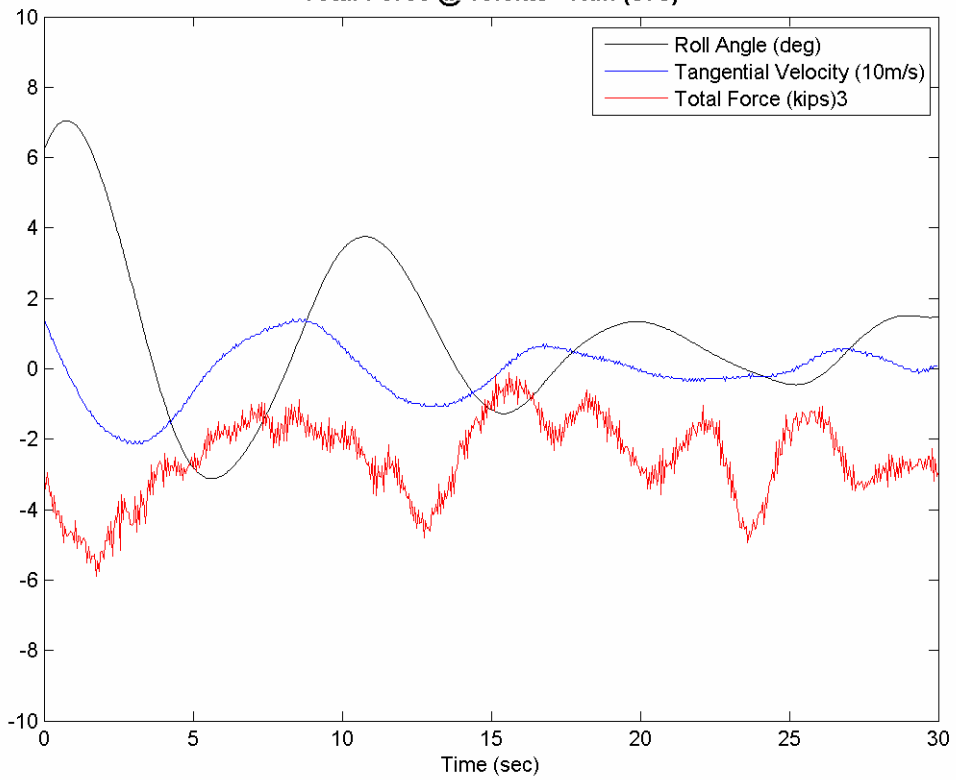


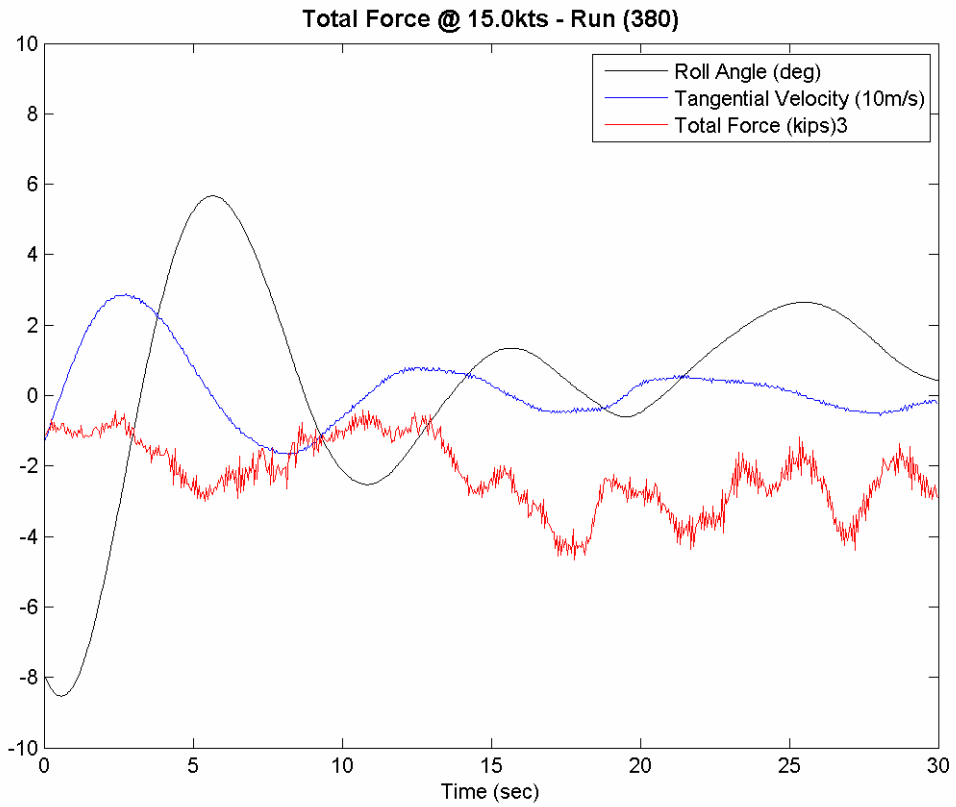
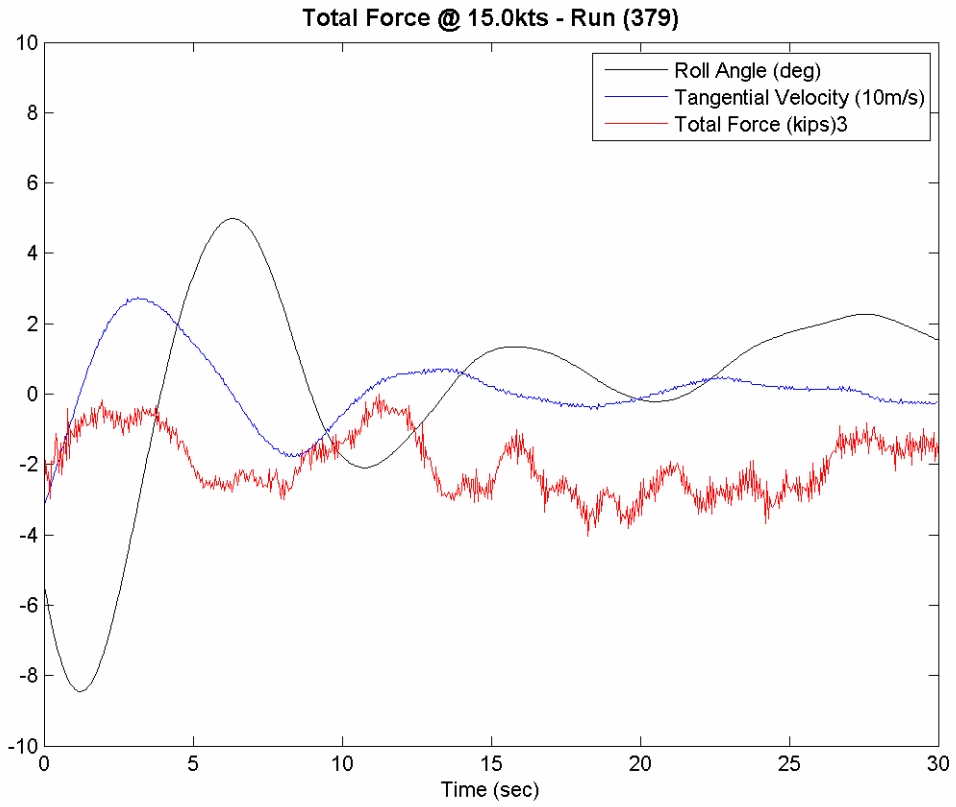


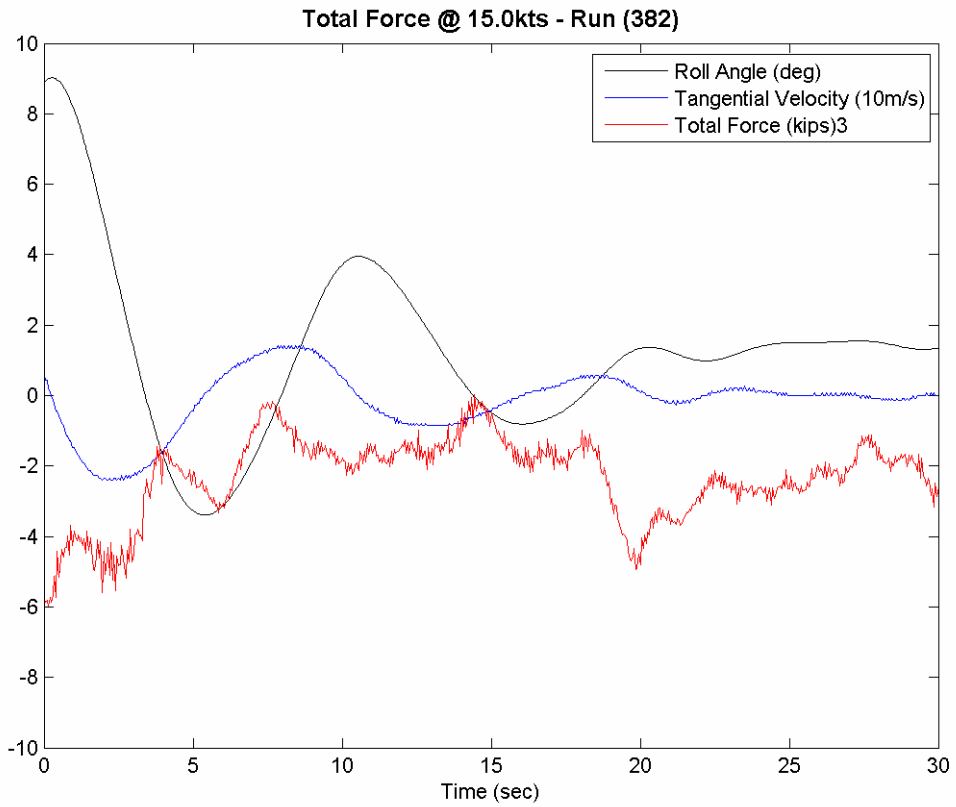
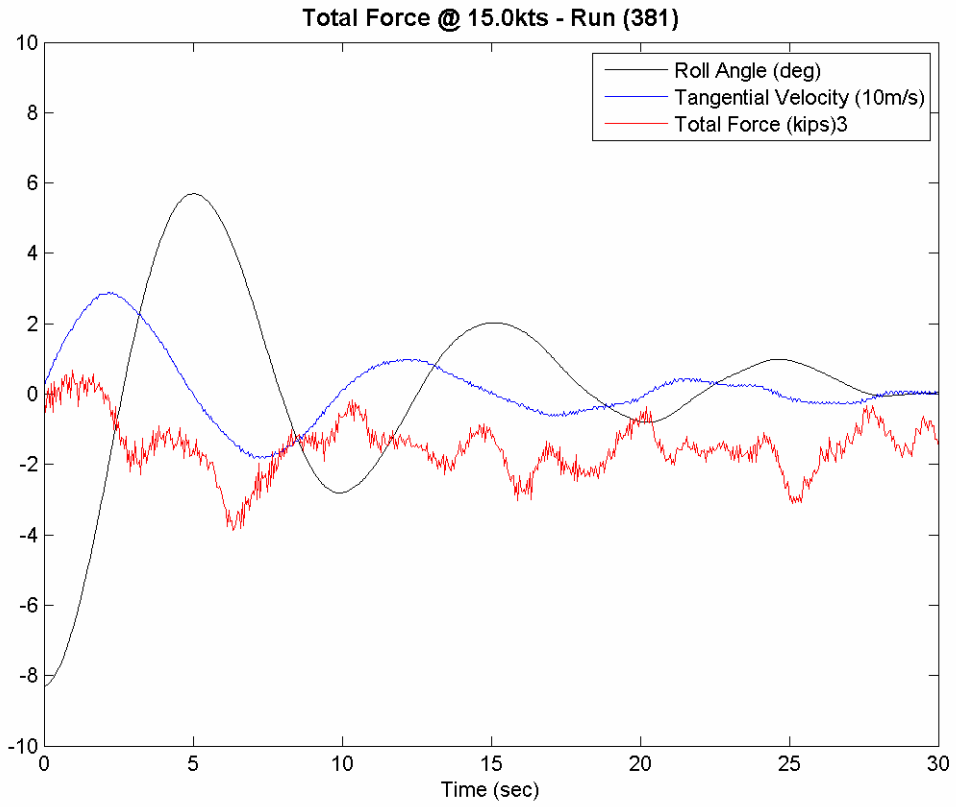
Total Force @ 15.0kts - Run (342)

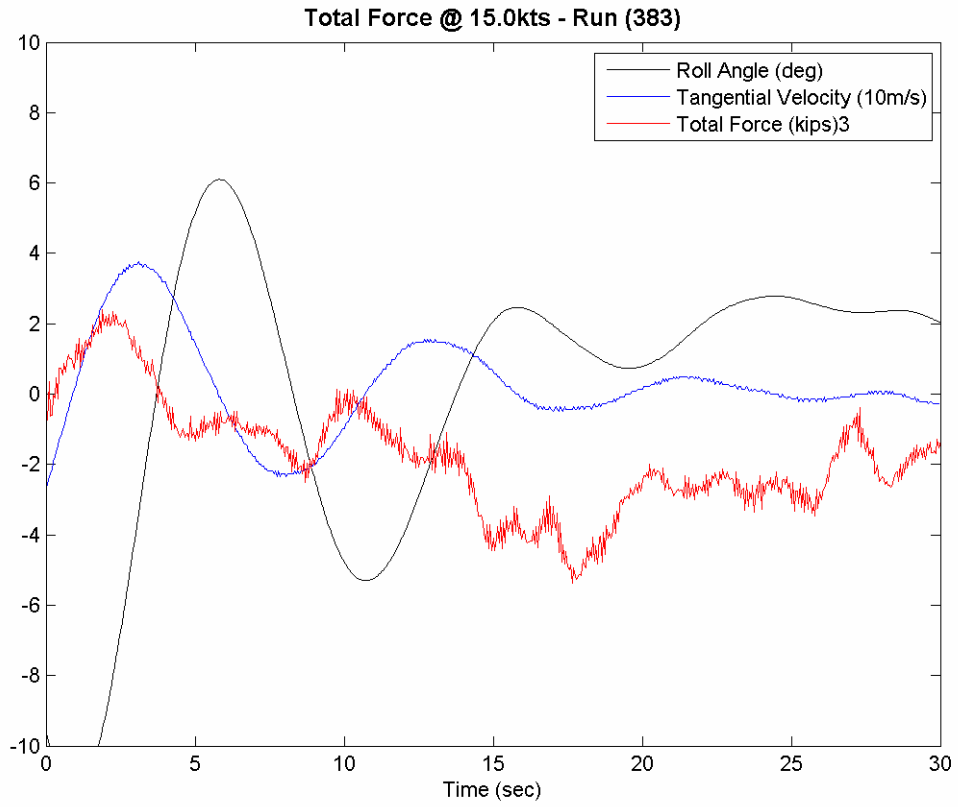


Total Force @ 15.0kts - Run (378)

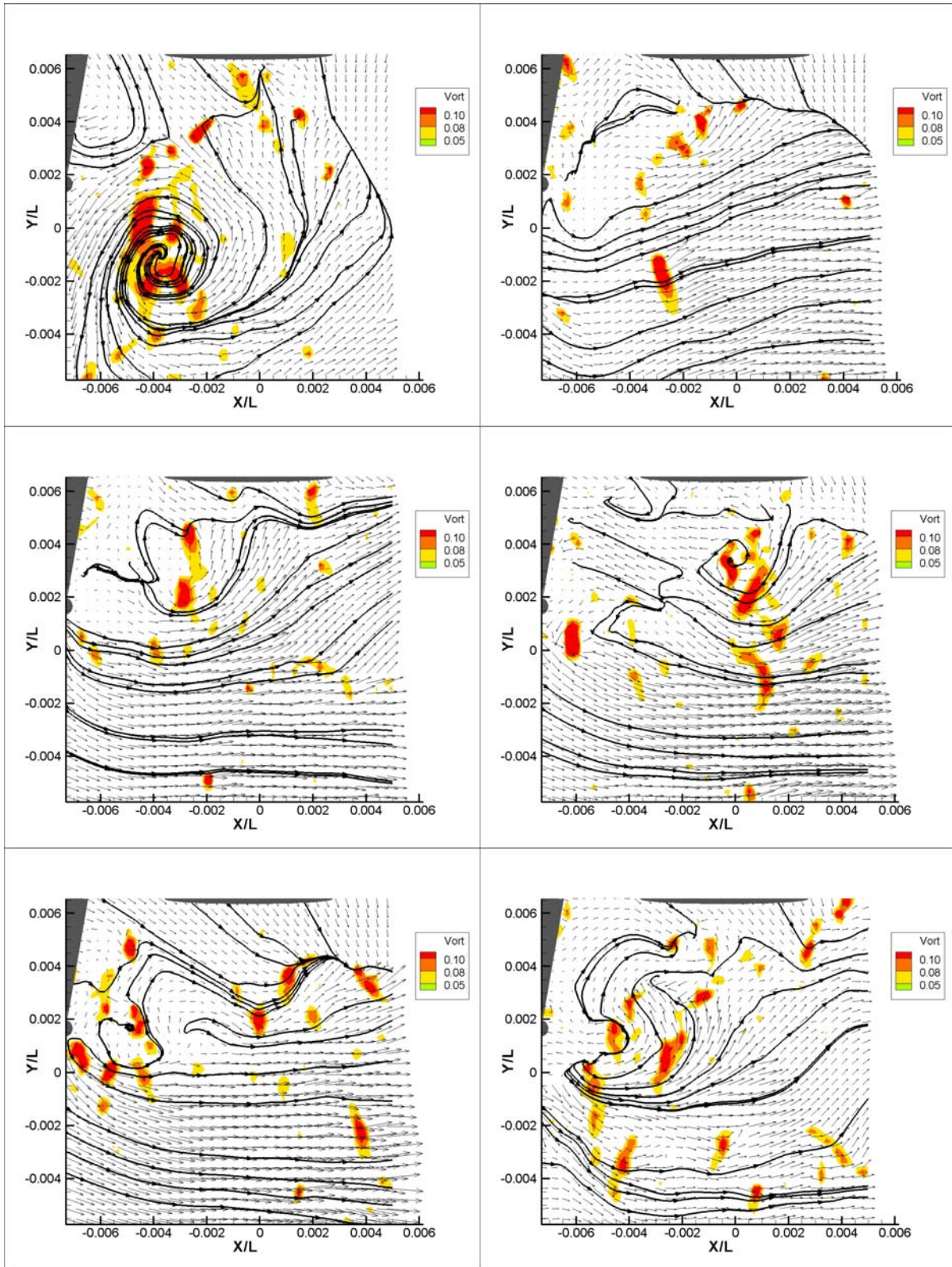




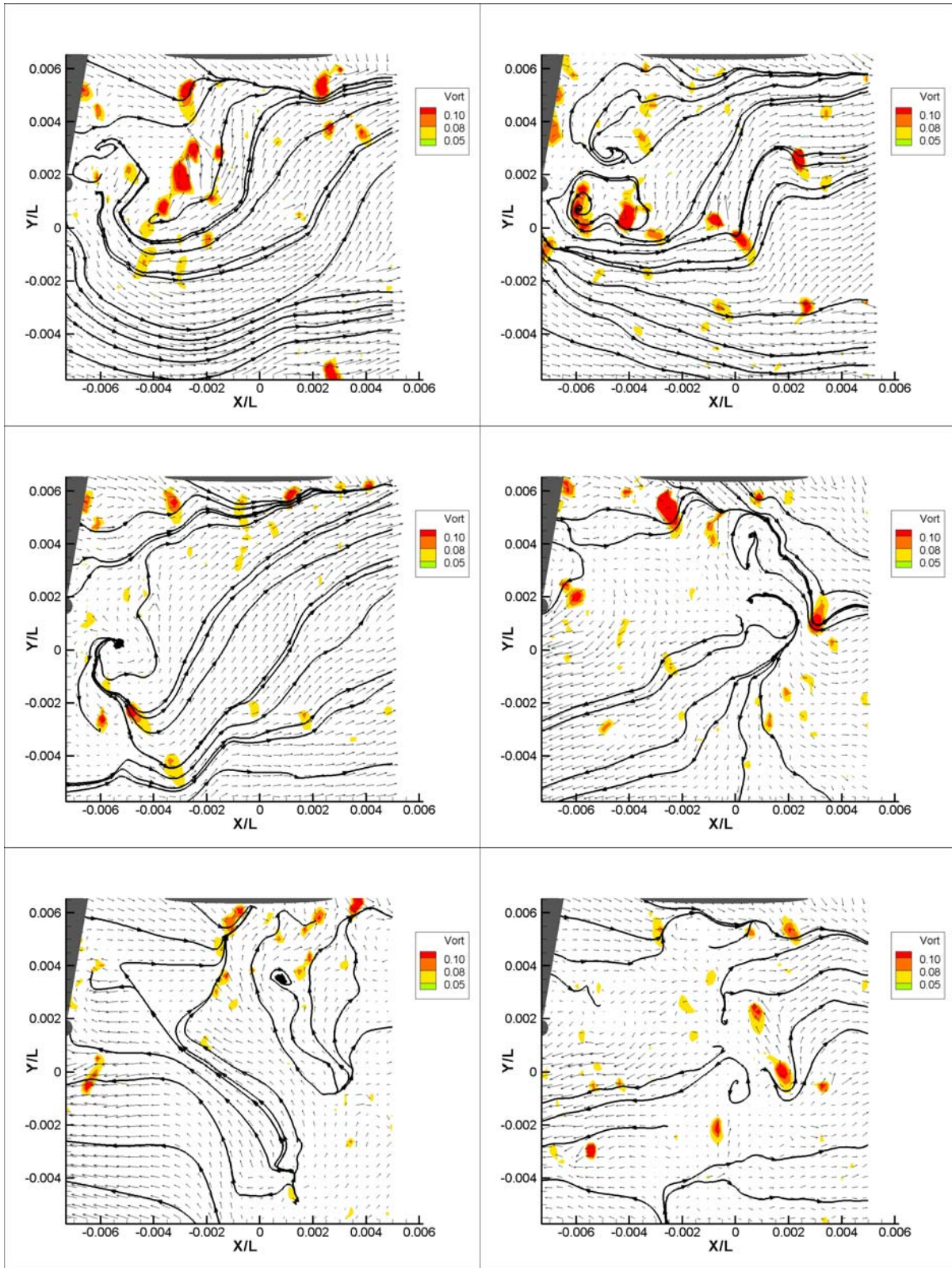




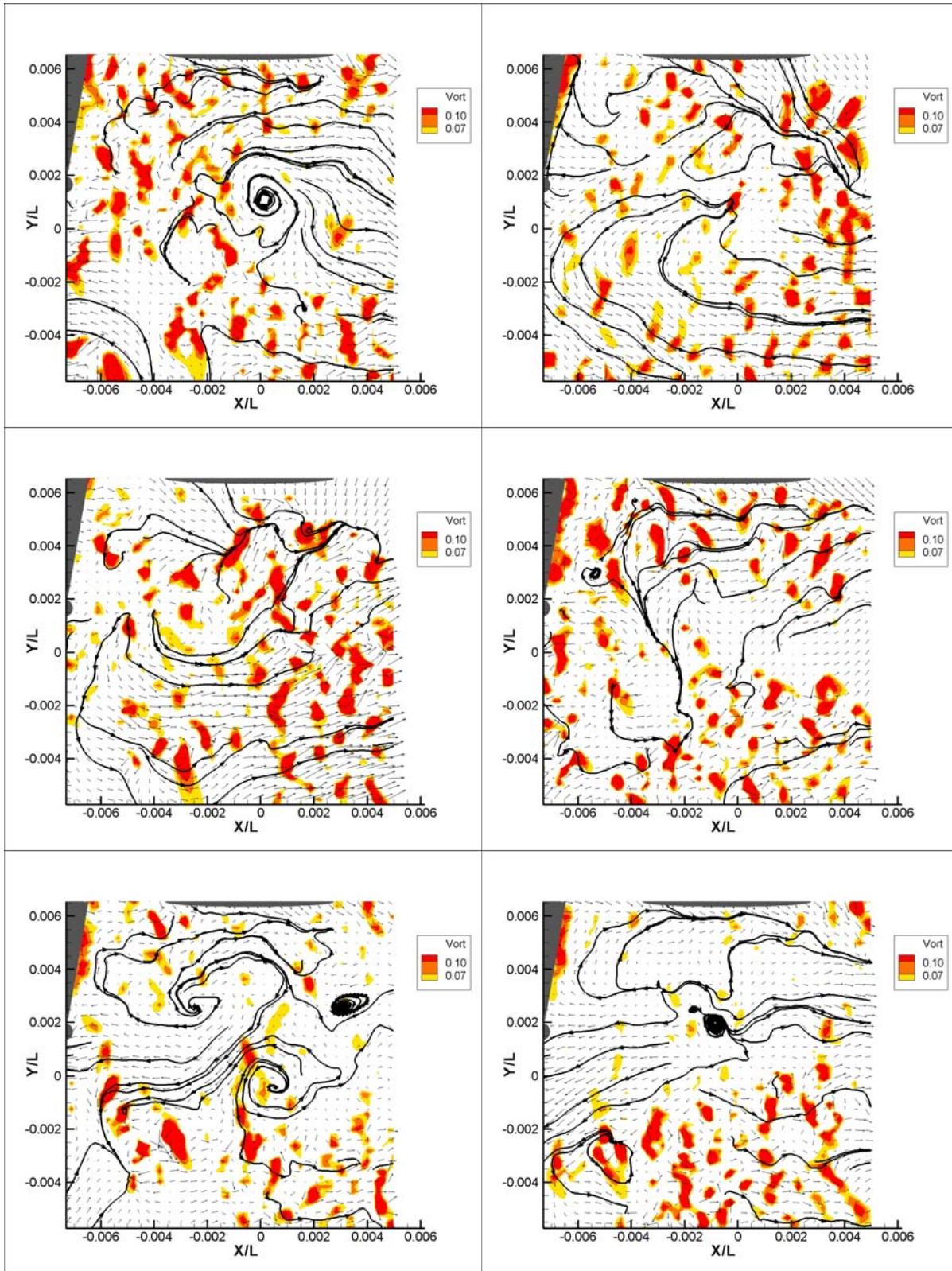
APPENDIX D – ADDITIONAL PIV IMAGE SERIES



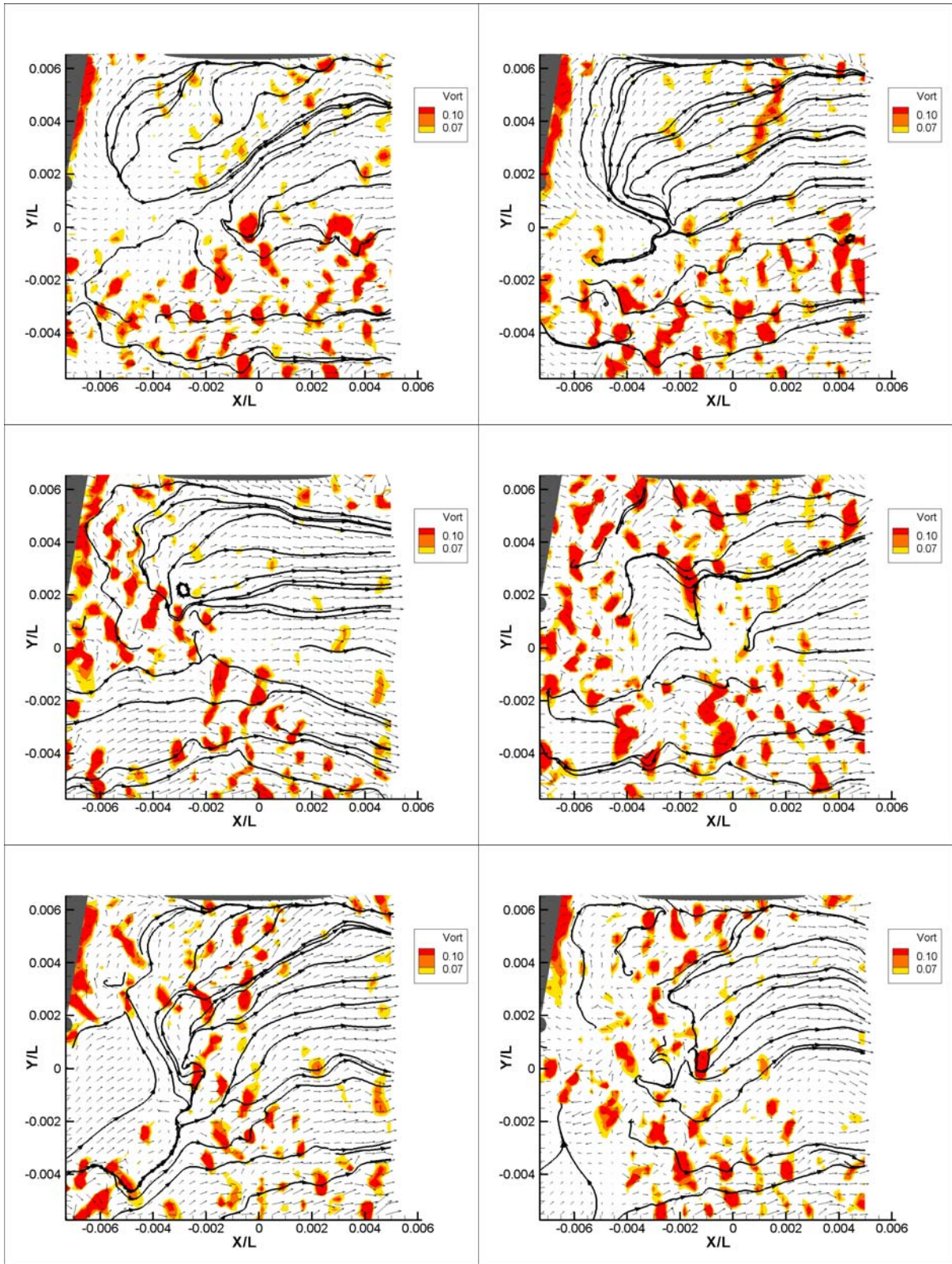
PIV Images at 5.0kts, Run 291 ($t = 0, 1, 2, 3, 4, 5s$)



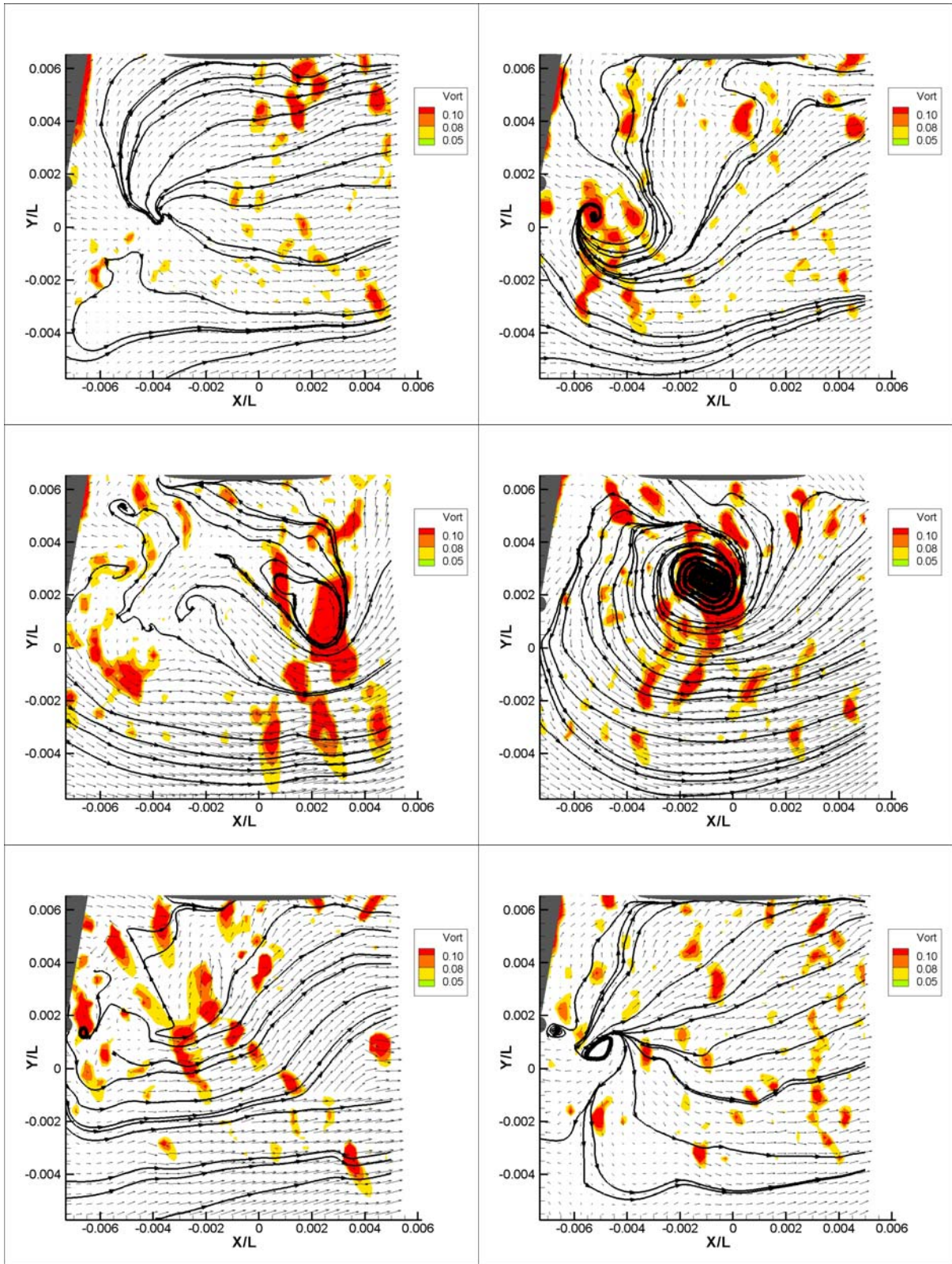
PIV Images at 5.0kts, Run 291 ($t = 6,7,8,9,10,11s$)



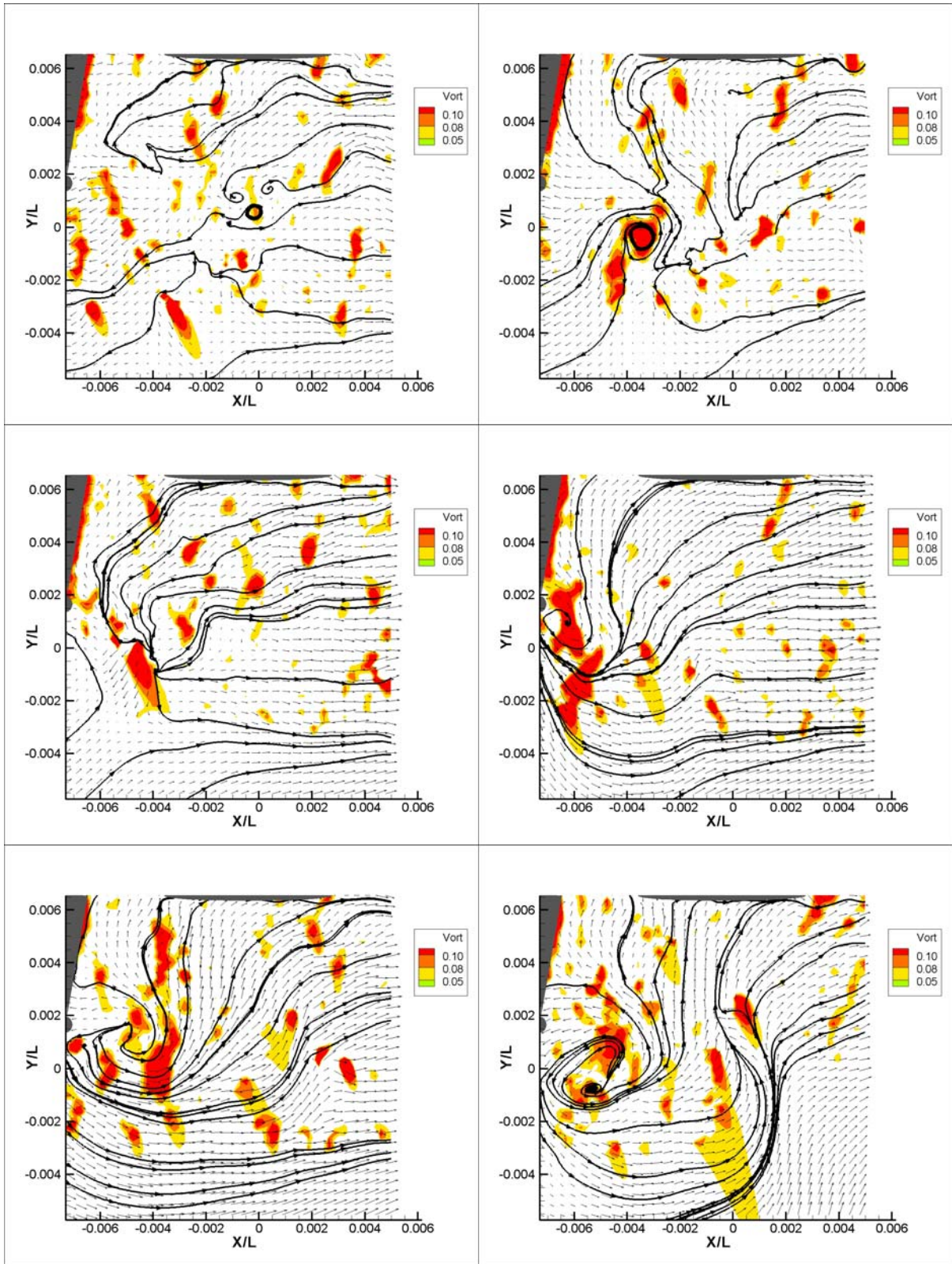
PIV Images at 7.5kts, Run 321 (t = 0,1,2,3,4,5s)



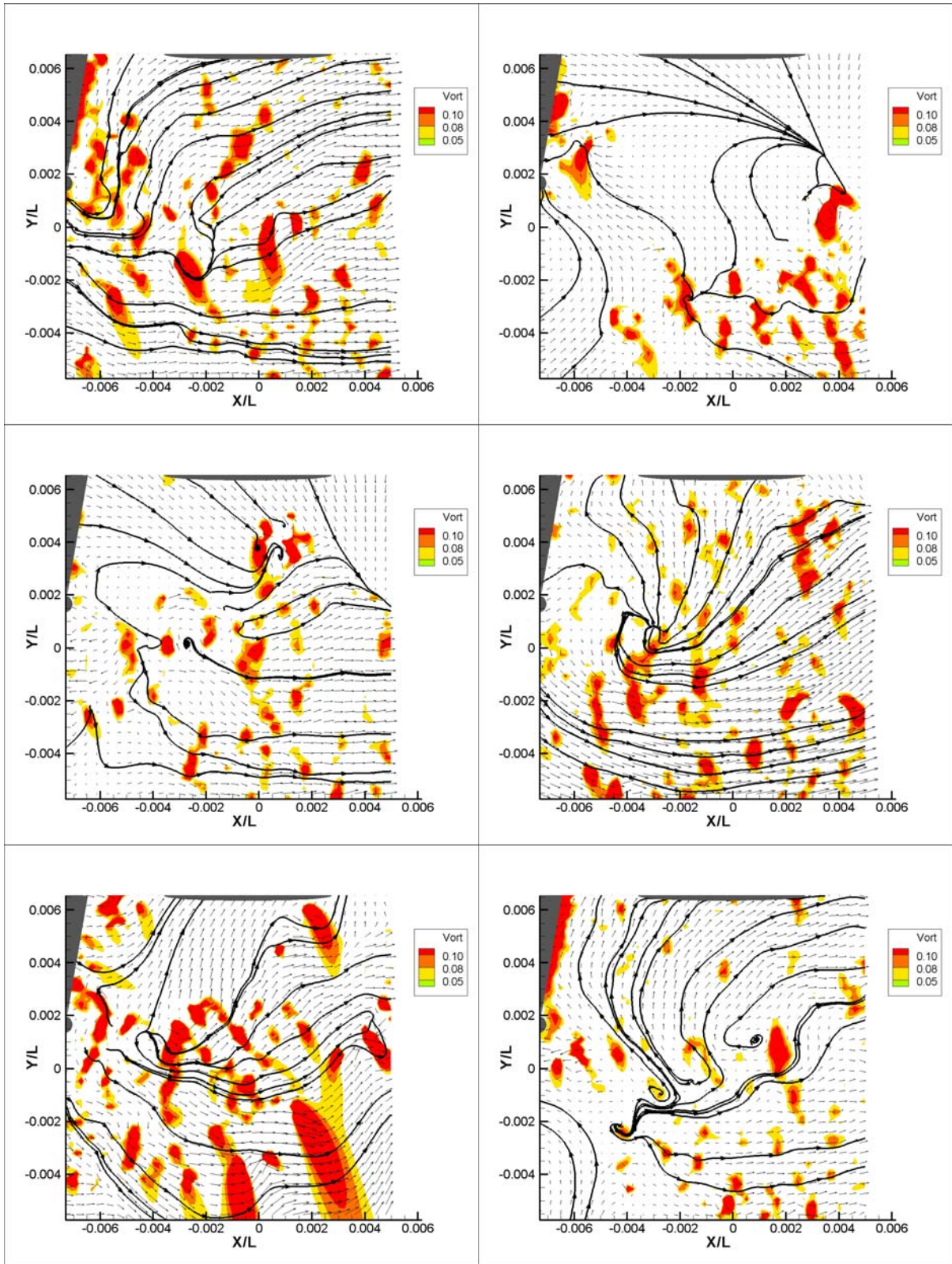
PIV Images at 7.5kts, Run 321 (t = 6,7,8,9,10,11s)



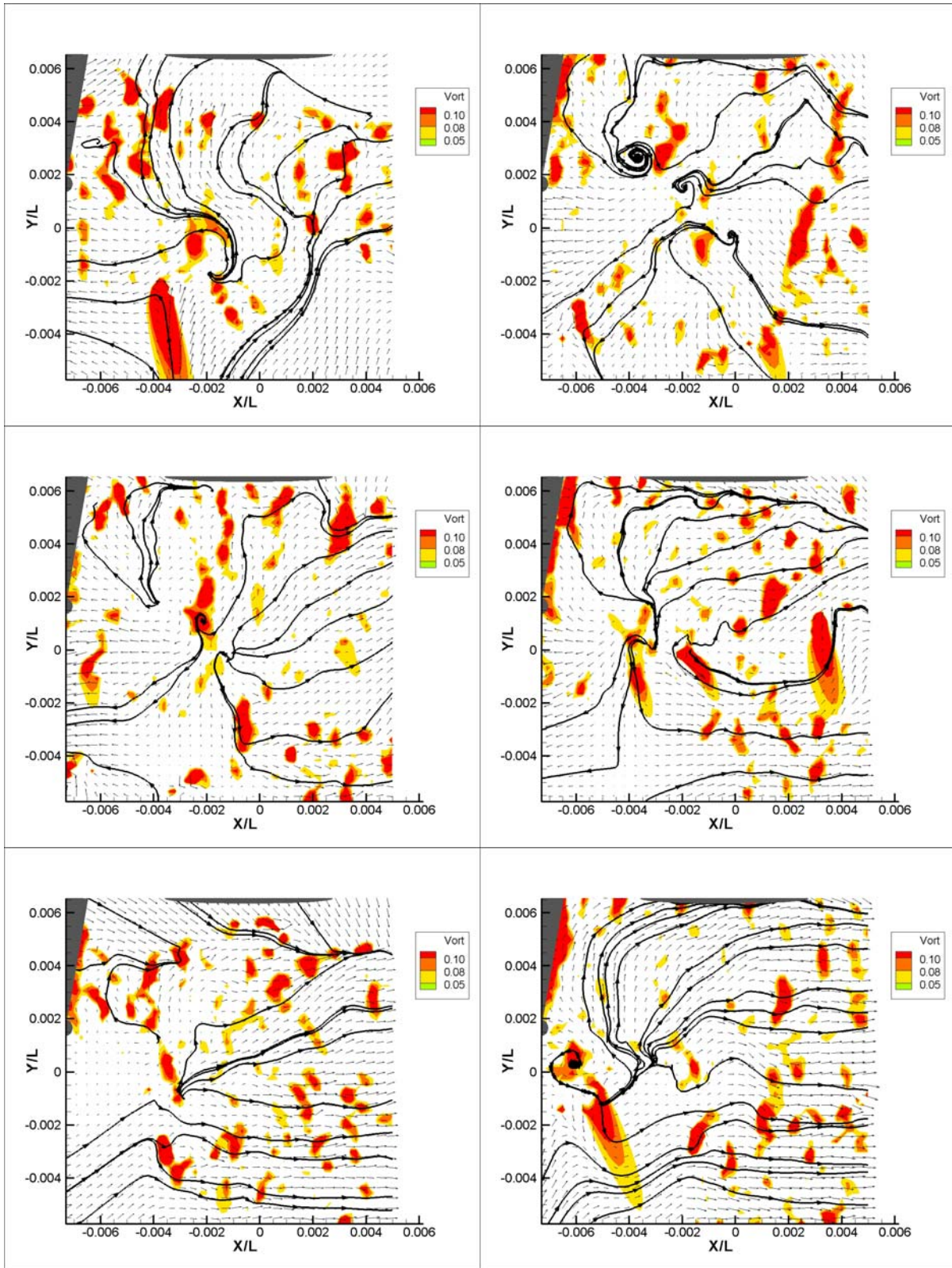
PIV Images at 10.0kts, Run 281 ($t = 0, 1, 2, 3, 4, 5s$)



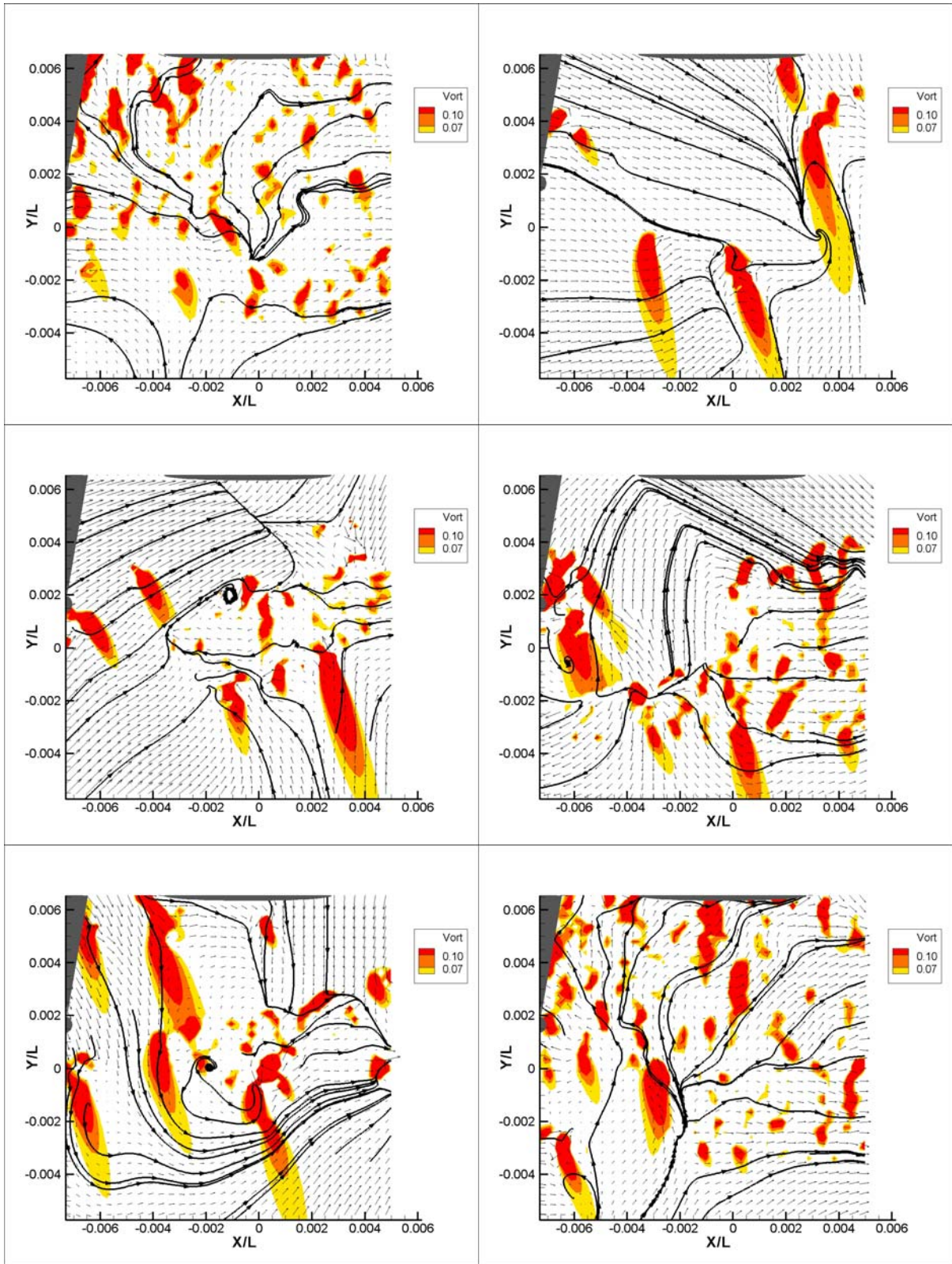
PIV Images at 10.0kts, Run 281 (t = 6,7,8,9,10,11s)



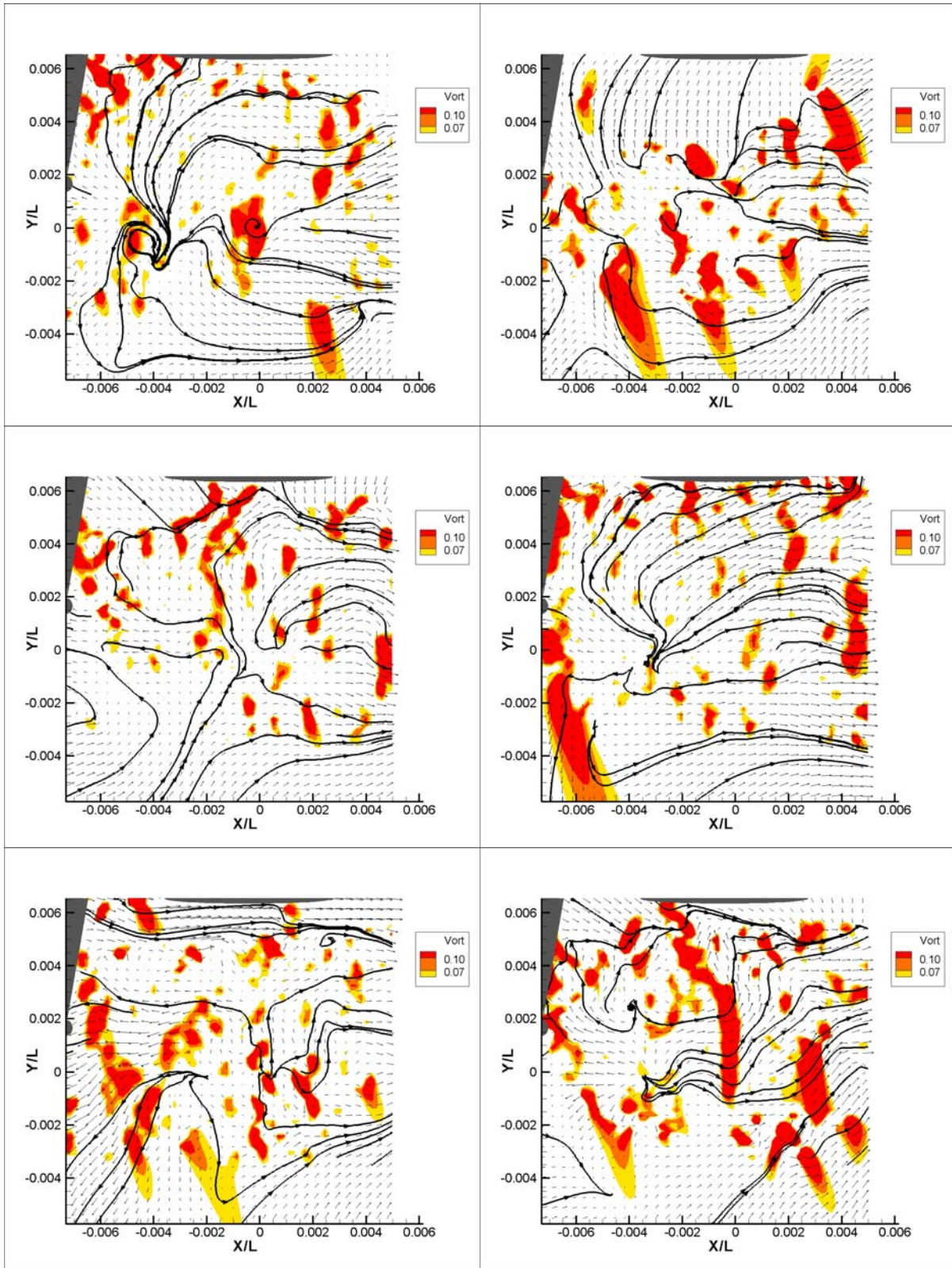
PIV Images at 12.5kts, Run 338 ($t = 0, 1, 2, 3, 4, 5s$)



PIV Images at 12.5kts, Run 338 (t = 6,7,8,9,10,11s)



PIV Images at 15.0kts, Run 341 (t = 0,1,2,3,4,5s)



PIV Images at 15.0kts, Run 341 ($t = 6,7,8,9,10,11s$)